Conversion of Coral Sand to Calcium Phosphate as a Drug Delivery System for Bone Regeneration

by

Joshua Chou

BSc. Hons. (UTS)

The thesis submitted in fulfillment of the requirements for the degree of

Doctor of Philosophy

Department of Physics and Advanced Materials, Faculty of Science,
the University of Technology Sydney

April, 2011

Declaration

Candidate's Certificate

This is to certify that the work presented in this thesis was carried out by the candidate in the Faculty of Science at the University of Technology Sydney and has not been submitted to any other university or institution for a higher degree. This work contains no material written or published by any other person except where due reference has been made.

Joshua Chou

Sydney, April 2011

Acknowledgements

I wish to express my deep sense of gratitude to Professor Besim Ben-Nissan and Dr. Stella Valenzuela from the Faculty of Science, the University of Technology Sydney, for their inspiring guidance, constant encouragement and support of my research work. I thank them very much for giving me the freedom to explore the realms of science and for sharing their wide knowledge and expertise. I very much appreciate the working environment they have provided to the group members, thereby leading to a highly productive atmosphere, where everyone understands their responsibilities and acts accordingly. I am deeply grateful to them for their support in times of difficulties, solving many problems and motivating me to progress ahead. In spite of their busy schedule, they have always made themselves available whenever I approached them and I sincerely thank them for being open and supportive to my suggestions. I am very grateful that they let me present the results of my research at both national and international conferences. From the Faculty of Science, I have had the privilege to work with several co-workers and I express my warmest thanks to all of them: Greg Heness PhD., Torsten Theis PhD., Julia Ting PhD., Barry Liu PhD., Norman Booth PhD. and Jerran Nadoo.

I express my thanks to all my family and friends for their support, friendship and love during the whole period of this work. Especially I would like to thank my parents, Joey and Jenny and my brother Jeremy, who always supported me and kept me motivated to finish my thesis

Finally, this thesis could not have been completed without constant encouragement, support and tender loving care, especially during difficult times, from my beloved Ellen, I love you.

Joshua Chou
Sydney, April 2011

Abstract

In this research, we have for the first time harnessed the architectural design of biospheres from coral beach sand, to capture and deliver the drug bisphosphonate alone, or in combination with antibiotics. Partnered with this we used lipid coatings to control drug elution by design. This is a study to utilise biomimetics for drug delivery using these marine structures. Importantly, release of the drug was sustained at physiologically relevant quantities for longer periods than those originating from other clinically practiced schemes such as, doping bone cements and oral administration. The simple concept of using natural structures directly for human therapeutics can yield enormous benefits to an increasingly ageing population. Currently researchers are striving to perfect the design and formulation of delivery vehicles that can be directed to an exact location and offload the pharmaceutical drugs at the site. There are many promising strategies including bio-inspired ones, but none using something as simple as coral beach sand with unique pore size, interconnectivity and architecture.

These calcium carbonate coral beach sand microspheres were converted to calcium phosphate and loaded with pharmaceutical drugs such as bisphosphonate. The drug bisphosphonate has an inherent affinity for calcium, and as the microspheres slowly degrade, the drug is released. Elution kinetics show sustained release of the adsorbed drug. This occurs for 21 days- long enough to influence early bone formation. Once the drug has been released, the spheres also safely dissipate. Drug functioning was positively determined by increased human osteoblast proliferation accompanied by osteoclast inhibition in direct association with bisphosphonate bio-spheres. The unique, complex topology and morphology enables the drug to be loaded and retained while the material is calcium phosphate and adsorbes the drug very efficiently.

In addition an antibiotic gentamicin was loaded at the same time to surmount the re-current problem of bacterial infections following bone and implant surgery. Biospheres therefore offer a more efficient and convenient alternative. Following complete drug release the vehicle degrades slowly in-situ. The elution kinetics can be further controlled by coating the spheres with lipid. In the future these can be incorporated with molecules that provide highly specific associations with a target tissue. Coral beach sand is plentiful and pre-designed to adsorb and release a variety of drugs, as indicated by this study. So far with this study we have shown this *in vitro*, but in principle this is applicable for any orthopaedic or maxillofacial drug of choice for bone repair and reconstruction. Biomimetics do not need to be complicated.

TABLE OF CONTENT

I. List of Figures

II. List of Tables

III. Publications

Book Chapter

1. B. Ben-Nissan, A.H. Choi, D.W. Green, B.A. Latella, **J. Chou** and A. Bendavid. Synthesis of Hydroxyapatite Nanocoatings by Sol-Gel Method for Clinical Applications, In Biological and Biomedical Coatings Handbook , CRC Press, Editor, S. Zhang, Taylor and Francis publishers. (In press, April 2011).

Full Papers in Peer-Reviewed Journals

1. **J. Chou**, B. Ben-Nissan, D.W. Green, S.M. Valenzuela, L. Kohan. (2011). Targeting and dissolution characteristics of bone forming and antibacterial drugs by harnessing the structure of micro-spherical shells from coral beach sand, Advanced Engineering Materials, 1: 1-2,93–99

2. **J.Chou**, D.W. Green and B. Ben-Nissan. (2010) New Slow Drug Delivery Materials and Systems for Biomedical Applications, Materials Australia, Sept, 43:3, 38-41

3. **J. Chou**, B. Ben-Nissan, P. Doble, C. Austin. (2010). Trace Elemental Imaging for Biomaterials by Laser Ablation Inductively Coupled Plasma-Mass Spectroscopy (LA-ICP-MS), Journal of Tissue Engineering and Regenerative Medicine (Accepted)

4. **J.Chou** and B. Ben-Nissan. (2009). Characterization of Slow Drug Delivery Microspheres for Bone Regeneration. In Bioceramics 22, Edited by Sukyoung Kim, 555-558.

5. **J.Chou**, R.Shimmon and B.Ben-Nissan (2009). Bisphosphonate determination using 1H-NMR spectroscopy for biomedical applications, Journal of Tissue Engineering and Regenerative Medicine, 3: 92-96

6. **J.Chou**, B.Ben-Nissan, A.H. Choi, R.Wuhrer, and D.Green (2007). Conversion of Coral Sand to Calcium Phosphate for biomedical application, Journal of Australia Ceramic Society, 43 [1], 44-48

7. K.Lewis, A.Choi, **J.Chou** and B. Ben-Nissan (2007). Nanoceramics in Medical Application, Materials Australia, Vol. 40, No.3, May/June 2007, 32-34

Full Papers in Conference Proceedings and Presentations

1. **J. Chou**, B. Ben-Nissan, and R. Shimmons. Bioinspired processing & laser ablation ICP-MS imaging of calcium phosphate microsphere. 10th International Conference on Ceramic Processing Science. May 2008. Oral Presentation

2. **J. Chou**, B. Ben-Nissan. Structure and characterization of coral sand and its conversion to calcium phosphate. 1st Asia Biomaterial Congress ABMC. December 2007. Poster

3. **J. Chou**, B. Ben-Nissan. Conversion of coral sand to calcium phosphate for biomedical applications. Materials & Austceram. July 2007. Oral Presentation

4. **J. Chou**, B. Ben-Nissan, R. Wuhrer. Conversion of coral sand for biomedical applications. 19th International Symposium on Ceramics in Medicine/ International Society for Ceramics in Medicine (ISCM). October 2006. Oral Presentation

1 Introduction

1.1 Introduction to the Research

Bone plays an important role in critical functions in human physiology and the importance becomes clear in the case of diseases such as osteogenesis imperfect, osteomyelitis, and osteoporosis in which bone deteriorates or does not function properly. These diseases along with traumatic injury and orthopedic surgery might lead to or induce bone defects or voids. The clinical and economic impact of treatments of bone defects is staggering. In the United States alone osteoporosis affects over 75 million people and this is projected to increase by 240% in the next fifty years (Ben-Nissan B., 2003) . Due to the large number of orthopedic surgeries that are performed each year, bone repair has become a subject of intensive investigation.

Most bone diseases pose serious health problems and directly impact on the patient's life-long mobility, activity and quality of life. Generally, a bone graft or implant is required where there is significant damage or loss of bone. The most desirable implants are autogenousi(natural materials which cause no immune rejection) or allogenic (from donors). However, sufficient material cannot always be derived from the patient or a suitable donor and current medical technologies are not yet able to synthesize these materials. As a consequence, artificial materials are substituted. However, these materials experience significant problems when implanted. They might bond poorly to living bones, resulting in micromotion and slippage when stressed.

The common aim in the development of bone tissue engineering is to produce a treatment for preventing bone loss which allows for complete regeneration of the bone to the pre-traumatic state. Many great ideas have been proposed over the years but amongst these the most attractive strategy is using a drug loaded scaffold that possesses a specific architecture to promotes and allows new bone regeneration. The premise behind this idea, that is also the core hypothesis behind this thesis, is that specific materials can be manipulated to facilitate cell colonization and proliferation.

The cells are encouraged to form the extracellular matrix, and grow into a fully functional replacement. Drug therapy can be used to promote a positive cellular response, and/or to limit any negative immunological or inflammatory response. The scaffold will degrade after implantation, breaking down into base constituents that can be tolerated and eliminated by the body. The final result will be a new functional bone, with no traces of the scaffold and hopefully none of the original trauma.

Resorbable calcium phosphate-based composite scaffolds are designed to match as closely as possible to the mineral composition of natural bone, thereby allowing the generation of bone trabeculae, provided the rate of resorption of the calcium phosphate is sufficiently slow for osteoblasts to be able to regenerate new bone (Blokhuis et al., 2000). In particularly, beta-tricalcium phosphate is one of the most widely used bone implant materials. Its crystal phase possesses a similar structure to that of natural bone. This facilitates osseointegration of the implant into the surrounding bone material, and stability. There is increasing effort in developing spherical particles, which are more suitable for implantation than non-homogeneous granules, since they conform better to irregular implant sites (Temeno and Antonios, 2000). Particles with uniform shape have a more predictable flowing property during injection (Ribeiro C.C., 2006). Paul and Sharma (1999) showed that irregularity with the surface morphology could cause inflammatory responses and slow the rate of bone formation compared to relatively smooth surfaces. Therefore the ideal microsphere delivery system will consist of a smooth surface with uniform pores. The effectiveness of these micro spherical materials can be highly improved if they can act simultaneously as carriers of biologically active molecules. In this sense, spherical materials with uniform pores will have additional advantages since they present additional surface area, which is an important parameter that strongly influences the drug loading capacity and release rates that can be achieved (Ribeiro C.C., 2006).

In the present research, the material investigated is a beta tricalcium phosphate microsphere manufactured from a marine structure by a hydrothermal conversion reaction, where the trabecular, bone imitating structure (pores size, interconnectivity and biocompatibility) of the microsphere remains unchanged and the calcium carbonate skeleton is converted to calcium phosphate. This study was designed to investigate the properties of natural marine microspheres to serve as both a bone substitute and as a drug delivery matrix.

1.2 Main Premise

The use of calcium phosphate bioceramic for bone regeneration is well documented and widely recognized due to the good biological response and adequate mechanical properties. The effectiveness of these calcium phosphates can be further enhanced by introducing pharmaceuticals that can assist in the bone regeneration. The development of microspheres is both a scientific and technical challenge which has yet been vercome. To date, there is -as yet- no microsphere developed that offers uniform porosity which is crucial as pore size and interconnectivity allows drug loading and controllable dissolution rates.

The use of corals as a biomaterial scaffold has already being demonstrated by many workers in animal experiments demonstrating bone growth and integration for small and medium sized bone defects (Guillemin et al., 1987). However the use of pure corals limitated to small bone defects as large defects were shown to undergo an osteogenic slackening, loss of strength, leading after some weeks to collapse and a lack of repair.

In order to overcome these weaknesses, the research described in this thesis was carried out to utilize the unique structure and architecture that natural coral exhibit, to convert it to calcium phosphate by hydrothermal conversion process, and to demonstrate if pharmaceutical medication can be incorporated into the coralline material to enhance the bone replacement process.

1.3 General Aims

The general aim of this thesis is to develop a new generation scaffold capable of drug delivery using natural materials to facilitate bone regeneration. This is realized through several objectives which describe the progression of scaffold development.

The thesis examines and discusses a specific marine structure, "coral beach sand microspheres" for the compositional and structural characteristics and both physical and biological properties using a range of analytical techniques.
Coral sand is one of the commercial names of *Foraminefera,* a unique marine structure or shell, and for simplicity the name "coral beach sand" rather than the species name is used throughout this thesis.

Basic aims:

I. To identify and characterize a natural spherical coral sand and convert to calcium phosphate by the hydrothermal method,

II. To evaluate the suitability of converted calcium phosphate microspheres for bone tissue regeneration applications via *in vitro* tests.

III. To investigate the drug loading and release behavior of the microspheres dependent on its specific characteristics, thereby allowing for the material to be individually tailored to the required delivery rates.

IV. To examine the *in vitro* efficiency of dual pharmaceutically loaded microspheres in promoting bone regeneration and inhibiting microbial infections post implant operations.

2 REVIEW OF THE LITERATURE

2.1 Bone Tissue Engineering and Regeneration

The development of bone tissue engineering is directly related to changes in materials and nanotechnology. While the inclusion of material requirements is standard in the design process of engineered bone substitutes, it is also critical to incorporate clinical requirements in order to engineer a clinically relevant device. There are multiple clinical reasons to develop bone tissue-engineering alternatives, including the need for better filler materials that can be used in the reconstruction of large orthopaedic defects and the need for orthopaedic implants that are mechanically more suitable to their biological environment. Bone regeneration requires four components: a morphogenetic signal, responsive host cells that will respond to the signal, a suitable carrier of this signal that can deliver it to specific sites then serve as scaffolding for the growth of the responsive host cells, and a viable and most importantly a well vascularized host bed (Croteau et al., 1999, Harakas, 1984). To develop successful drug delivery systems for treatment of bone disease, a sound rationale based on bone anatomy and biology is needed. To this end, an overview on the structure and biological functions of the bone tissue is presented.

2.2 Bone Anatomy and Physiology

Bone is a complex mineralized living tissue, exhibiting the property of marked rigidity and strength whilst maintaining some degree of elasticity. In general, there are two types of bones in the skeleton, namely, the flat bones (eg. skull bones, scapula, mandible, ilium) and the long bones (eg. tibia, femur, humerus). In principle, bone serves three main functions in the body: (i) act as a mechanical support; (ii) the site of muscle attachment for locomotion, protective, for vital organs and bone marrow; and (iii) to assist metabolism, it acts as a reserve of ions for the entire organism, especially calcium and phosphate. Bone consists of metabolically active cells and is comprised of osteogenic precursor cells, osteoblasts, osteoclasts, osteocytes, bone lining cells and the hematopoietic elements of the bone marrow.

The bone remodeling process primarily involves the coordinated activity of cells from two distinct lineages, the osteoblasts and the osteoclasts, which form and resorb the mineralized tissue. There are two main forms of bone, woven bone and lamellar bone. Woven bone is a primitive and immature bone that is formed during bone development, fracture healing, tumours and metabolic diseases. Woven bone forms rapidly and is characterized by a random orientation of collagen fibers, with irregularly shaped vascular spaces and calcification occurring as irregularly distributed patches.

As time passes, woven bone is gradually replaced by organized lamellar bone, which is the form that constitutes most of the mature skeleton. Lamellar bone is made up of collagen fibers formed in highly organized sheets in which successive layers of fibers are oriented perpendicular to each other with little interfibrillar space, and calcification occurs in an orderly manner.

2.2.1 Osteoblast and Bone Formation

Osteoblast lineage cells originate from multipotent mesenchymal stem cells which are adjacent to all bone surfaces. Differentiation of osteoblast cells proceeds along an osteogenic pathway progressing from osteoprogenitors, preosteoblasts to fully mature osteoblasts and then to lining cells or osteocytes. This process is controlled and monitored by a cascade of events that involves a combination of genetic programming and gene regulation by various hormones, cytokines, growth factors and other soluble factors (Hughes et al., 2006). The osteoblasts are cuboidal or slightly elongated cells that are located at the bone surfaces undergoing remodeling. Their primary function is to lay down the extracellular matrix and regulate its mineralization. The osteoblast is a typical protein-producing cell which has an extremely well-developed rough endoplasmatic reticulum and a large circular Golgi complex. There are approximately 100-400 osteoblast cells per bone-forming site producing a highly organized organic extracellular matrix called the osteoid.

The osteoblast has a lifespan of around one month, during which it lays down 0.5-1.5 m^3 osteoid per day (Sommerfeldt and Rubin, 2001). During the remodeling process some osteoblasts may become "trapped" in the newly formed matrix, after which they are then converted into osteocytes, whereas others remain on the bone surface as bone lining cells or undergo apoptosis. The inorganic component of the bone consists primarily of calcium phosphate, with small quantities of magnesium, fluoride and sodium. Bone mineral is often referred as hydroxyapatite. It is four times smaller than any naturally occurring apatites and less perfect in structure, being more reactive and soluble which facilitates chemical turnover.

2.2.2 Osteoclast and Bone Resorption

The osteoclast cells are formed by the attraction of hemopoietic myelomonocytic precursors to the resorption site, followed by their fusion, and attachment of the subsequent multinucleated cell to the bone surface (Sims and Gooi, 2008). The interaction between receptor activator of nuclear factor-kappaB (RANK) and RANK ligand (RANKL) is the pathway used by the osteoblasts to control bone resorption. Osteoblasts produce RANKL, a cytokine of the tumour necrosis factor (TNF) family. RANK (the receptor) resides on the cell surface of osteoclasts and pre-osteoclasts. RANK-RANKL binding stimulates the formation, activation and maturation of osteoclasts. The catabolic effects of RANKL are opposed by osteoprotegrin (OPG), which is also a member of the TNF family that acts as a decoy receptor for RANKL, thus inhibiting RANK-RANKL binding (Villiers and Tobias, 2009).

The osteoblast lineage is responsible for the production of OPG which is a very effective inhibitor of osteoclast formation that acts locally as a "brake" on osteoclast formation (Sims and Gooi, 2008). The relative balance between RANKL and OPG is a major determinant of osteoclast activity (Villiers and Tobias, 2009). While RANKL is membrane bound and acts to promote osteoclast precursor fusion, it is CSF-1 that is secreted by osteoblasts that promotes osteoclast precursor proliferation as well as promoting RANK expression by these precursors.

The differentiation of osteoclasts can be controlled by osteoblasts which can limit the movement of osteoclast precursors towards each other (allowing fusion) and to the bone surface (allowing attachment) through the release of chemoattractants (Sims and Gooi, 2008). Chemo-attractants acting on monocytic osteoclast precursors include osteocalcin, α_2 HS-glycoprotein (fetuin-A) and collagen-I fragments (Malone JD, 1982). For these matrix-associated proteins to act as chemo-attractants, it is possible that they are released by resorbing osteoclasts during the early phase of resorption (demineralisation) and attract further precursors to continue resorption of the bone surface. Recent studies on bone ageing shows that when collagen-I is isomerized, and aged bone, which has a higher ratio of / collagen isomers compared to younger bovine bone, has been shown to support the formation of many more osteoclasts from human osteoclast precursors which would suggest a supporting role for matrix constituents in the control of osteoclast formation (Henriksen K, 2007). The bone resorption process involves the osteoclast bone cell, which originates from hematopoietic stem cells that undergo proliferation and differentiation into preosteoclasts and osteoclasts.

Osteoclasts are highly migratory, multinucleated and polarized cells that present abundance of Golgi complexes, mitochondria and transport vesicles loaded with lysosomal enzymes. The most prominent feature of the osteoclast is the presence of deep folding of the plasma membrane in the area facing the bone matrix, the ruffled border that is surrounded by a ring of contractile proteins (actin, vinculin and talin) serving to attach the cell to the bone surface and sealing off the resorbing compartment. Protons and lytic enzymes are secreted across the ruffled border to the resorbing compartment. The low pH level (between 2 and 4) allows for the dissolution of the mineral while exposing the organic matrix. Subsequently, a variety of enzymes (including tartrate-resistant acid phosphatase, TRAP), at low pH, degrades the matrix components. The resultant residues are either internalized or transported by transcytosis and released at the basolateral membrane. An activated osteoclast is able to resorb 200,000 m^3 per day, an average amount of bone formed by seven to ten generations of osteoblasts with an average lifespan of 15-20 days (Sommerfeldt and Rubin, 2001).

2.2.3 The Bone Remodelling Process

The production of RANKL by osteoblast-lineage cells is stimulated by microdamage within the bone matrix. These microdamage (microcracks) are small defects in the bone matrix that occurs in both pathological conditions and with normal skeletal loading. Studies conducted under experimental loading has shown to initiate bone remodelling and that resorption and replacement of the bone compromised by this damage is one of the important mechanical functions of bone remodeling (Sims and Gooi, 2008). The microdamage within the bone is sensed by osteocytes, which are terminally differentiated osteoblasts that have been shown to sense changes in pressure within the matrix.

Bone is regarded as a dynamic tissue that is constantly being formed and resorbed in response to changes in mechanical loading, altered serum calcium levels and in response to a wide range of paracrine and endocrine factors. The bone remodelling process is co-ordinated by the actions of osteoblasts (cells that form bone), osteoclasts (cells that destroy bone) and osteocytes which exist within the bone matrix and osteoblast derived lining cells that cover the surface of the bone**.** The remodelling process begins with the initiation of forming osteoclast, osteoclast-mediated bone resorption, a reversal period, and an extended period of bone matrix formation mediated by osteoblasts, followed by mineralisation of the matrix. This continuous process of remodelling maintains normal skeletal size and bone strength, and provides a mechanism for the repair of damaged bone (Villiers and Tobias, 2009). These remodelling processes are commonly regarded as independent process, but in reality both resorption and formation are closely linked within discrete temporary anatomic structures, first described by Frost who later named these “basic multicellular units,” later abbreviated as BMU (Parfitt, 2002). Defects in this remodelling cycle can result in a range of metabolic and congenital bone diseases including osteoporosis and Paget’s disease of the bone.

2.2.4 The Bone Healing Process

Every injury sustained by the human body initiates a series of coordinated events that is directed towards restoring the injured tissue to as near normal as possible which can be defined as the healing process. Bone healing is considered as regeneration rather than repair since it restores the tissue to its original physical, mechanical and functional properties. The healing process is regulated by a complex interplay of systemic and local factors and occurs in three distinct but overlapping stages: the early inflammatory stage, the repair stage and the late remodeling stage (Kalfas, 2001, Hollinger and Wong, 1996). In addition, inflammatory cell activation at the orthopedic implant site may occur by the presence of bacteria. One type of inflammatory cell is the macrophages which migrates to the bone-implant interface and becomes activated soon following implantation. Macrophages clearly form the first line of defense against bacteria, viruses and foreign implanted materials. Therefore, it may be key to design a delivery system that can down regulate the macrophage activities so that wound healing can occur quickly and bone growth and mineral deposition by osteoblasts are promoted shortly thereafter (Webster et al., 2009).

The initial biological response is to stop the bleeding from ruptured vessels. A hematoma develops within the injury site during the first few hours and days and is accompanied by a typical inflammatory response. The hypoxic tissue environment stimulates the migration of inflammatory cells and fibroblasts to the injured zone, and the initial hematoma is replaced by granulation tissue. The establishment of the repair stage is initiated by the ingrowth of vascular tissue, which favours the migration of mesenchymal stem cells. Fibroblasts than begin to lay down a stroma that supports the vascular ingrowth, while osteoblastic cells secrete osteoid, which is subsequently mineralized by the formation of a callus around the repair site. In these early stages the immature bone consists of an array of collagen fibers and randomly oriented spicules of bone. The bone healing process is only complete during the remodelling phase in which various cellular molecular and functional regulators modify woven bone to organized lamellar bone, restoring the original shape, structures and mechanical strength.

The remodelling process is a slow process which can take over months or even years and is strongly influenced by local mechanical stress placed in the bone (Kalfas, 2001).

2.3 Biomaterials

The use of biomaterials in medicine is not a novel concept. As early as 2000 years ago, dental implants made of gold or iron were already been used [REF] . However, the practical use of implants in that era is not comparable to their present use. The increasing demand for safe and reliable implants has resulted in the evolution of biomaterials science as a distinct discipline. The importance of prostheses and implants in medicine is continuing to grow due to mankind's desire to increase life expectancy. This will require a growing number of synthetic devices to overcome the problems associated with deterioration of failing body parts. Implants are produced from biomaterials that share a common property: biocompatibility.

At the dawn of the 21st century, biomaterials are widely used throughout medicine, dentistry and biotechnology. Just 50 years ago biomaterials as we think of them today did not exist. The word "biomaterial" was not used. There were no medical device manufacturers, no formalized regulatory approval processes, no understanding of biocompatibility, and certainly no academic courses on biomaterials. Yet, crude biomaterials were used, generally with poor to mixed results, throughout history. Most implants prior to 1950 had a low probability of success because of a poor understanding of biocompatibility and sterilization. The first study assessing the *in viv*o bioreactivity of implant materials was performed by Levert in 1829 (Ratner et al., 2004).

The worldwide market for all types of biomaterials was estimated at over $5 billion USD in the late 1980s, but grew to about $25.5 billion in 2008 and is likely to exceed $252.7 billion by 2014. The rate of market growth has been estimated at about 12 to 20% per year. For the United States, the biomaterials market has been estimated at about $9 billion as of the year 2000, with a growth rate of about 20% per year. Approximately 3.6 million orthopedic operations are carried out per year in the United States, four out of the ten most frequently involving metallic implants. In Australia 2.2 million Australians are affected by osteoporosis with a total costs of $7.4 billion per year of which $1.9 billion are direct costs (Sambrook et al., 2002).

2.3.1 Classification of Biomaterials Based on Biological Interactions

Any material incorporated into a human needs to abide by defined properties that will assure that there are no side effects when interacting with living tissue. Biomaterials for bone repair or substitution are both organic (e.g. polymers) and inorganic (calcium phosphates, bioglass, calcium carbonates, calcium sulfates). Inorganic biomaterials are designed to replace a part or a function of the human body in a safe, reliable, economic, physiologically and aesthetically acceptable manner (Hench, 1982). Since biomaterials are inorganic structures they do not include renewable materials obtained from natural sources such as wood, plant fibres, hides, sinew, bone, ivory and others. One of the more important properties of biomaterials is their biocompatibility. This is not an individual property *per se*, but relates to the various interactions the material is subjected to at a cellular or tissue level, hence a systems approach is required (Williams, 1985). A modern view of biocompatibility often refers to the ability of a material to perform in the presence of an appropriate host response, for a specific application. Hence biocompatibility is neither a single event nor a single phenomenon but is meant to be a collection of processes involving different but interdependent interaction mechanisms between material and living tissue (Williams, 1990).

According to their biologic interaction, synthetic materials are classified as:

Bioresorbable materials - substances/material that are released but in non-toxic concentrations that may lead to only benign tissue reactions such as formation of a fibrous connective tissue capsule or weak immune reactions that cause formation of giant cells or phagocyte. These materials are often refered to as ***biotolerant*** and include austenitic stainless steels or bone cement consisting of polymethylmethacrylate (PMMA)

Bioinert materials do not release any toxic constituents but also do not show positive interaction with living tissue. The usual response of the body to these materials is the formation of a non-adherent capsule of connective tissue around the bioinert material. In such cases the bone remodelling manifests itself by a shape-mediated *contact osteogenesis*. Through the bone-materials interface only compressive forces will be transmitted ("bony on-growth"). Typical bioinert materials are titanium and its alloys, ceramics such as alumina, zirconia and titania, and some polymers, as well as carbon, see Table 1.2.

Bioactive materials demonstrate a positive interaction with living tissue that includes the differentiation of immature cells towards bone cells. In contrast to bioinert materials there is chemical bonding to the bone along the interface, thought to be triggered by the adsorption of bone growth-mediating proteins at the biomaterials surface. Hence there will be a biochemically-mediated strong *bonding osteogenesis*. In addition to compressive forces, to some degree tensile and shear forces can also be transmitted through the interface ("bony ingrowth"). Typical bioactive materials are calcium phosphates and bioglasses.

Bioactive materials such as calcium phosphate fulfill the requirements as a bone graft material: "to become an integral part of the organism".

2.3.2 Properties of Biomaterials

In order to function appropriately, biomaterials must possess properties that allow them to be used successfully for their intended applications. This is therefore influenced by their bulk properties and surface properties. The bulk and surface properties of biomaterials used for medical implants have been shown to directly influence, and in some cases, control the dynamic interactions that take place at the tissue-implant interface. Bulk properties determine the strength of an implant, whereas the surface properties are important with regard to the eventual interactions of an implant with the surrounding biological systems. Since the interaction of a synthetic device and biological system takes place at the biomaterial-tissue interface, it is evident that the surface properties of a biomaterial are pivotal for the regulation of implant integration.

Several factors determine the surface characteristics of a material, including composition, roughness, release of ions, charge, and energy. Obviously the interaction of biological constituents with the surface of a biomaterial device must not cause any detrimental effects to the surrounding viable cells, tissues, and organs. For that reason, the surface molecules of a biomaterial should not be toxic, carcinogenic, pyrogenic, cytotoxic, or antigenic to living cells in any way. For most applications, biomaterials are in contact with cells and tissues, often for prolonged periods. Thus, rational and sophisticated use of biomaterials and design of medical devices requires some knowledge of the general concepts concerning the interaction of cells with nonphysiological surfaces. Cell interactions with the external environment are mediated by receptors in the cell membrane, which interact with proteins and other ligands that adsorb to the material surface from the surrounding plasma and other fluids (Lauffenburger D.A., 2001). Cell adhesion triggers multiple functional biochemical signaling pathways within the cell. Most tissue-derived cells require attachment to a solid surface for viability, growth, migration, and differentiation. The nature of that attachment is an important regulator of those functions.

Moreover, the behavior and function of adherent cells depend on the characteristics of the substrate, particularly its adhesiveness. Following contact with tissue or blood, the surface of a biomaterials becomes rapidly coated with proteins that are adsorbed from the surrounding body fluids.

The chemistry of the underlying substrate controls the nature of the adherent protein layer. Moreover, although cells are able to adhere, spread, and grow on bare biomaterials surfaces *in-vitro*, proteins absorbed from the adjacent tissue environment or blood and /or secreted by the adherent cells themselves markedly enhance cell attachment, migration, and growth. Cell adhesion to biomaterials is mediated by cytoskeletal associated receptors in the cell membrane, which interact with cell adhesion proteins that adsorb to the material surface from the surrounding plasma and other fluids. Fixation of an implant in the human body is a dynamic process that remodels the interface zone between the implant and living tissue at all dimensional levels from the molecular up to the cell and tissue morphology level and at all time scales from the first second up to several years after implantation (Kasemo, 1991).

Besides the surface irregularities as mentioned earlier, porosity can also be considered as surface irregularity. Porosity can occur only at the substrate surface or can completely penetrate throughout a bulk material. It consists of individual openings and aspacings or interconnecting pores. Porosity can be created intentially by a specific production process, such as sintering of beads, leaching of salt, sugar or starch crystals, or knitting and weaving of fibers. For many biomedical applications, there is a need for porous implant materials. They can be used for artificial blood vessels, artificial skin, drug delivery, bone and cartilage reconstruction, periodontal repair, and tissue engineering (Lanza RP., 1997). Promoting bone ingrowth the optimum pore size is in the range of 75-250 μm (Pilliar, 1987). On the other hand , for ingrowth of fibrocartilagenous tissue the recommended pore size ranges from 200 to 300 μm (Elema et al., 1990). Besides pore size, other parameters play a role, such as compressibility, pore interconnectivity, pore interconnecting throat size, and degradability of the porous

material (de Groot et al., 1990). The mechanism behind the use of virtually inert microporous materials is the ingrowth of tissue into pores on the surface or throughout the implant (Ohgushi et al., 1992). The increased interfacial area between the implant and the tissues results in an increased resistance to movement of the device in the tissue. The interface is established by the living tissue in the pores. Consequently, this method of attachment is often termed "biological fixation". It is capable of withstanding more complex stress states than "morphological fixation." The limitation with porous implants, however is that in order for the tissue to remain viable and healthy, it is necessary for the pores to be greater than 50 to 150 μm. The large interfacial area required for the porosity is due to the need to provide a blood supply to the ingrown connective tissue. Also, if micro-movement occurs at the interface of a porous implant and tissue is damaged, the blood supply may be cut off, the tissues will die, inflammation will ensue, and the interfacial stability will be destroyed.

2.4 Bone Substitute Materials

Bone substitute materials can be categorized as osteoconductive, osteoinductive and osteogenic (Frayssinet et al., 1998). Osteoconductive materials are designed to provide a framework which guides the bone healing tissue. There is direct contact between the bone with the material but without any interposition of cells or tissue. Examples of osteoconductive materials consist of hydroxyapatite and/or beta tricalcium phosphate (β-TCP). Osteoinductive materials on the other hand acts on the differentiation of the nearby cells by inducing phenotypic evolution of multipotent stem cells or mesenchymal cells towards osteogenic phenotypes. Osteoinductive material can induce bone formation regardless of the environment and in addition it can induce ectopic bone formation. The implantation of a bone substitute following surgical intervention always takes place at a bone healing site. This leads to a series of histologic reactions which characterise the bone healing process (Frayssinet et al., 1998).

These reactions may be observed in the following four stages after the site has become stabilised: *1) inflammatory stage; 2) fibrous callus stage; 3) bony callus stage; 4) remodeling stage.*

Regardless of what material is used as the bone substitute, upon implantation into the bone tissue this elicits an onslaught of monocytes and macrophages from the first stage onwards while becoming fixed to the material surface. These cells will try to phagocytose the material or the debris released from it, depending on the property of the material. Particles less than 50pm in size are usually phagocytosed while larger particles are surrounded by groups of macrophages and giant cells. Bioactive materials do induce these tissue, cellular and molecular reactions, however the degree of inflammation is lower, and for a shorter period of time compared with non-biocompatible materials. The healing process is characterized by the differentiation of osteoblasts from fibroblasts present in the connective tissue which has replaced the hematoma. Most of the osteoblasts differentiate in close proximity to the ceramic and are apparently immobilised at the material surface as they are at the surface of the bone trabeculae.

2.4.1 Calcium Phosphate

The primary objective in bone tissue engineering is to mimic native bone tissue, and the first challenge lies in the selection of a bulk biomaterial. The bulk material composition determines the overall success of the scaffold material. The use of some calcium phosphate materials for bone substitution, augmentation and repair has gained clinical acceptance in many areas of orthopaedics and dentistry. These materials have consistently demonstrated excellent cellular and tissue responses both *in vitro* and *in vivo*. Calcium phosphate ceramics are synthetic scaffolds that have been employed in orthopedics since the 1980s (LeGeros, 1988). Different composition of calcium phosphates differ in their crystallographic structure and therefore in internal bonding strength which is reflected in their stability and solubility or dissolution properties (LeGeros, 1993).

Calcium phosphate materials of identical composition but different crystallographic structure (e.g. α-TCP versus β-TCP) vary considerably in their dissolution properties *in vitro* and are also expected to vary in the extent of their biodegradation. The order of relative solubility of some Ca-P compounds are as follows:

Tetracalcium Phosphate ($Ca_4P_2O_9$) > Amorphous calcium Phosphate > alpha-Tricalcium Phosphate ($Ca_3(PO_4)_2$) > beta-Tricalcium Phosphate ($Ca_3(PO_4)$ 2) >> Hydroxyapatite ($Ca_{10}(PO_4)_6(OH)_2$) (LeGeros, 1993)

Biodegradation/bioresorption of the material is assumed also to be related to solubility of the Ca-P materials,24'45' 87,99~101,132,161,185 which in turn is, related to the bioactivity, and ultimately to the bone formation of the bone/material interface. Factors affecting biodegradation/bioresorption are both materially and environmentally related concerning the properties of the calcium phosphate materials themselves and those of the biological environment. The most common types of calcium phosphate materials investigated for synthetic bone scaffold development are: hydroxyapatite (HAp), $Ca_{10}(PO_4)_6(OH)_2$, tricalcium phosphate (TCP), $Ca_3(PO_4)_2$ and biphasic calcium phosphates (BCP).
A detailed explanation on the chemical and physical interactions of hydroxyapatite and tricalcium phosphate materials with bone cells and tissue is provided below.

2.4.2 Hydroxyapatite

Hydroxyapatite (HA) is the most commonly used polycrystalline calcium phosphate ceramic mineral as an artificial bone graft substitute. Mature bone consists of 60–70 % calcium phosphates of its dry weight. Hydroxyapatite is the main element in the mineral bony substance of the vertebrate's skeleton, where the organic matrix is embedded. Unlike the other calcium phosphates, hydroxyapatite takes a longer period of time to break down under physiological conditions.

In fact, it is thermodynamically stable at physiological pH and actively takes part in bone bonding, forming strong chemical bonds with surrounding bone. This property has been exploited for rapid bone repair after major trauma or surgery. While its mechanical properties have been found to be unsuitable for load-bearing applications such as orthopaedics, it is used as a coating on materials such as titanium and titanium alloys, where it can contribute its 'bioactive' properties, while the metallic component bears the load.

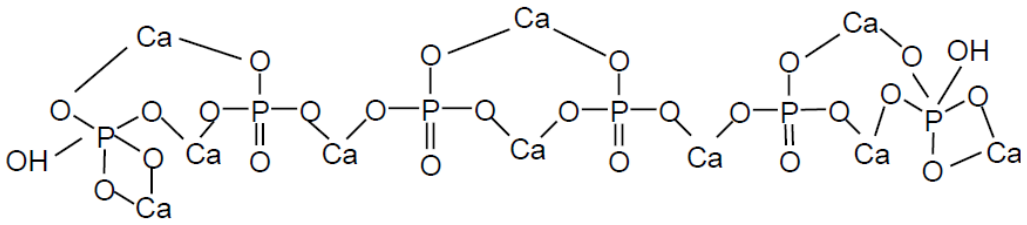

Figure 2.1 Chemical structure of hydroxyapatite, $Ca_{10}(PO_4)_6(OH)_2$

Hydroxyapatite, either as porous or dense implants or in a granular form, has shown to become directly bonded to the surrounding bone once implanted. Direct bonding refers to lack of local inflammatory, foreign-body or local toxicity reactions. This type of direct bonding is refer to as “chemical bonding”, “bone-bonding” or “natural bone cementing” mechanism (Jarcho, 1981). This is applicable to all calcium phosphate implant materials. Ion exchange is part of the solid-solution equilibrium which ultimately calcifies forming mineral crystals depositing on the surface of the hydroxyapatite (Jarcho, 1977). This is supported by the findings that Ca:P ratio measured with the electron probe microanalysis technique around the implants increases during six months from 1.50 to about 1.67 with the latter corresponding to those found in the normal bone mineral around the implant. According to all findings detected in the zone of bone bonding, the bonding zone appears to be similar to the acellular bone matrix derived from differentiating osteoblasts. Another electron microscopic study revealed a direct chemical bonding between bone and the hydroxyapatite without any unmineralized tissue layer at the interface (Tracy and Doremus, 1984).

From all these interface studies on hydroxyapatite it can be concluded that the body does not consider hydroxyapatite to be a foreign material but rather a normal bone component due to its chemical resemblance to natural bone and consequently, bone grows directly onto the surface of hydroxyapatite.

2.4.3 Beta-Tricalcium Phosphate (β-TCP)

Tricalcium phosphate (TCP) ceramics are particularly attractive candidates for applications such as temporary implants in the human body to fill parts of bones. Tricalcium phosphates has been studied extensively either alone or in its different forms of composites with hydroxyapatite (Nasca RJ., 1989, Shima T., 1979, Steffen T., 2000). Tricalcium phosphate is available in two crystallographically different forms, alpha tricalcium phosphate (α-TCP) and beta tricalcium phosphate (β-TCP). TCP possesses many favourable properties such as biocompatibility with bone tissue; bioactivity, and significant biodegradation behaviour. The solubility and bioresorption of different TCPs are dependent on the possible incorporation of foreign ions (i.e. fluoride and magnesium) and on the size of the particle crystals. The smaller the particle size, the greater the solubility. α-TCP has not been used as bone substitute due to its fast solubility rate (Bohner M., 2001). Due to the bioresorption characteristics of tricalcium phoshphates, it provides a positive influence on the local tissue interactions for a short period to generate an optimal interface and tissue ingrowth for long-term function (Jarcho, 1981).

Beta-tricalcium phosphate (β-TCP), which possesses stoichiometry similar to amorphous biologic precursors to bone mineral, is one of the most attractive biomaterials for bone repair because it shows excellent biological compatibility, osteoinductivity, and safety in living tissues which has a Ca-to-P molar ratio of 1.5. The crystal structure of β-TCP is very closely related to that of a natural mineral, whitlockite, which contains small amounts of Fe, Mn, Mg, and H. It has been discerned that new regenerating bone from skeletal margins surrounding a ceramic implant grows into the pores of the ceramic in centripetal fashion.

The rate of β-TCP bioresorption is typically in the range of 1-2 years (Bohner M., 2001). It has been learned that if TCP degrades too rapidly fibrous union takes place across the opening without osseous repair.

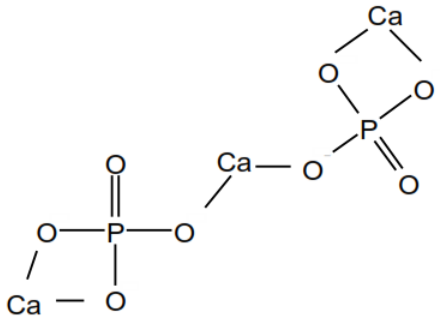

Figure 2.2 Chemical structure of tricalciumphosphate, $Ca_3(PO_4)_2$

2.5 Biomimetics

Engineers, scientists, and business people are increasingly turning toward nature for design inspiration. The field of biomimetics, the application of methods and systems, found in nature, to engineering and technology, has spawned a number of innovations far superior to what the human mind alone could have devised. The reason is simple. Nature, through billions of years of trial and error, has produced effective solutions to innumerable complex real-world problems. The rigorous competition of natural selection means waste and efficiency are not tolerated in natural systems, unlike many of the technologies devised by humans. The concept of biomimetics has been explored by several authors under different perspectives.

Based on this concept, Kokubo and Takadama, (2006) developed a technique for coating different organic, inorganic and metallic materials, with bioactive layers, which has been designated as biomimetic coating. The main aim of this biomimetic process is to mimic the biomineralization, leading to the formation of a bone-like carbonated apatite layer on the surface of a substrate. The methodology has been claimed to be very useful for producing highly bioactive and biocompatible composites with different mechanical properties.

Nature makes economic use of materials by optimising the design of the entire structure or system to meet multiple needs and to create a bewildering variety of life forms. Natural materials are mostly constituted from organic, inorganic crystals and amorphous phases. The organic phase generally occupies a very small fraction of the total volume and has functions ranging from toughening the tissue to synthesising highly functional minerals. The inorganic components can be single crystals or aggregates of them arranged in wellordered arrays to give a hierarchy of length scales. The interfaces between the soft organic matter and the relatively hard inorganic material is of paramount importance in determining the properties of the composite and nature has devised strategies for assuring integrity of the interfaces under demanding conditions of stress. Natural materials are self-generating, hierarchical, multifunctional, nonlinear, composite, adaptive, self-repairing and biodegradable.

Biomimetics is the field of scientific endeavour, which attempts to design systems and synthesise materials through biomimicry. *Bio* meaning life and *mimesis* meaning imitation are derived from Greek. Biomedical engineers consider biomimetics as a means of conducting tissue engineering and trace the origins of biomimetics to ancient times when Mayan, Roman and Chinese civilizations had learnt to use dental implants made of natural materials. Material scientists view biomimetics as a tool for learning to synthesise materials under ambient conditions and with least pollution to the environment. Biologists study biomimetics not only for an understanding of the biological processes but also to trace the evolution of various classes of organisms.

Overall, the field of biomimetics addresses more than one issue. Those engaged in this field of research activity try to mimic natural methods of manufacture of chemicals in order to create new ones, learn new principles from phenomena observed in nature, reproduce mechanisms found in nature and copy the principles of synthesizing materials under ambient conditions and with easily available raw materials.

2.5.1 Natural Coral

While synthetic materials are widely used in the biomedical field with great success, natural structural materials are recently starting to surpass this by providing an abundant source of novel biomedical applications. Natural bioceramics such as corals are known to be designed through natural optimization methods to physically support and maintain a range of tissues for a variety of functions. During the last decade, there has been an increasing understanding of biomineralization which has initiated improvements in biomimetic synthesis methods and leading to the production of new generation biomaterials (Ben-Nissan B., 2003). Coral mineral (aragonite or calcite forms of calcium carbonate) has had considerable success due to its porous structure (ranging from 150 to 500 μm) is similar to cancellous bone and is one of a limited number of materials that will form chemical bonds with bone and soft tissues *in-vivo*. Corals obtained from the sea is first cleansed from all organic material and then sterilized and manufactured as blocks and in granular form. The calcium carbonate skeletal structure of the coral is preserved, making it highly resorbable. The resorption process is from observing osteoclasts histologically in contact with coral. The enzymatic process via carbonic anhydrate dissolves the carbonate coral skeleton. Guillemin and colleagues (Guillemin et al., 1987) have demonstrated (a) initial invasion of the coral structure by bone marrow elements accompanied by blood vessels, followed by (b) osteoclastic resorption and (c) osteoblastic bone formation. It was also noted that there was a gradual transformation of the crystalline structure of aragonite to poorly crystallized apatite.

These properties of biocompatibility, resorbability and substitution by the host bone have made natural coral a biomaterial useful for bone filling applications (Guillemin et al., 1993).

2.5.2 Coralline Materials

The term natural coral is to be distinguished from coralline materials in which calcium carbonate is converted to calcium phosphate through a replacement process. Coralline apatites can be derived from sea coral. As coral is a naturally occurring structure, it has optimal strength and structural characteristics. The pore structure of coralline calcium phosphate produced by certain species is similar to human cancellous bone, making it a suitable material for bone substitute applications. Coral and converted coralline hydroxyapatite have been used as bone grafts and orbitals implants since the 1980s. This is because the porous nature of the structure allows ingrowths of blood vessels to supply blood for bone, which eventually infiltrates the implant. Size and interconnectivity of pores are of utmost importance when hard and soft tissue ingrowths are required. Bone pore sizes range from 200 to 400 μm in trabecular bone and 1 to 100 um in normal cortical bone and the pores are interconnected. Kuhne et al. (1994) showed that implants with an average pore size of around 260 μm had the most successful ingrowths as compared to no implants (that is, simply leaving the segment empty). It was further reported that interaction of the primary osteons between the pores via the interconnections allows propagation of osteoblasts. It was reported that complete replacement of aragonite ($CaCO_3$) by phosphatic material was achieved using less than 533K and 103 MPa. During the hydrothermal conversion treatment, hydroxyapatite replaces the aragonite whilst preserving the porous structure. The following exchange takes place:

$$10CaCO_3 + 6(NH_4)_2HPO_4 + 2H_2O \rightarrow Ca_{10}(PO_4)_6(OH)_2 + 6(NH_4)_2CO_3 + 4H_2CO_3$$

The resulting material is known as coralline hydroxyapatite, be it in the porous coralline structure or in powdered form.

2.5.3 Kokubo's Simulated Body Fluids

The development of bone-bonding materials with different chemical and biological characteristics with adequate mechanical properties is desired. This desire leads to two questions: what type of material bonds to living bone; and are animal experiments the only one way to test for bone bonding, that is, to identify a material with *in-vivo* bone bioactivity. In the last three decades, a large number of investigators have proposed that the essential requirement for an artificial material to bond to living bone is the formation of bonelike apatite on its surface when implanted in the living body. In 1991 Kokubo (Kokubo et al., 1990) proposed that *in-vivo* apatite formation on the surfaces of many biomedical materials can be reproduced in Kokubo's simulated body fluid (SBF) with ion concentrations nearly equal to those of human blood plasma. In essence this means that the *in vivo* bone bioactivity of a material can be predicted from the apatite formation on its surface in SBF (Kokubo and Takadama, 2006).

Hydroxyapatite layers can be easily produced on various organic and inorganic substrates when submerged in Kokubo's simulated body fluid. In 1989, Kokubo and co-worker showed that after immersion in SBF, a wide range of biomaterial surfaces initiated very fine crystallites of carbonate ion-containing apatite, and since then a large number of work shows that osteoblasts can proliferate and differentiate on this apatite layer. Since then, SBF have been produced in order to provide insight into the reactivity of the inorganic component of blood plasma, and predict the bioactivity of implants, bone scaffolds, as well as other novel biomaterials. On the other hand, SBF also has been used to prepare bioactive composites by forming hydroxyapatite on various types of substrates. Simulated body fluid solutions in close resemblance to the Hanks balanced salt solution (HBSS) (Hench and West, 1990), are prepared with the aim of simulating the ion concentrations present in the human plasma. To mimic human plasma, SBF solutions are prepared to have relatively low calcium and phosphate ion concentrations, namely, 2.5 and 1.0 mM, respectively.

Furthermore, to mimic human plasma, the pH value of SBF solutions is adjusted to the physiological value of 7.4 by using organic buffers, such as Tris or Hepes. These compounds are not present in human plasma (Kokubo and Takadama, 2006).

SBF has ionic concentrations of 142.0 mM Na^+, 5.0mM K^+, 1.5mM Mg^{2+}, 2.5mM Ca^{2+}, 147.8mM Cl^-, 4.2mM HCO^{3-}, 1.0mM HPO_4^{2-} and 0.5mM SO_4^{2-} and a pH of 7.40, nearly equal to those in human blood plasma at 36.5ºC. The SBF usually is prepared by dissolving reagent-grade chemicals of NaCl, $NaHCO_3$, KCl, $K_2HPO_4 \cdot 3H_2O$, $MgCl_2 \cdot 6H_2O$, $CaCl_2$ and Na_2SO_4 into distilled water and buffering at pH 7.40 with tris (hydroxymethyl) aminomethane ($(CH_2OH)_3CNH_3$) and 1.0M hydrochloric acid at 36.5ºC.

2.6 Drug Delivery Systems

As the life expectancy in developed countries continue to increase, this has led to a serious rise in the number of musculoskeletal disorders, such as osteoporosis and osteoarthritis. The number of medications to prevent and treat these diseases has also expanded in recent times due to scientific advancements. The development of new drugs and active substances, allows treating some of these diseases even in their initial stages. Drug delivery systems are different from conventional drug dosage forms (pills, tablets, ointments, creams, injectables) in that they reside in the body at a particular location for a prolonged period of time to achieve their purpose continuously over that period of time. The pattern of the drug release may be constant, oscillating, declining continuously, or even pulsating periodically. The feature of a drug delivery system is that the pattern is at least a qualitative design feature of the system.

The key issue that has been explored in recent times with regards to these treatments is the ability to maximize the drug access to specific bone sites, and most importantly to be able to control the release of the drugs, in order to maintain a desired drug concentration level for long periods of time without reaching a

toxic level or dropping below the minimum effective level. For these reasons, major efforts have been made, focussing on the development of biodegradable materials that are capable of releasing drugs with reproducible and predictable kinetics (Ginebra et al., 2006, Williams, 1990). For bone repair surgery, biphasic calcium phosphate bone substitutes derived from hydroxyapatite and β tricalcium phosphate (β-TCP) are the most promising materials for bone drug delivery systems. This type of drug delivery system is able to release a therapeutic agent in situ to produce an action promoting the osteoconductivity of the material (Rao, 2002). During the last decade major attention has been paid to antibiotics due to their wide areas of application as prevention against infection during surgical interventions or in general in the treatment of bone infections. Other drugs such as anti-inflammatory or substances stimulating bone regeneration has been a prime focus in recent years.

2.6.1 Characteristics of Drug Delivery Systems

The local response to a drug delivery system may be complicated by the presence of an increased level of the drug in the tissues. While the drug concentration in the carrier is high, the local tissues are protected from exposure to pure drug by the membrane. Notwithstanding this, the drug must move from the external surface of the carrier to the tissue across a concentration gradient indicated in Figure 2.3 as the difference (C_i- C_{px}), where C_i is the concentration of the drug at the external surface of the carrier and C_{px} is the drug concentration required in the tissue for therapeutic effect. To avoid any local toxic response occurring due to the high concentration of the drug at the surface of the carrier, the focus is to design a system that ensures that most of the change in concentration occurs within the carrier. This type of system is called “controlled drug delivery systems” because the rate of drug release is controlled by mechanisms within the delivery system, independent of the conditions in the surrounding tissue. The characteristic of controlled delivery not only reduces the probability of local toxic tissue response but also results in a predictable performance of both the rate of release of the drug and the duration of the therapy that can be achieved with such systems.

The material selected for the incorporation of drug must not only provide the intended mode of operation but also be biocompatible and compatible with the many constraints imposed during manufacturing (Buckels, 1977, Buckles, 1983).

2.6.2 Problems Associated with Current Drug Carriers

As mentioned previously wound contamination, or postoperative infections following fracture repair, implantation of joint prosthesis or spine surgery, can cause serious problems. For these reasons, antibiotics are often provided as prophylactics, either orally or intravenously. However, limited accessibility to the site of infection often prolongs the treatment of bone infections. A common method used in controlling bone infections is implanting poly-methylmethacrylate spheres (PMMA) loaded with gentamicin sulphate to the infected site. However, PMMA spheres are not biodegradable and must be removed after certain periods of time to be replaced with new spheres or other substitute material. Moreover, it is difficult to shape ceramics with complex form in order to be fitted into any type and size of bone defect (Ginebra et al., 2006). The treatment of bone infection remains difficult because of problems with local penetration of systemically administered antibiotics. Furthermore, bacteria adhere to bone matrix and orthopaedic implants, eluding host defenses and antibiotics by developing a slimy film or acquiring a very slow metabolic rate (Baro et al., 2002). Effective treatment against infection may be possible by killing the bacteria during the early stages of colonization and the continuous delivery of antibiotics. Surgical placement of polymethylmethacrylate (PMMA) spheres at the site of infection, which then release antibiotic for approximately 6 weeks, has been the method of choice for the past decade. Although this system functions effectively in terms of antibiotic delivery and eradication of infection, because of their non-biodegradable nature, the spheres must be removed once the vascularity of the region has returned to normal, a process that could be avoided if a biodegradable drug delivery system was used (Rossi S, 2004).

One of the most common infections to occur during post-operations is infections like osteomyelitis which remains a considerable problem in orthopaedic surgery (Laurent F, 2008). The main reason for this is the poor accessibility of the infected bone site by systematic administration of antibiotics (Tadic et al., 2004). For infected prostheses, often it requires the complete removal of the implant which can lead to severe functional disability and be costly in terms of quality of life. Systemic antibiotics should be administrated in high concentrations for prolonged periods of time. However such high concentrations of drugs in the blood may induce toxicity. Systemic antibiotic administration does not always allow for efficient concentrations, mainly because of poor blood flow to the bone tissue (Meseguer-Olmo et al., 2002). Furthermore, for prolong treatments, antibiotic-resistant microbial strains can emerge because of selective pressure induced by antibiotics. Such resistant-strains are a major problem in the hospitals where antibiotics are widely used (Laurent F, 2008).

2.6.3 Parameters Defining Drug Release Kinetics

The rate at which drug is released from any type of drug delivery system is dependent on various factors such as the microstructure, the solubility of the drug, the type of bond between the drug and the matrix of the carrier, and the mechanism of degradation (if any) of the carrier. In the initial stages (until approximately 60% drug released) the drug release kinetics follows Higuchi's law (Higuchi, 1963). Generally the porosity and other microstructural parameters of the carrier plays a vital part in the drug release kinetics. In the case when the drug is poorly soluble, the release kinetics do not follow the Higuchi law, since it would be controlled by the dissolution of the drug, the release being proportional to the time. In cases where porosity does not remain constant, drug release kinetics also does not follow Higuchi's law and the drug diffusion through the carrier's matrix is no longer the only mechanism which controls the drug release. As previously mentioned, Higuchi's law is valid for the initial stage of drug release (the mass of the drug release is proportional to the $\sqrt{t}$.

Another model by Tung (1995), during the second stage, the release of the drug is proportional to the time, followed by a third stage at which the liberation is stabilized as the concentration of the antibiotic in the environment increase. With this particular model, the existence of the second stage would solely depend on the type of antibiotic being incorporated and its solubility. The release kinetic of the second stage can be explained by a low solubility of the drug and hence a dissolution-controlled release, proportional to the time.

2.6.4 Current Trends in Biomimetics

Even though the field of biomimetics is still in its infancy some tangible applications are on the horizon. The British biotechnology company Zeneca, a subsidiary of ICI, manufactures a biodegradable polymer Biopol which is produced by the bacterium A*lcaligenes eutrophus*. The polymer, which is similar to polypropylene, is used to produce moulded items such as bottles and has also been used in the controlled release of drugs. The young discipline of biomimetics has already proved that it is capable of contributing to sustainable technologies. If the characteristic features of natural synthesis such as energy and raw material consumption efficiency, use of readily available materials, multifunctionality etc., are further copied and developed synthetically, we shall see a change in manufacturing strategies and greater movement towards sustainable development.

Although the nanoscale modeling of synthetically manufactured hybrids and composites is still in its early stages, mimicking natural microstructures while using strong synthetic molecules may lead to a new generation of biomaterials, whose physical characteristics will be comparable with the materials available in nature. A formidable challenge remains regarding the optimization of the morphology and bioactivity in these novel hybrid composites.

2.7 Concluding Remarks

Due to limitation with current bone grafts for the treatment of critical-sized defects in bone have motivated this dynamic field of bone tissue engineering. The focus is the design of synthetic biodegradable replacements for bone. Various technologies and strategies reviewed have shown progressive development of synthetic components capable of mimicking the physiochemical attributes of bone. However, no single tissue engineering scaffold to date has demonstrated the ability to meet the comprehensive requirements that is needed to overcome the current challenges. The scaffold discussed herein demonstrates several obstacles that have already been overcome. Arguably, an elegant union of solutions to each of those individual challenges will likely result in the most positive patient outcomes. In the near term, such technological unions are unlikely to be able to match the close spatial and temporal control over the bone environment that has been observed in healthy bone. The best strategies to developing bone scaffolds will be to incorporate cross-functional interdisciplinary approaches aimed at enhancing key events rather than exerting start-to-finish control over the bone development process.

3 PHYSICO-CHEMICAL CHARACTERISATION OF CORAL AND CORALLINE MICROSPHERES

3.1 Characterization of Coral Microspheres

3.1.1 Introduction

The first step in a complex series of biophysical/biochemical processes related to the interaction of an implanted material with host biological tissue consists of the spontaneous formation of a proteinaceous layer absorbed onto the implanted materials (LeGeros and Daculsi, 1990). Therefore, the surface properties are crucial for successful biomaterial biocompatibility and must be considered in their selection for biomedical applications. Chemical composition, structural characteristics, impurities amongst many others are well known parameters that influence the complex process of biomaterials, and their subsequent influence on the attachment and spreading of cells that ultimately determine the success or failure of the implant during service.

This chapter examines and discusses the characterization of the coral and coral sand microspheres for the compositional and structural characteristics and properties using a range of analytical techniques. As stated earlier coral sand is the commercial name of *Foraminefera* materials and for simplicity oral sand rather than species name is used throughout the thesis.

3.1.2 Equipment and Procedures

Material processing - Natural coral sand grains were washed in bleach and in distilled water in a sonicator (Transtek System's Soniclean) to remove any salt and residues from the ocean. The samples were then fired to 300°C for 24 hours to remove any organics. Coral sands exist in nature as calcium carbonate and as such extensive chemical analysis into the morphological and both physical and chemical properties of the coral sands are required. In the past four decades various characterization techniques have been developed to reveal the structure of materials, such as scanning electron microscopy. Scanning electron microscopy (SEM) is useful for the direct observations of surfaces because it offers better

resolution and depth of field than optical microscopy and allows direct observation of variability of mineral densities and mineral-to-organic ratios in calcified tissues, such as bone and dentine. Combined with the energy dispersive spectrometer detector, analysis can be performed to investigate the qualitative chemical analysis of the specimen. A Philips (FEI) XL 30 ESEM was used for surface characterization. The microscope was operated in low vacuum mode at 0.8 Torr, 25kV accelerating voltage and a working distance of 10mm, using the back scattered electron detector (BSE) and gaseous secondary electron detector (GSE). An EDAX energy dispersive spectrometer (EDS) mounted on the XL30 ESEM was used to determine the elements within the sample.

It is important to note that changes in the Ca:P ratio (and hence phase composition) have been demonstrated to have a profound effect on the biological response (LeGeros R.Z., 2001) they elicit *in-vivo*, therefore it is important to analyze the phase composition of the coral microspheres before and after the hydrothermal conversion. Phase transformations and interstitial and/or substitution of trace elements of the coral spheres were examined by X-ray diffraction (XRD) and fourier transform infrared spectroscopy (FTIR) which are both well recognized in the characterization of both calcium carbonate and calcium phosphate materials.

X-ray diffraction (XRD) has emerged as an excellent tool for crystallographic characterization of bioceramic materials. The results are matched with international JSPD standards. Fourier transform infrared spectroscopy (FTIR) was used to characterize the organic and mineral phases present and revealed the presence of absorptions characteristic to that of calcium carbonate and calcium phosphate. X-ray diffraction analysis was performed in Siemens D5000 using CuKα of 1.54A, with 2θ ranging from 15 to 60, and compared with International Centre for Diffraction Data (ICDD) Joint Committee on Powder Diffraction Standards (JCPDS) database records. The samples were prepared by crushing approximately 1.5 – 2.0 g of the coral sample in a mortar and pestle.

Differential thermal analysis and thermal gravimetric analysis (DTA/TGA) were used to examine the decomposition of calcium carbonate from the coral sand. The differential thermal analysis and thermogravimetry analysis (DTA/TGA) instrument is used to study the decomposition and reaction of the coral sand during melting thus determining the transition temperatures. DTA/TGA is a powerful thermoanalytical technique that identifies the temperature regions and any critical events during a firing process. TGA measures the weight loss of the coral sand from the process of structural water release and carbonate decomposition. Thermogravimetric and differential thermal analysis (TGA/DTA) were performed on a TA Instruments SDT 2960 at 10°C/min.

FTIR analysis - A Nicolet 760 Fourier-Transform Infra Red spectroscopy (FTIR) with diffuse-reflectance accessory, were scanned 120 times between 400cm^{-1} to 4000cm^{-1} with the subtraction of KBr background. Samples were prepared by grinding with KBr in a mortar and pestle.

Chemical analysis - Inductively coupled plasma mass spectrometry (ICP-MS) was performed on the Agilent 7500ce to identify and quantify trace elements. 0.2g of the coral was heated in a 100°C furnace for 14 hours and into a 10mL vial pre-cleansed with 1% nitric acid. 5mL of 64% nitric acid was added into the vial than immediately filled up to the 10mL line with distilled water. The vial was than shook until the coral was dissolved and left for an additional 2 hours. The solution in the vial was then analyzed for trace elements.

3.1.3 Results and Discussions

3.1.3.1 Fourier Transform Infrared Spectroscopy (FTIR)

FTIR spectra of the coral sand samples presented in figure 3.1 shows peaks associated with those of calcium carbonates. The results showed peaks of carbonate v_2 (866cm^{-1}, representing amorphous calcium carbonate) and v_3 (1420cm^{-1}) vibrational modes. These peaks are due to the vibration of carbon-oxygen double bonds in the carbonate ions. The broad peak around 3000 cm^{-1} is due to the FTIR exposed to air which can be reduced by allowing more time for the air to dissipate from the FTIR instrument.

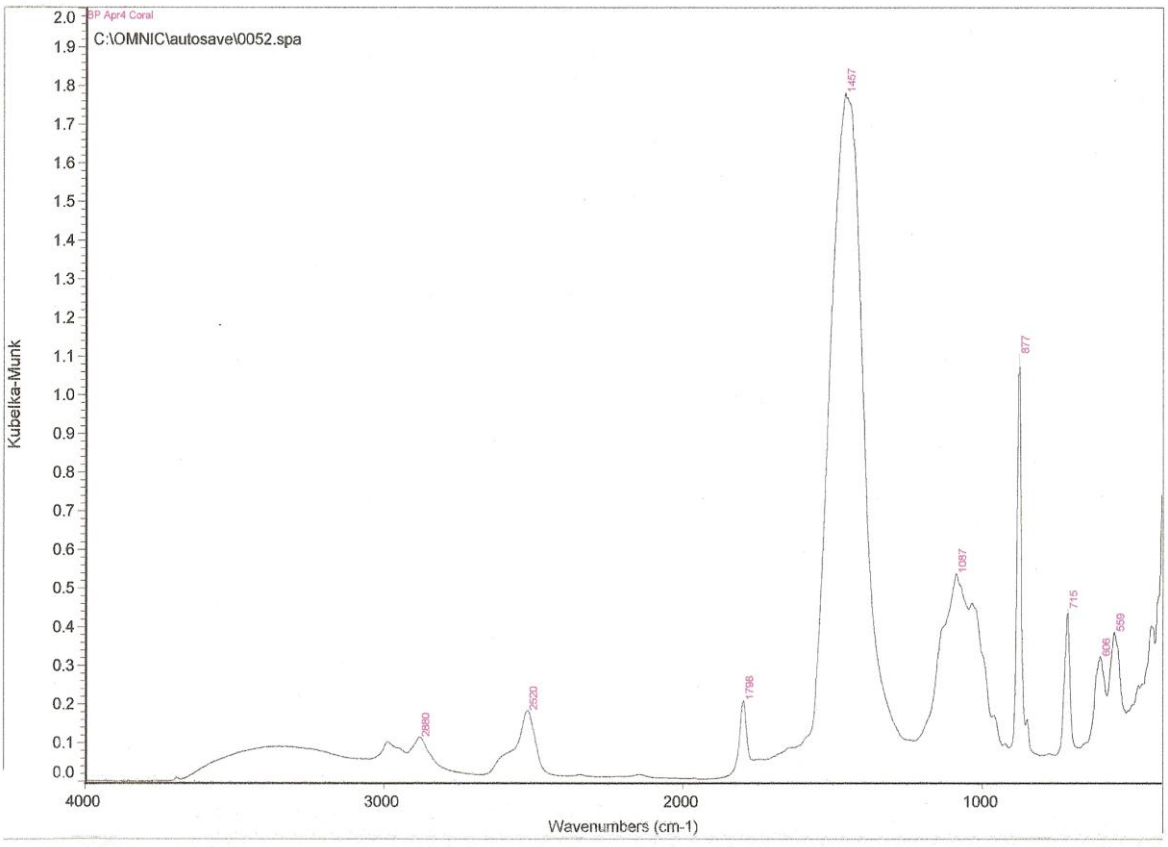

Figure 3.1 FTIR spectra of unconverted coral sample showing peaks matching those of calcium carbonate.

3.1.3.2 Scanning Electron Microscopy

Figure 3.2 (a) shows a low magnification SEM image of the coral sample and reveals a coral sand with diameter of approximately 1mm. Figure 3.2 (b) shows a higher magnification image, revealing a porous structure with the coral. The average pore size was found to be approximately 3-4 μm.

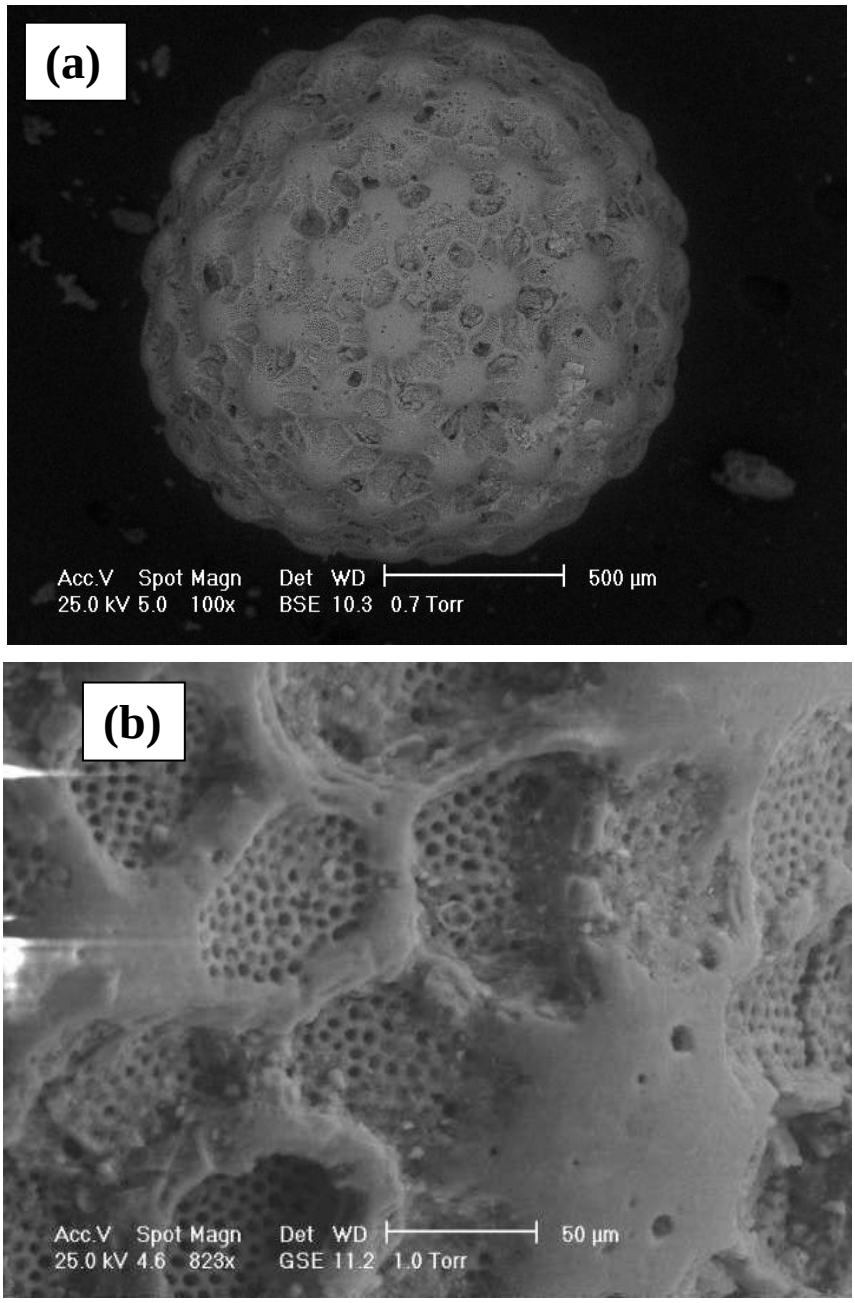

Figure 3.2 (a) Low magnification SEM image of coral sand topography. (b) High magnification SEM image of coral surface topography

From Figure 3.3(a) and Figure 3.3 (b), imaging of a cross section of the coral sand revealed that the coral sand also contains uniform internal porous network both on the top surface and internally. The interconnective porous network seems uniform, having grown outwards from central core/nucleus (Lee and Anderson, 1991)

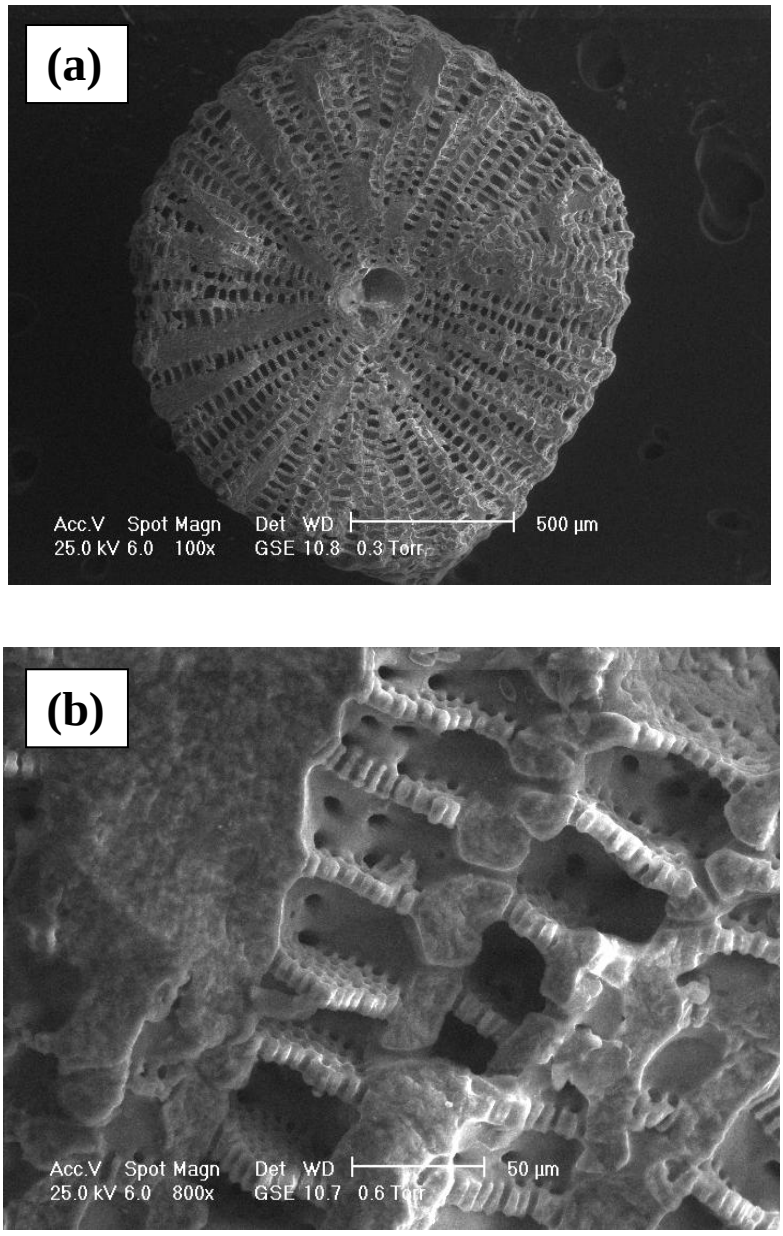

Figure 3.3 (a) Cross sectional images of the microspheres (b) Close up showing direction of porous network shows that the coral sand has a uniform porous network both connecting out from both the horizontal and vertical direction.

3.1.3.3 X-Ray Diffraction (XRD)

XRD patterns, presented in Figure 3.3, were analysed to determine the phase composition of the coral sand samples. All samples (n=3) were calcium carbonate consisting of aragonite and calcite phases. Additional phases were not detected. These were matched with JCPDS database.

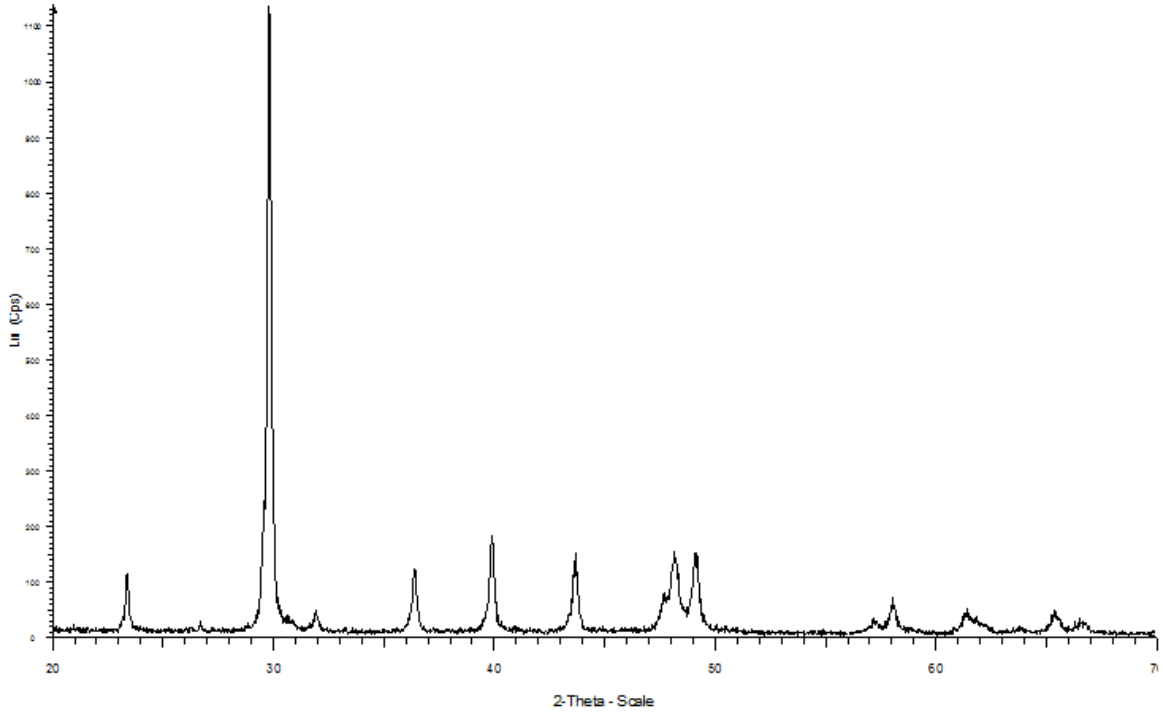

Figure 3.4 XRD result of the coral beach sand

3.1.3.4 Differential Thermal Analysis/ Thermogravmetric Analysis (DTA/TGA)

Figure 2.4 shows the decomposition of calcium carbonate. The DTA output (blue line) shows the coral started dissociating from calcium carbonate into calcium oxide between 600-800°C. The TGA output (red line) shows a 44.54% decrease in the mass of the coral sand. This result matches those of typical calcium carbonate dissociation thus reinforcing our analysis that the coral sand is composed of calcium carbonate. The following is the chemical equation for the dissociation of calcium carbonate.

$$CaCo_3 + Heat(932^{\circ}F) \rightarrow CaO + CO_2$$

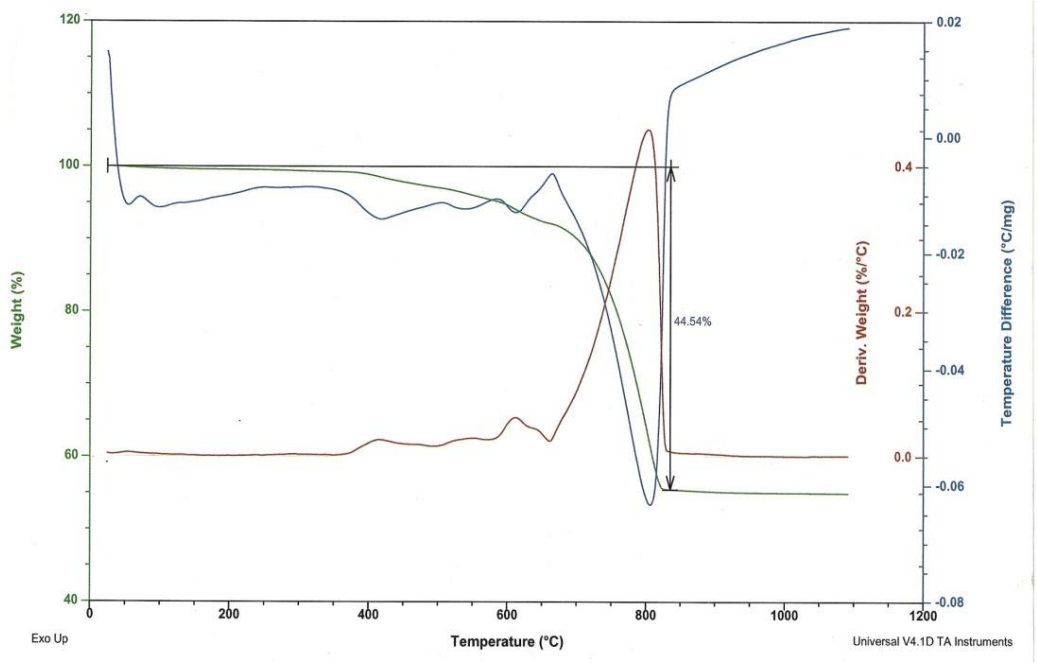

Figure 3.5 DTA results showing dissociation of calcium carbonate of calcium carbonate to calcium oxide and TGA results showing loss of mass from the coral.

3.1.3.5 Inductively Coupled Plasma- Mass Spectroscopy (ICP-MS)

Trace amount of several elements in the coral samples were identified and quantified using ICP-MS.Trace quantities of strontium (5.4ppm), sodium (1.1ppm) and magnesium (6.3ppm) were detected.

Table 3.1 Trace element results from the coral sand

Elements	Concentration (ppm)
Sr	5.4
Mg	6.3
Na	1.1

3.1.3.6 Porosity and Surface Area of Coral microspheres

The surface area of the coral sample measured a BET surface area value of 4.1 m^2/g. The corals had an average weight of 0.003g and based on these values an approximate calculation of 365 Pa per gram of coral sample. The inner matrix of this HA is coralline derived from the mineral skeleton of the marine coral with average pore sizes ranged from 5 to 10 μm with both micro and nanopores.

It should be noted that the BET surface area measurements presented here was obtained under difficulty and therefore the may not reflect on the actual values. There is no instrumental reason for this. The samples could not be exposed to the conditions needed to make a surface area measurement, vacuum, liquid nitrogen etc. The samples were sent to three independent measurement services but results obtained were all inconclusive.

3.1.4 Conclusion

The coral sand was identified by FTIR and XRD to be calcium carbonate, which was further corroborated by the results from DTA/TGA dissociation of the coral sand. Trace elements within the coral sand was identified and quantified by ICP-MS showing the presence of strontium, magnesium, sodium and iron of which none are toxic to the human body. This is crucial as the proposed material is to be used for implanting into the human body. The surface morphology of the coral sand was characterized by scanning electron microscopy and revealed a uniform distribution of interconnected pores. The uniform distribution of the pores is an important factor to the application of the coral sand as one of the key focuses of the present research is the production of a uniform porous microsphere that cannot be otherwise produced. The results from the characterization of the coral sand shows that the material at hand is suitable for hydrothermal treatment for conversion to calcium phosphate.

3.2 Hydrothermal Conversion of Coral Microspheres to Beta-Tricalcium Phosphate (β-TCP)

This section introduces and discusses the process and mechanism behind the hydrothermal conversion from calcium carbonate to calcium phosphate and the subsequent characterization and examination on the bioactivity of the microspheres after the conversion process.

3.2.1 Introduction

The word "hydrothermal" came from British geologist, Sir Roderick Murchison (1792-1871), in relation to the action of heated water bringing about change within the Earth's crust. Work on hydrothermal process was first started in 1845 by Schafhäult. Hydrothermal conversion reactions works at elevated temperature above 100 °C and within a few atmospheric pressures. The heart of the hydrothermal treatment is performed within a sealed reaction container known as the crucible which is composed of thick walls internally composed of platinum, to contain the pressures generated. The crucible is commonly made of platinum (Pt). As previously mentioned the hydrothermal synthesis involves heating the sample and the liquid reagent coupled with a suitable solvent in the tightly sealed crucible at temperature of up to 250°C. Despite having elevated temperatures and high pressure generated within the crucible, this is less severe in contrast to traditional ceramic methods of solid-state chemistry. These processes have allowed an insight into numerous materials leading to important applications. The use of the hydrothermal processes has shown to be quite successful in the preparation of homogenous fine powders. This results in fine crystallised powders with a certain stoichiometric composition. Thus hydrothermal synthesis has met the increasing demands in the preparation of crystalline ceramics (Somiya, 2006). The cost saving factor and less energy consumption are further reasons for its use.

Previously studies conducted by D.M. Roy and S.K. Linnehan using porite corals and *acanthaster planci* as templates for aragonite and calcite phases of calcium carbonates immersed with di-ammonium hydrogen phosphate solution to replace the coral skeletal carbonate with phosphatic material (Roy DM, 1974). The complete replacement with the phosphatic material was essentially achieved with the interconnecting porous structure preserved. These were observed via scanning electron microscopy (White 1972).

The examination of the coral sands collected was identified to be calcium carbonate and thus a suitable material for hydrothermal conversion. One of the key benefits of the hydrothermal conversion treatment is the ability to control the calcium phosphate phase of the resulting material. The different phases of calcium phosphate contribute to different solubility rate of the material. Beta-tricalcium phosphate (β-TCP) is one of the most attractive biomaterials for use in bone repair due to its good biocompatibility, osteoconductivity and a faster dissolution rate compared with hydroxyapatite.

3.2.2 Equipment and Procedure

The coral microspheres were characterized after the hydrothermal conversion process. The compositional analysis was carried out using fourier transform infrared spectroscopy (FTIR) and x-ray diffraction (XRD) spectroscopy. Scanning electron microscopy (SEM) was use to examine the structural morphology of the converted material to determine if the structure was preserved after the hydrothermal conversion. micro-CT analysis which is an additional non-destructive technique was utilised to look at the coral samples in a three dimensional view.

Conversion process - Hydrothermal conversion was carried out in a Parr reactor at 250°C and 8.0MPa pressure with diammonium hydrogenophosphate $(NH_4)_2HPO_4$ from Sigma Aldrich.

Electron microscopy - A Philips (FEI) XL 30 ESEM was used for surface characterization. The microscope was operated in low vacuum mode at 0.8 Torr, 25kV accelerating voltage and a working distance of 10mm, using the back scattered electron detector (BSE) and gaseous secondary electron detector (GSE).

FTIR analysis - A Nicolet 760 Fourier-Transform Infra Red spectroscopy (FTIR) with diffuse-reflectance accessory, were scanned 120 times between $400cm^{-1}$ to $4000cm^{-1}$ with the subtraction of KBr background. Samples were prepared by grinding with KBr in a mortar and pestle.

X-Ray diffraction analysis - X-ray diffraction analysis was performed in Siemens D5000 using CuKα of 1.54A, with 2θ ranging from 15 to 60, and compared with International Centre for Diffraction Data (ICDD) Joint Committee on Powder Diffraction Standards (JCPDS) database records.

Chemical analysis - Inductively coupled plasma mass spectrometry (ICP-MS) was performed on the Agilent 7500ce to identify and quantify trace elements.

Bioactivity analysis - Converted β-TCP microsphere were immersed in Kokubo's simulated body fluid (SBF) solution with CO_2 at 37°C for 3 and 7 days to test for *in-vitro* bioactivity. Chemicals for simulated body fluid (SBF) outlined in table 3.2 were all purchased from Sigma Aldrich Australia Ltd. The compositions of the SBF solution are outlined in table 3.2 (Kokubo et al., 2003).

Table 3.2 Chemical composition for simulated body fluid (SBF) solution

Chemical	**Amount (g)**
$NaHCO_3$	1.134
$MgSO_4 \cdot 7H_2O$	0.124
KCl	0.068
NaCl	3.37
K_2HPO_4	0.115
$CaCl_2$	0.139
Tris(hydroxymethyl)-aminomethane	3.03

3.2.3 Results and Discussion

The conversion process in addition to the processing factors is directly associated to the Ca/P ratio during the hydrothermal conversion. To obtain β-TCP, a Ca/P ratio of 1.50 is required as oppose to the 1.67 ratio for hydroxyapatite. However this chemical control has to be verified with other structural characterisation methods.

3.2.3.1 Environmental Scanning Electron Microscopy (ESEM) Analysis

ESEM analysis revealed no significant changes in the morphology of the coral after conversion to β-tricalcium phosphate (Figure 3.6). The morphology and pore distribution shows significant similarity to those of natural bone structures. The interconnecting structure of both corals was preserved with a little increase after conversion. This has a distinct advantage in drug delivery usage where the encapsulated drug could dissociate faster.

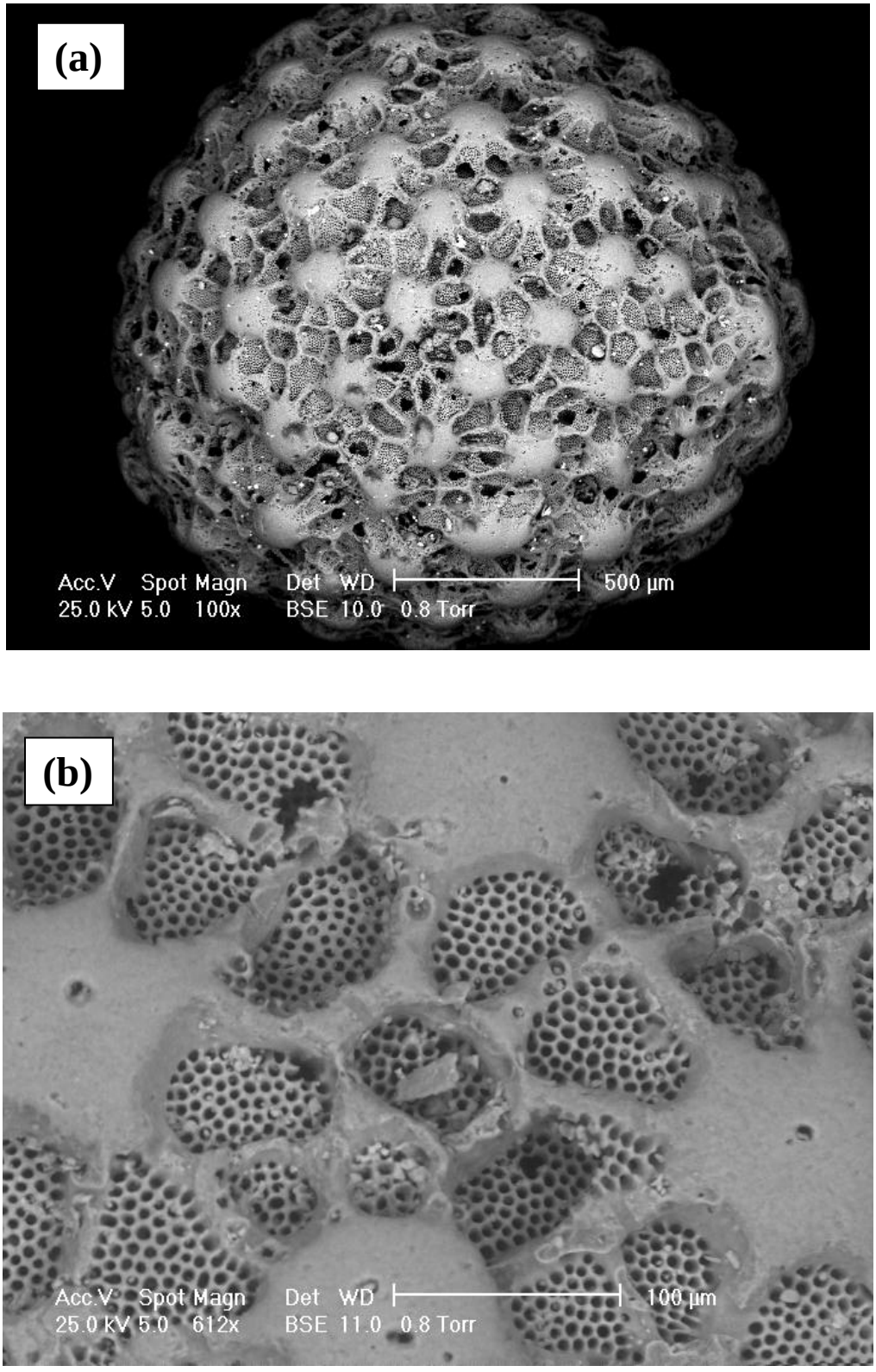

Figure 3.6 ESEM micrograph of the after hydrothermal converted β-TCP microsphere (a) lower magnification (x100) and (b)at a higher magnification (x612)

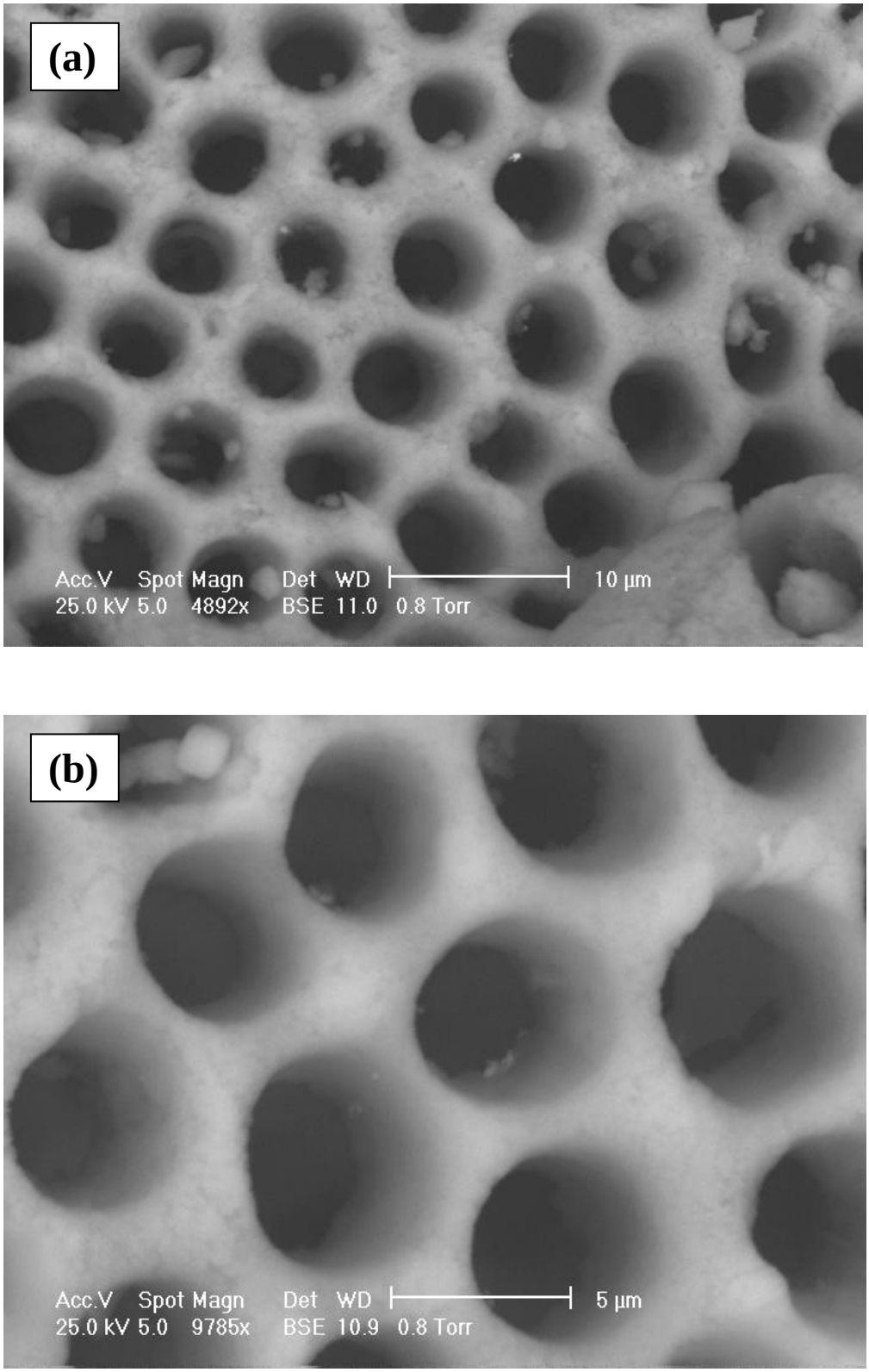

Figure 3.7 ESEM micrograph at high magnification (a) focusing on the pore distribution at the surface of the β-TCP microsphere and (b) average surface pore size of 5µm.

3.2.3.1 Microtomographic (Micro-CT) Analysis

Microtomography, as a non-destructive method, was used to compile a three-dimensional reconstruction of the coral sand. It revealed the coral sand's internal structure to be permeated by a uniform distribution of interconnecting micropores. Figure 3.8 shows that the pores are uniformly distributed externally as well as internally and they all appear to lead to a central chamber core from which the original coral spore grew (Lee and Anderson, 1991). The pores seem to be interconnected by channels, forming a continuum without dead ends. The micro-CT analysis generated cross-sectional slice of the images which enable us to see the elaborate internal architecture that the microsphere possesses an indication as to how the drug would be incorporated and released.

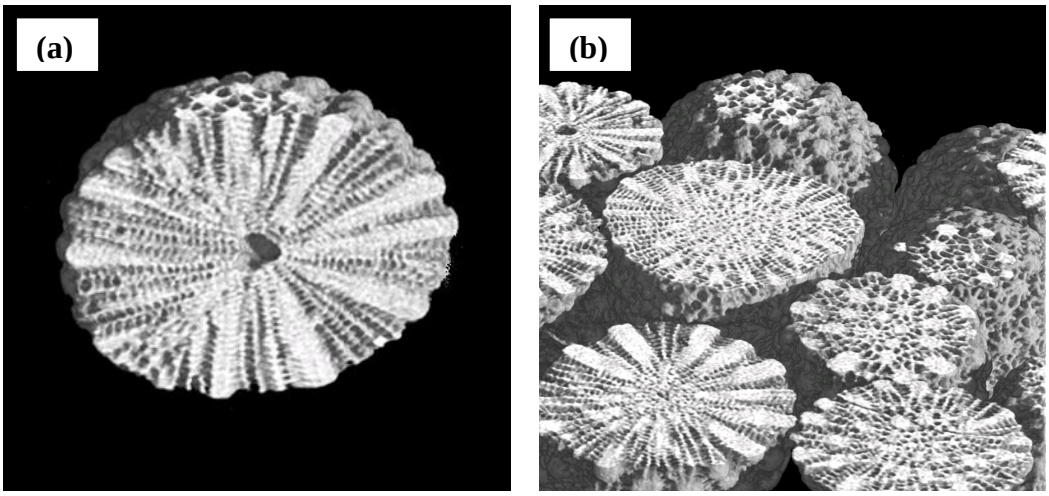

Figure 3.8 Reconstructed microtomographic images of the β-TCP microsphere showing (a) uniform distribution of the interconnecting pores and (b) different levels of internal architecture.

3.2.3.2 Fourier Transform Infrared Spectroscopy (FTIR)

Fourier transform infrared spectroscopy analysis showed peaks (Figure 3.9) corresponding to both calcium carbonate and β-tricalcium phosphate. In biological apatite's infrared absorption spectra, it displays characteristic bands due to OH^-, PO_4^{3-} and CO_3^{2-}. The coral sample FTIR did not display any OH^- vibration. The coral derivatives showed mixture of peaks with 715 cm^{-1}, 879 cm^{-1}, 1082 cm^{-1} assigned to the calcium carbonate peaks and where the 875cm^{-1} and 1420-1457 cm^{-1} peaks are indication of the presence of β-TCP (CO_3^{2-} ions substituting for PO_4^{3-} ions). The broad and intense bands associated at the PO_4^{3-} vibrations in calcium phosphate material is around 1082 cm^{-1} (antisymmetric stretching mode) and 560 cm^{-1}, 609 cm^{-1} (antisymmetirc bending mode). Apart from CO_3^{2-} substituting for PO_4^{3-}, other anions such as Cl^- and F^- can readily substitute for OH^- in the lattice structure of biological apatites. CaO peaks were unable to be observed as the spectrum has a major absorption band at 300cm^{-1} which is out of the FTIR analysis range. FTIR analysis further reinforces the identification of the converted corals to be a mix of calcium carbonate and β-tricalcium phosphate.

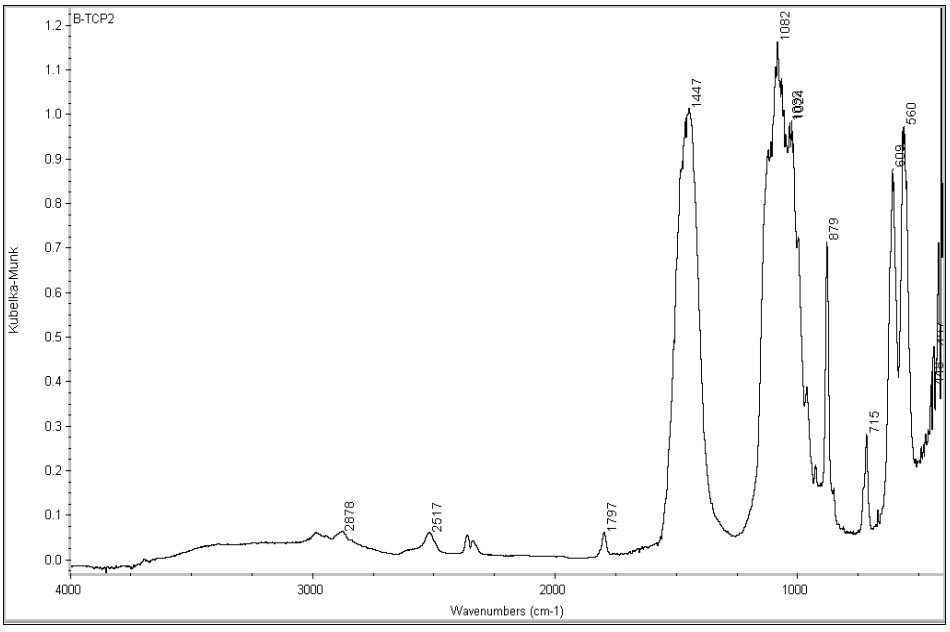

Figure 3.9 FTIR spectra of after conversion coral sand sample showing Ca_3PO_4 related vibrations

3.2.3.3 X-Ray Diffractometry (XRD)

XRD analysis showed that the microstructure of the coral sand microsphere (Figure 3.10) after conversion was composed of mainly β-tricalcium phosphate (whitlockite) with some HAp and calcium carbonate peaks.

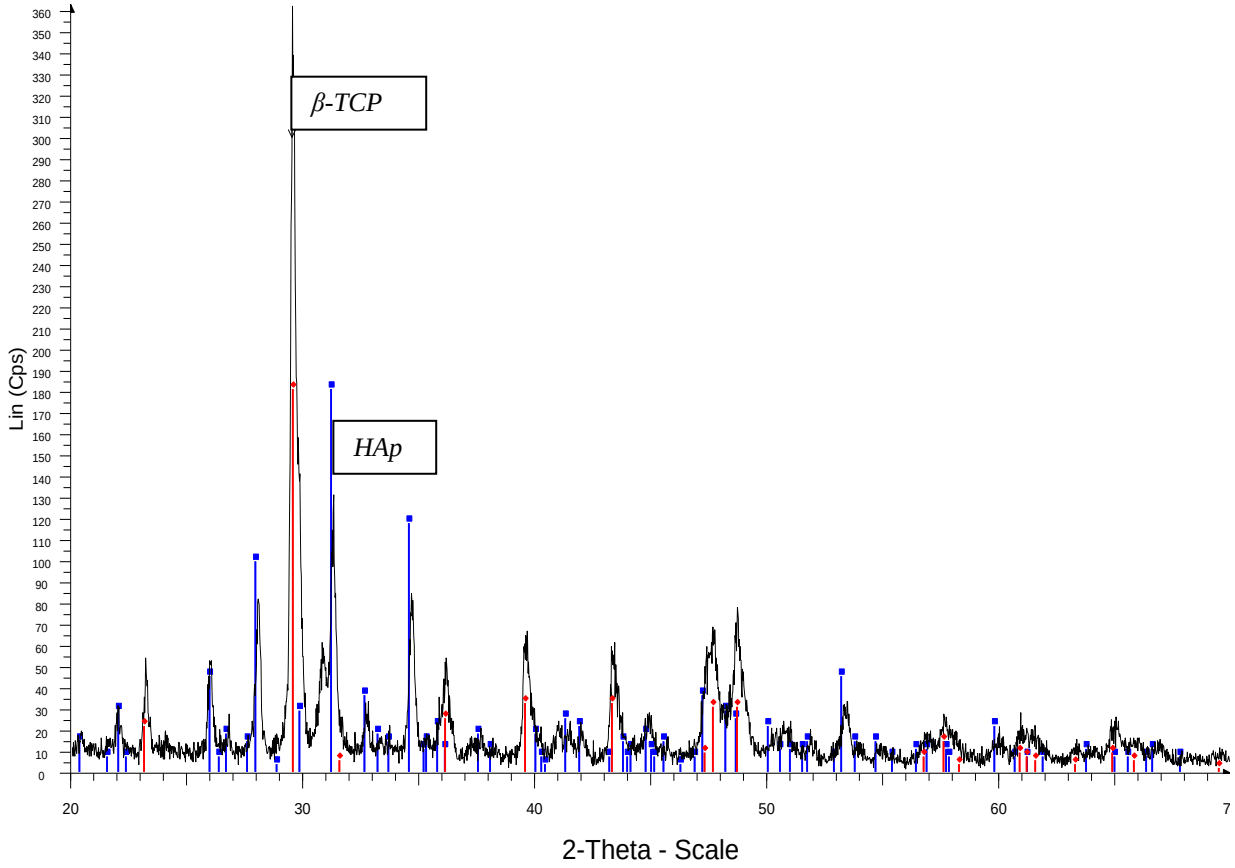

Figure 3.10 patterns showing after hydrothermal conversion peaks corresponding to β-TCP (blue) and other phases such as HAp and calcium carbonate (red)

3.2.3.4 Bioactivity of β-TCP Microspheres

The *in-vitro* bone bioactivity was investigated by immersing the microspheres into Kokubo's simulated body fluid (SBF) solution and observing the precipitation of calcium and phosphate ions. The EDS spectrum in Figure 3.11 shows the atomic composition of the precipitates after 7 days immersed in the SBF solution. The existence of calcium (Ca) and phosphate (P) are at a higher intensity for the SBF sample (yellow peaks) when compared with normal β-TCP microsphere (red peaks). Figure 3.12 shows the SEM morphology of the microspheres after immersion in SBF for 7 days. Precipitates were observed throughout the surface of the microspheres covering the majority of the pores on the surface. These *in-vitro* results support the notion that the hydrothermally converted β-TCP microspheres will be bioactive and possess the necessary properties as a biodegradable material for drug delivery.

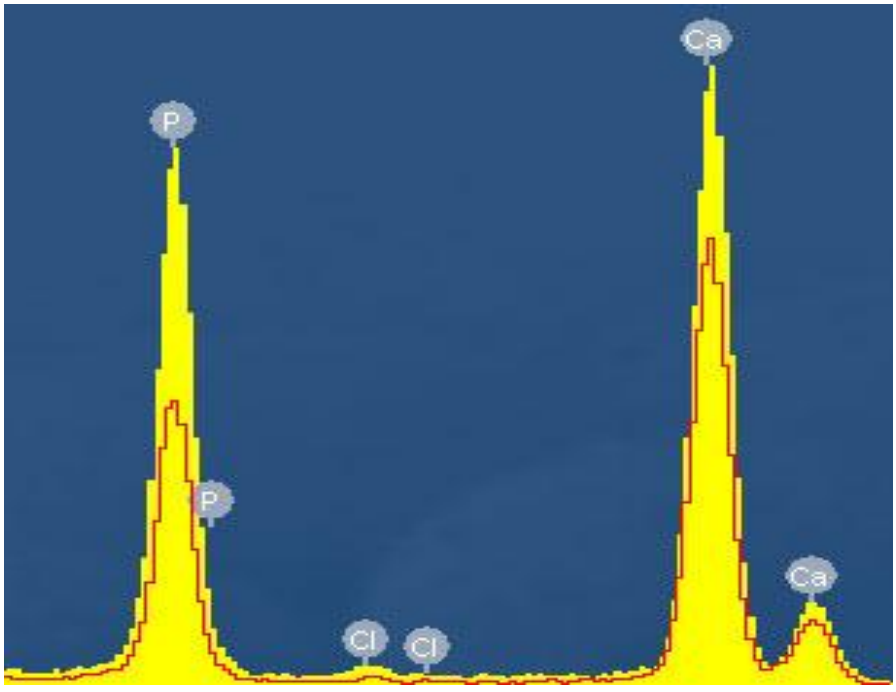

Figure 3.11 EDS analysis showing the higher intensity of the calcium and phosphate peaks of the precipitated β-TCP microsphere (yellow) compared with normal non SBF treated β-TCP microsphere (red).

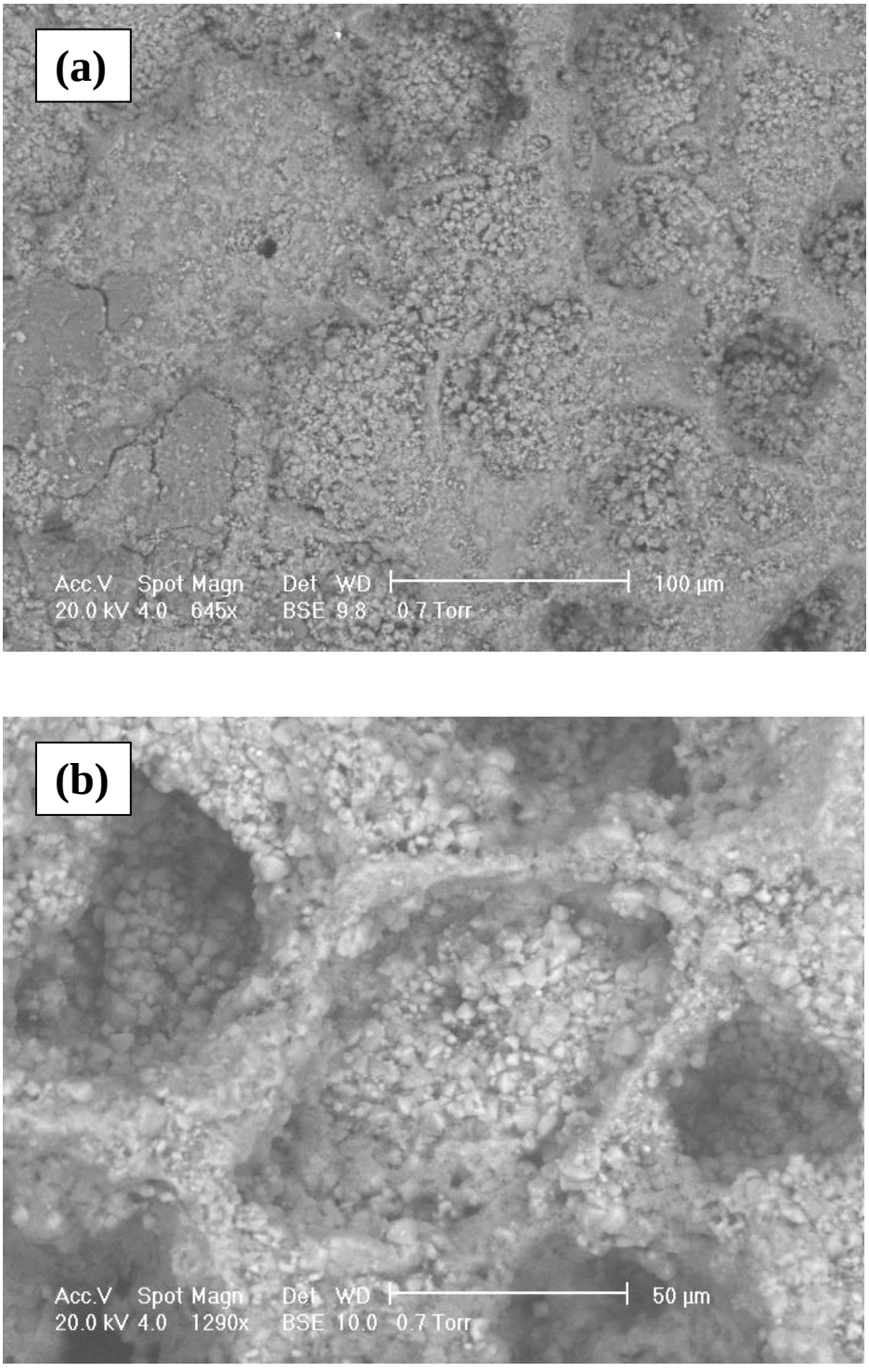

Figure 3.12 β-TCP microspheres immersed in SBF solution for 7 days showing precipitation of calcium phosphate phase throughout the surface and in between the pores.

3.2.3.5 Inductively Coupled Plasma- Mass Spectroscopy (ICP-MS)

It was important to investigate the chemical composition of the microspheres after hydrothermal conversion. The compositional analysis results by ICP-MS (table 3.3) showed the original concentration for both strontium and magnesium had slightly decreased possibly due to the dissolution during the conversion process.

Table 3.3 ICP-MS results showing chemical compositions of the after conversion β-TCP microspheres

Element	Before Conversion Concentration (ppm)	After Conversion Concentration (ppm)
Strontium	2.25	1.4
Magnesium	6.3	2.6

3.2.4 Conclusion

The resulting product from the hydrothermal process was identified by X-ray diffraction to be a mix of calcium carbonate and β-TCP microsphere. Evidence shows a minor change to the pore size of the coral before and after treatment. The overall structure did not change the original un-transformed structure making it available for adsorption of candidate drug compounds. Micro-computed tomography (micro-CT) and scanning electron microscopy (SEM) imaging confirmed that the microspheres were internally permeated by a 3-dimensional network of microscopic channels measuring 5-10μm in diameter. This preservation of structure can be used for implant allowing ingrowth of tissues. This work has shown under controlled hydrothermal conversion, a mix product of calcite and β-TCP can be derived from the coral sand grains while retaining its porous structures. This mixed composition will provide a faster dissolution rate which is suitable as a biodegradable material for drug delivery.

3.3 Biodegradation of Beta-Tricalcium Phosphate Microspheres

This section describes the protocols developed and utilized for studying the release profile of the β-TCP microsphere. The release studies are aim at estimating the amount of calcium released from the microspheres in physiological solutions. General dissolution behaviors were studied under distilled water solution and the effects of electrolyte constituents at physiological pH of 7.4 was studied using tris-buffer solution.

3.3.1 Introduction

Beta-tricalcium phosphate phase was selected as it had a dissolution rate suitable for drug delivery. *In-vitro* dissolution tests, although far from the ideal method, can give some insights on the stability of the materials prior to implantation. In fact, since these studies are carried out in solution they always simulate the worst case low-end service environment.

In the early 1970s, Driskell used beta-tricalcium phosphate to repair hard-tissue avulsive wounds and oro-facial fractures (Driskell et al., 1973). When placed in proximity to the freshly cut and bleeding bone, the ceramic matrix is rapidly invaded by bone-forming tissues. Meanwhile, the implant is resorbed and the process continues for approximately 6-18 months (Metsger et al., 1982). It has been reported that TCP is more bioresorbable than hydrxoyapatite, which has a relatively slow resorption rate compared to rates of new bone formation (Garey et al., 1991, Klein et al., 1983). The bioresorption of tricalcium phosphate (TCP) is assumed to take place by both cell mediated and solution-driven processes. Research has shown that TCP has a much higher dissoulution rate than that of stoichiometric HAp (Park and Lakes, 1992, Jarcho, 1981, LeGeros, 1993). Ducheyne et al. compared the dissolution rates of six different calcium phosphates in calcium and phosphate free solution at pH 7.3 (Ducheyne et al., 1993).

Even though pure TCP has good resorbability, the higher the solubility, the faster the dissolution rate which can result in strength reduction during the bone remodeling process which can eventually lead to implant failure. The ideal material would be one that can resorbed at a rate while maintaining the strength and simultaneously supporting the activity of osteoblasts in the development of new bone.

The continuous degradation of an implant causes a gradual load transfer to the healing tissue, preventing stress shielding atrophy and stimulates the healing and remodeling of bones. Some requirements must be fulfilled by the ideal prosthetic biodegradable materials, such as biocompatibility, adequate initial strength and stiffness, retention of mechanical properties throughout sufficient time to assure its biofunctionality and non-toxicity of the degradation by-products. After implantation, the surface of any graft is rapidly colonized by cells. Much more biology, than chemistry and material science altogether, is involved into these very complex processes and many specific details still remain unknown. In order to simplify the task, the biodegradability of the biologically relevant calcium phosphates might be described by a chemical dissolution (Dorozhkin, 2009).

3.3.1.1 Effect of Strontium and Magnesium on Calcium Phosphate Dissolution

Dedhiya et al. (1974) investigated the inhibition of hydroxyapatite dissolution by strontium and magnesium in acetate buggers containing phosphate. They reported that both strontium and magnesium alone have modest retarding effects on hydroxyapatite dissolution. A solution containing $1x10^{-4}$ M concentration of strontium or magnesium in combination with 1 ppm fluorine would cause about a 50% reduction in hydroxyapatite solubility. Dedhiya, Young, and Higuchi (1972) have suggested that the inhibitory effect of strontium may be due to the formation of a calcium-strontium-apatite complex of the composition Ca_6Sr_4-$(PO_4)_6(OH)_2$ at the hydroxyapatite crystal surface.

3.3.1.2 Stoichiometric and Non-Stoichiometric Dissolution Model

Stoichiometric or non-stoichiometric dissolution can be measured by either the ionic concentrations in a solution or the surface composition of apatite during dissolution. Ions present in a solid may dissolve either simultaneously with dissolution rates proportional to their molar concentrations (stoichiometric dissolution) or non-simultaneously with different values of the dissolution rates for each ion (incongruent dissolution). The latter case always results in a situation where the surface layer with a chemical composition different from that of the bulk of solid is formed. At the fundamental level the reactions that occur between solids and liquids involves a coupled sequence of mass transport, adsorption/desorption phenomena, heterogeneous reaction, chemical transformations of intermediates, whose identification, separation and kinetic quantification are all necessary if the mechanism of the process is to be fully understood and described. It is also generally agreed that during dissolution, lattice ions undergo the following processes:

1) Detachment from a kink site
2) Surface diffusion away from the crystal steps
3) Desorption from the surface
4) Diffusion into the bulk solution

In the case of calcium phosphate, it is found that calcium dissolution is faster when compared with that of phosphate (Rey C., 2006, O'Neill W.C., 2007, Wopenka B., 2005). The dissolution of hydroxyapatite in aqueous medium appears to be always non-stoichiometric at the beginning, but when the solid has successively equilibrate at any given pH, the solution's Ca:P ratio approached a limiting value of 1.67. Once this value is reached, the solid only maintains this ratio by dissolving stoichiometricaly (Dorozhkin, 2002).

3.3.1.3 Comparison of Different Dissolution Models

Over the years, various models to simulate and study the dissolution of apatites have been proposed and these have provided significant information on calcium phosphate materials. Nevertheless, there are still a lot of elements missing. Each model has its own limitations and drawbacks. Moreover, most of the models were elaborated for apatite dissolution in slightly acidic or nearly neutral ($4 < pH < 8$) solutions, with relatively small values of solution undersaturation, and within the temperature range of 25 and 37°C only. However, there is no doubt that each of the proposed models is correct for the specific experimental conditions studies. The different models focus on the different aspects of the same process of apatite dissolution and are likely to complement each other. Unfortunately, it is still impossible to obtain a complete understanding for all the processes involved. Stochiometric hydroxyapatite was found to be the least soluble (most stable) amongst the materials tested (LeGeros, 1993). The variability in dissolution measured for the various materials studied is evidence that although materials may appear similar in terms of elemental analysis, their respective solubility characteristics in solution may differ. The dissolution characteristics of calcium phosphates are governed by a large number of factors related either with the *in-vitro* solution environment or with the properties of the material. The use of deionized water provides a general dissolution profile of the microsphere whereas the tris-buffer solution provides an insight into the dissolution properties of the microspheres under a more complex solution system. The release profile will provide a general overview on the characteristics of the microspheres under the two different conditions. There are various models for performing *in-vitro* dissolution tests which vary in complexities. The dissolution model performed in this study is based on the measurement of the calcium ions released into the respective solutions over a predetermined period of time using a calcium ion-selective electrode. As the acidity of the solution has a direct effect on the dissolution rate, the pH was adjusted to physiological pH of 7.4 for all experiments and measurements of the pH were recorded for further analysis.

3.3.2 Equipment and Procedure

Preparation of solution - Dissolution tests were carried out on the β-TCP microspheres in distilled water and tris-buffer solution which simulates, in a very simplistic way, the *in-vitro* physiological environment. Tris-buffer solution was prepared by dissolving 300g tris-(hydroxymethyl)-aminomethane (Sigma Aldrich Australia Ltd.) in 50 mL of deionized water and with 0.1M KCl solution (0.75g/100mL) as KCl is the ionic strength adjustor (ISA) for the calcium ion selective electrode. It was than stabilized to pH 7.4 with HCl and incubated at 37°C with 5% CO_2 atmosphere in a shaker.

Calcium ion measurement - The evaluation of the dissolution behavior was made by measuring the concentration of calcium ions released into the solutions at 24 h intervals for 14 days using a calcium ion selective electrode (ISE). The ISE was calibrated prior to each reading for accuracy and all dissolution results were repeated in triplicate.

Electron microscopy - The surface morphology of the β-TCP microspheres after immersion in solution was examined using a scanning electron microscope Philips (FEI) XL 30 for surface characterization. The microscope was operated in low vacuum mode at 0.8 Torr, 25kV accelerating voltage and a working distance of 10mm, using the back scattered electron detector (BSE).Three replicates of each condition were studied.

3.3.3 Results and Discussion

The experimental approach used in this study consisted of following the dissolution kinetics of the β-TCP microspheres with pH- and calcium ion-selective electrodes (Figure 3.13, Figure 3.14). Over time, the dissolution rate decreases and other factors such as the ionic product of the surrounding medium became more important. The increase of dissolved Ca^{+} in the solution will favour some degree of re-precipitation, which can also contribute to the decrease in the dissolution rate. The dissolution profiles of Ca^{+} indicate that the dissolution rate reached a constant level after 18 days. The dissolution studies were continued for 150 days which further confirmed that the dissolution rate remained constant (Figure 3.13, Figure 3.15). It should also be noted that there remains calcite composition within the microsphere which would essentially increase the dissolution rate further compared with pure β-TCP.

The test solution was not replenished with fresh solution for the duration of the experiment and the solution's initial composition was not maintained. This approach was adopted to avoid introducing other variables into the experiments. However, one must point out that dissolution *in-vivo* does not occur in a constant fluid milieu. This is because *in-vivo* once the material starts dissolving, the respective ions can be transported away from the dissolution sites by fluid flow. Therefore equilibrium condition may never be reached. These *in-vitro* studies may provide an indication on the implant behavior of the β-TCP under *in-vivo* conditions.

The trend of solubility of the β-TCP microspheres obtained in this study are in agreement with previous findings that the solubility of apatites increase with increasing ionic substitutions into the apatite lattice and decreasing crystallinity.

3.3.3.1 Dissolution Behaviour in Double Distilled Water

Figure 3.13 shows the changes in the dissolution behavior, by means of calcium ions released into the solution, and the respective pH values over time. It can be seen that the concentration of the calcium ions increases until it reaches equilibrium. Whereas the pH value drops initially from 7.4 to approximately 6.9 before stabilizing at a pH of about 6.6 (Figure 3.14). The dissolution of the metastable components obviously occurs at the initial stage of the immersion tests and similar reactions would be expected for the *in-vivo* condition, especially when a decrease in pH value occurs due to infection and inflammation. However, large pH changes are unlikely to occur around an *in-vivo* implant as blood, which is extremely well buffered, is present in large volume and constantly circulating.

Scanning electron microscopy imaging shows that the top surface layer of the microsphere was found to have dissolved first during the immersion tests, while more micro-pores appeared as shown in Figure 3.17. The dissolved top layer exposes the micropores already present within the microspheres allowing further ingrowth of blood vessels and replacement of new bones over time.

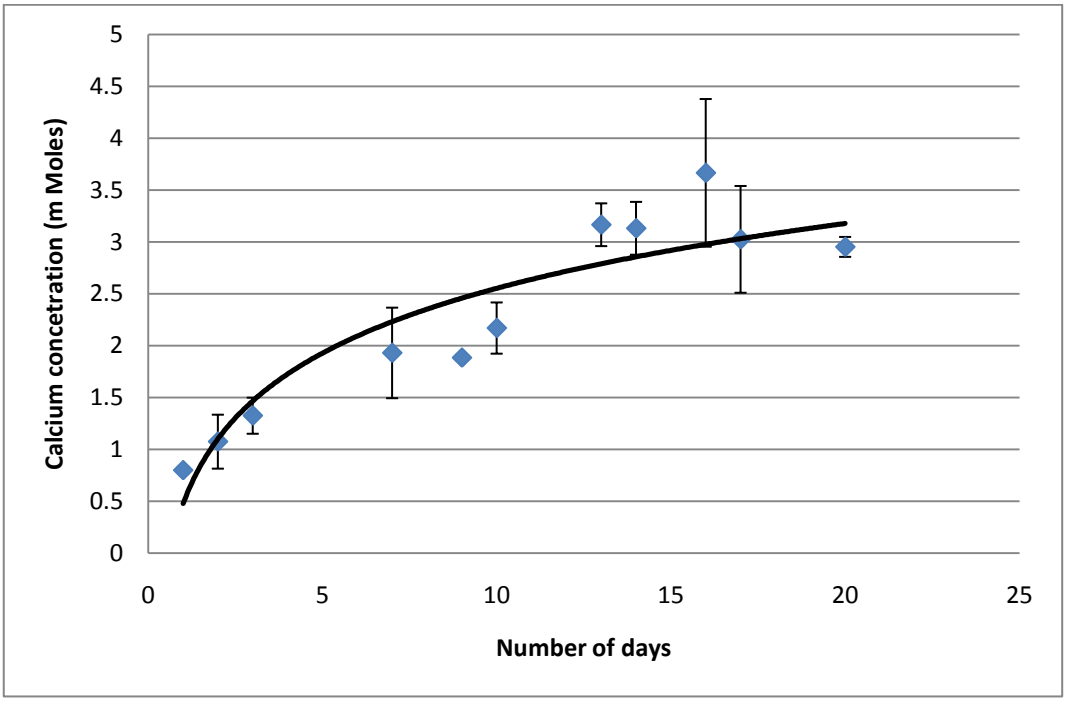

Figure 3.13 Release of calcium ions from β-TCP microspheres immersed in double distilled-deionized water over 20 days.

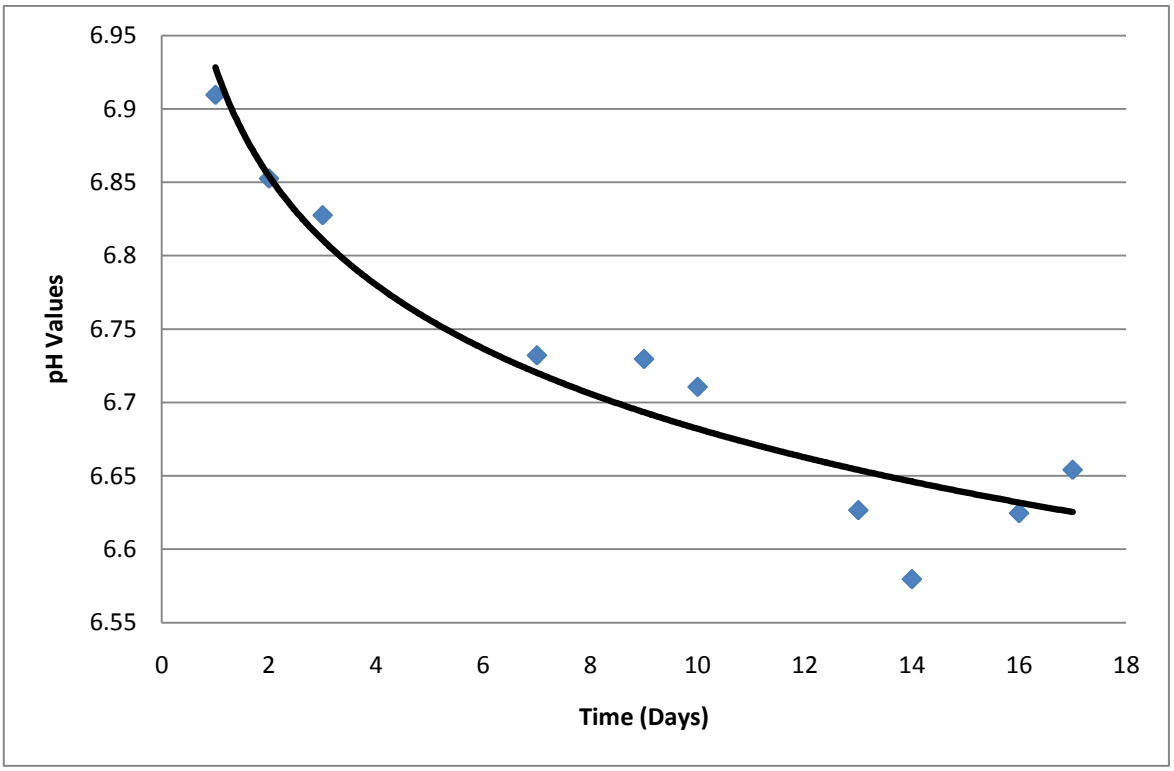

Figure 3.14 Changes in pH with respect to time of β–TCP microspheres immersed in double distilled-deionized water.

3.3.3.2 Dissolution Behaviour in Tris-Buffer Solution

Dissolution studies undertaken under calcium and phosphate free tris-buffer solution underwent a similar reaction trend was observed in the double distilled-deionized water study, except that the dissolution rate was more rapid and greater in magnitude. This is shown in Figure 3.15.

The effects of electrolyte constituents at a physiological pH 7.4 were also studied using tris-buffer solution (Figure 3.16). Tris-buffer [$(CH_2OH)_3CNH_2$], which contains three active hydroxyl ion groups can be stabilized by HCl, may react with the calcium ions released from the microspheres. This creates an active environment to induce more dissolution to occur, especially for the calcium ions, until it reaches an equilibrium stage as compared to the immersion in deionised water. A study conducted by Reis and Monteiro (1996) demonstrated the effects of Hank's Balance Salt solution (HBSS) on the dissolution behavior of hydroxyapatite coatings, and they concluded that the more complex the test solution is, the more aggressive it is in reducing the coatings stability.

A comparison between the dissolution profiles of Ca^{2+}, it can be seen that the dissolution trend of the curves is quite similar. The dissolution rate of Ca^{2+} is higher during the first 10 days. This can be correlated with the nature of the calcium phosphate material. In a dissolution study by Zhang (2003) using tris-HCl solution it was demonstrated that at the early stages of the dissolution process, the morphology, crystallinity and crystal size governs the rate. Since the material under investigation is spherical in structure it will have a high surface contact area with the solution that will further favour the dissolution process.

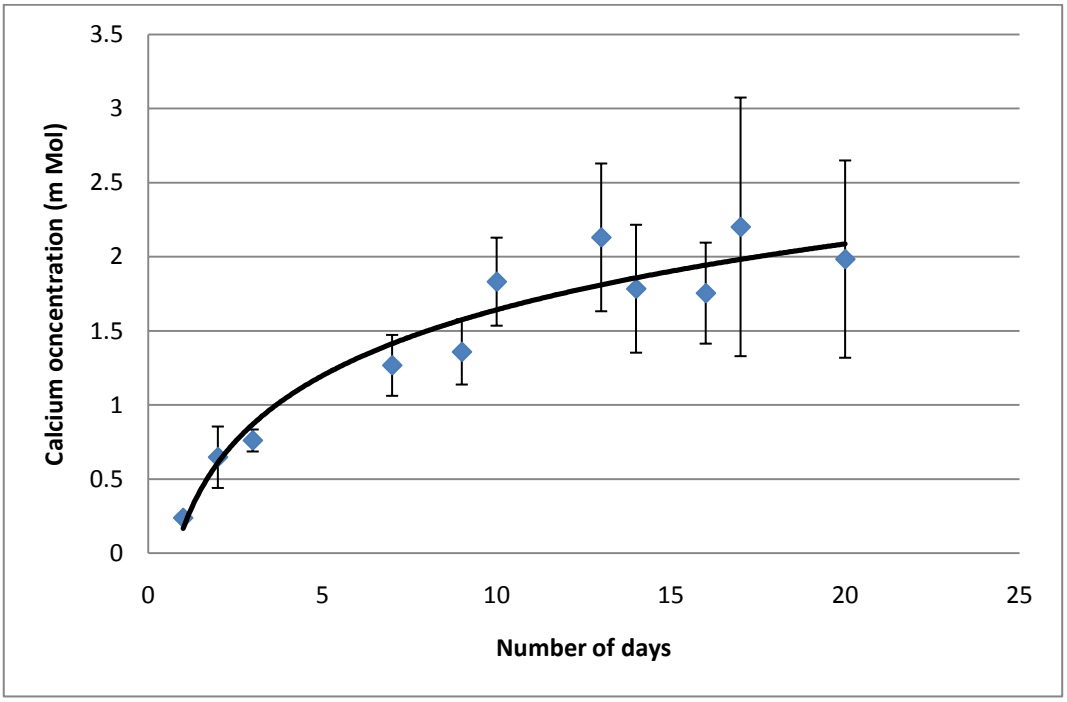

Figure 3.15 Release of calcium ions from β-TCP microspheres immersed in tris-buffer solution over 20 days.

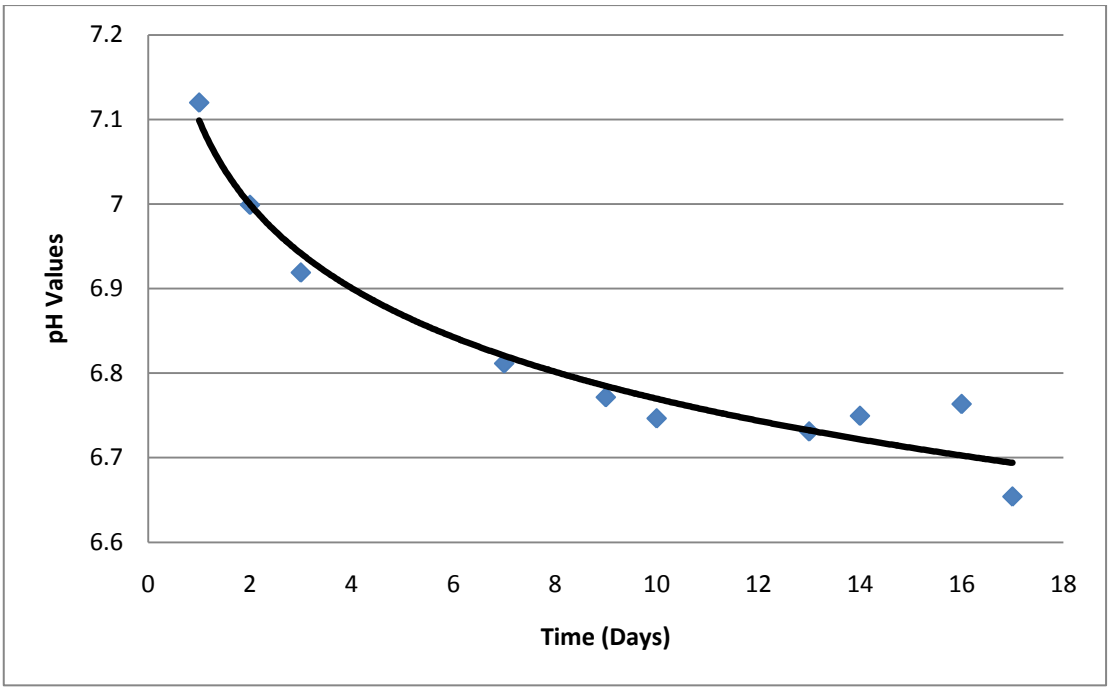

Figure 3.16 Changes in pH with respect to time of β–TCP microspheres immersed in tris-buffer solution.

3.3.3.3 Comparison of Dissolution Behaviours

When analyzing the dissolution profiles of Ca^{+} from the microspheres, one can observe that for the various solutions studied, different dissolution kinetics is observed. The dissolution rates depend heavily on the pH, since Ca-Ps are more soluble in acidic rather than neutral conditions. As expected, when comparing the two dissolution media, the microspheres dissolve at a higher rate when immersed in distilled water. Nevertheless the dissolution characteristics of calcium phosphates are governed by a large number of other factors related either to the *in-vitro* solution environment or with the properties of the material. Besides the pH, the environmental factors include the type and concentration of the buffered or unbuffered solutions, the degree of saturation, ionic strength, porosity, surface morphology such as cracks, loading conditions, duration of immersion and the presence of proteins and cells; the material properties include chemical composition, crystallinity, crystal particle size and density.

From the dissolution diagram it was calculated that by 20 days, 0.12% and 0.18% of the calcium had dissolved into the tris-buffer and distilled water respectively. A comparison between the dissolution rate in distilled water and tris-buffer solution shows a 33% increase in calcium dissolution. Recordings of the calcium ion concentration from both solutions were made for up to 1 year, with no significant found between the two samples.

The immersion test shows that the dissolution rate of the microspheres occurs at a comparatively slower rate. The dissolution rate is dependent not only on the crystallinity but also on the microstructure and density of the material. From the previous SEM characterization, it was observed that the surface of the microspheres had a higher density of pores. The high density of the outer layers of the microspheres makes the dissolution more difficult compared with other calcium phosphate materials which have a loose structure.

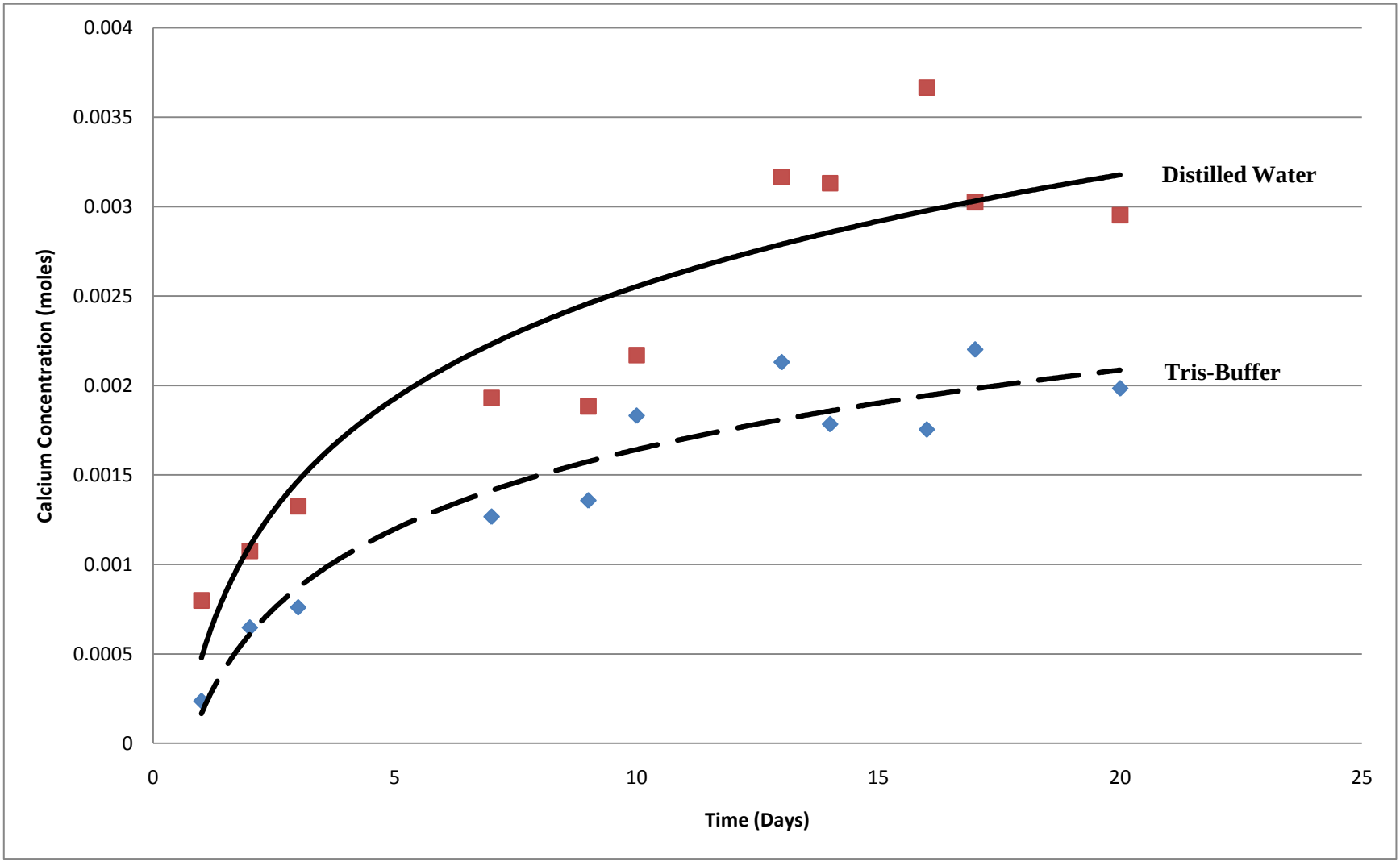

Figure 3.17 Comparison of calcium ions released in distilled water (red) and tris buffer (blue) solution.

3.3.3.4 Surface Characterization of β-TCP Microsphere Degradation

The surface morphology of the β-TCP microspheres was characterized by SEM to study the effect of the degradation after immersion for 3 months in distilled water and tris-buffer solution. Figure 3.18 (a) shows the degradation of the microsphere in distilled water. Interestingly it can be observed that a small percentage of the sphere has degraded resulting in larger pores whilst many of the original pores have also been maintained. [Figure 3.18 (b)]

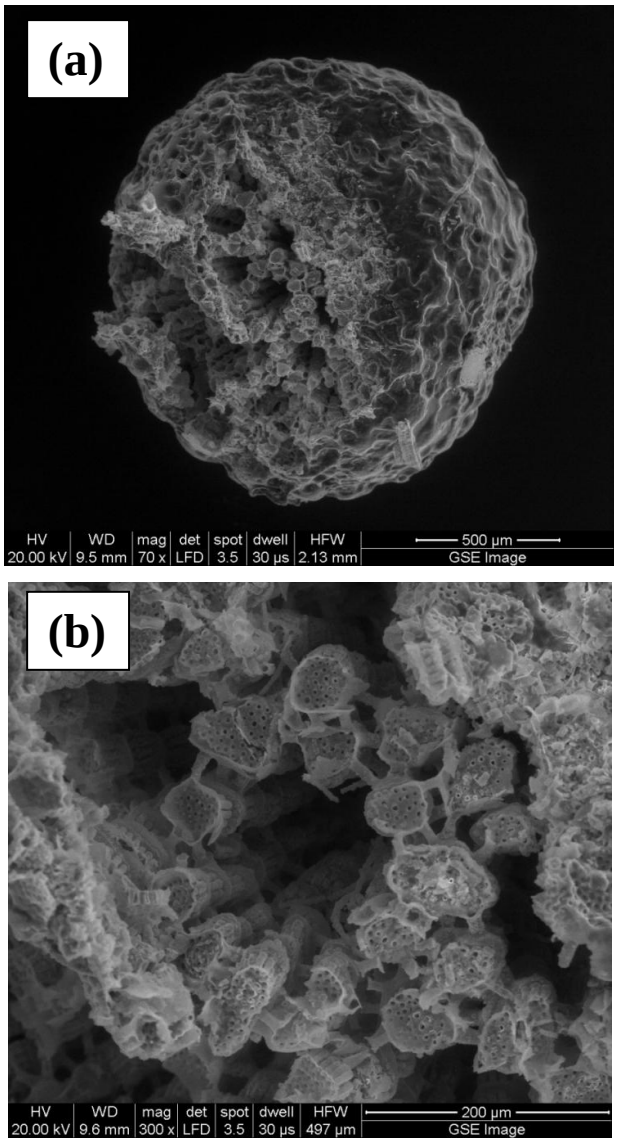

Figure 3.18 SEM micrograph of β-TCP microspheres (a) immersed in distilled water for 3 months and revealing larger pores as a result of the dissolution process (b).

Figure 3.19 shows the surface morphology of the microspheres after 3 months immersed in a tris-buffer solution. Compared with distilled water tris-buffer, has a slower degradation rate. The SEM images reaffirms this, revealing interestingly that the degradation is occurring from the big surface humps and thus generating bigger pores of approximately 150µm whilst maintaining the original network of micropores and exposing the internal porous network which can be beneficial for bone integration.

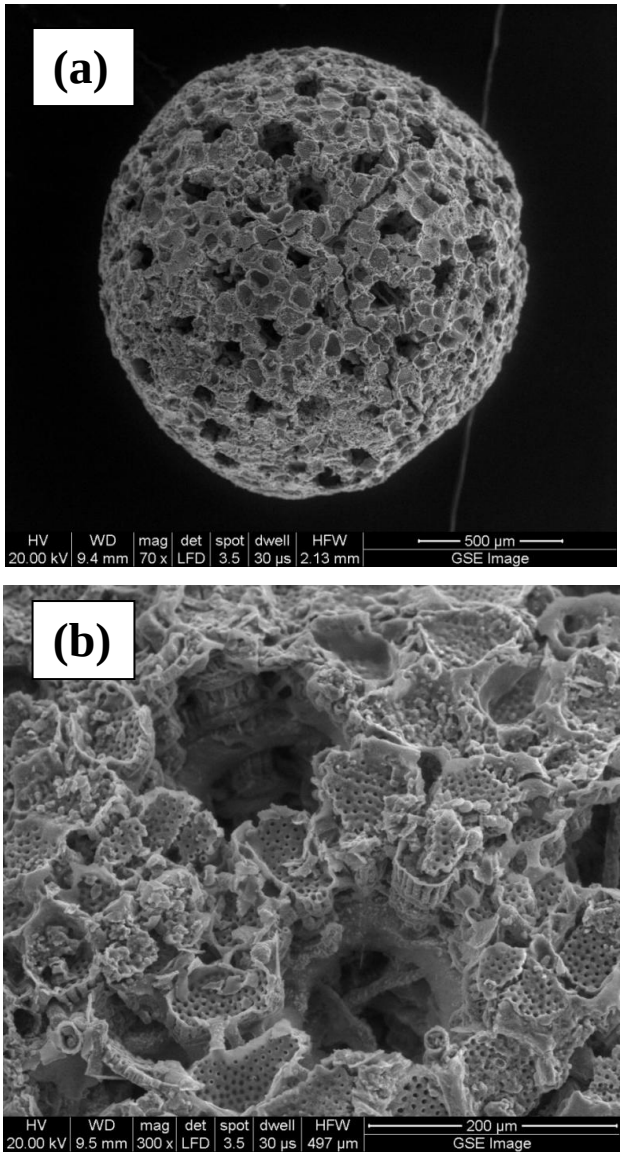

Figure 3.19 SEM micrograph of β-TCP microspheres immersed in tris-buffer solution for 3 months showing a slower surface degradation compared with distilled water.

3.3.4 Conclusions

In vitro dissolution studies undertaken in double distilled-deionized water demonstrate that the metastable components of the β–TCP microspheres dissolve under aqueous conditions and hence increase the calcium ions in the solution. The presence of the electrolyte constituents in the test solution, such as calcium and phosphate free tris-buffer solution, tend to decrease the rate of dissolution as compared to the deionized water alone.

The dissolution study was carried out over a one-year period, over which time, no difference in the concentration of the free calcium ions was observed after it reached equilibrium (Presented figures only show 20 days as that was the time frame the equilibrium was reached) . SEM examination of the surface morphology of the microspheres suggest that the changes in the surface structure following dissolution in water, would promote better bone integration due to exposure of the internal porous network whilst maintaining the micropores from its original structure. It was estimated that only 0.18% (2mM) of the total calcium was released in 18 days, which is a key period for early bone formation, which would suggest that the microspheres are an ideal candidate with a suitable degradation period as a scaffold or to be used as a biodegradable drug delivery carrier.

4 EVALUATION OF DRUG DELIVERY EFFICACY OF CORALLINE SCAFFOLD FOR BONE TISSUE ENGINEERING

4.1 Introduction

Following physico-chemical characterization of the β-TCP microspheres, it appears that they indeed could be used as a novel scaffold material offering uniformly sized pores and an interconnected porous network. The effectiveness of the β-TCP microspheres as a scaffold material can be further enhanced by incorporating pharmaceuticals. These can include and are not limited to drugs that promote bone regeneration and antibiotics to prevent bacterial infections which can lead to implant failures and such a system would prove to be highly advantageous in enhancing the integration between bone-implant interface. The aim of this chapter is to investigate the ability of the microspheres to act as a drug delivery carrier allowing direct delivery and sustained release of the drug into its surrounding.

4.1.1 The Use of Bisphosphonate for Promoting Bone Regeneration

Bisphosphonates are a class of drugs developed for use in the treatment of various bone and calcium-related pathologies like cancer, hypercalcemia, Paget's disease or osteoporosis (Oliveira et al., 2010). It has also been reported that bisphosphonates can be beneficial when administered after bone replacement, decreasing the primary failure mode of total hip arthroplasty, which is aseptic loosening following peri-implant osteolysis (Oliveira et al., 2010). This effect could be further improved if the time needed for the bisphosphonate to reach the bone-implant interface could be reduced. This can be achieved by a localized delivery of the drug to the site producing a more stable and integrated interface between the implant and bone at the early stage of implantation, which is when a significant amount of bone loss can occur. Several studies using different types of bisphosphonates has already shown success with this method. For example, Kajiwara et al. (2005) treated calcium ion-implanted titanium implants with pamidronate which significantly accelerated new bone formation in a rat tibia.

Yoshinari et al. (2009) have studied the effect of pamidronate incorporated into plasma sprayed hydroxyapatite coated titanium dental implant in beagle mandibular bone, which increased the bone-implant contact area. From these studies one can envisage that incorporation of bisphosphonate into a biodegradable drug delivery system would be an advantageous strategy for enhancing tissue integration and regeneration. Combined with a biodegradable drug delivery system the effectiveness of bisphosphonate can be enhanced by exposing the unique properties of bisphosphonate directly to the site of interest. This will hopefully promote a faster and better bone regeneration and integration. Orally injected bisphosphonates are poorly absorbed (<1%) and must be taken whilst fasting. The patient is required to remain upright and fast for 30 mins. Failure to do so may cause gastrointestinal side-effects or inadequate absorption of the drug. Intravenous dosing avoids the gastrointestinal side-effect and ensures compliance but may cause mild flu-like symptoms for a few days following administration (Villiers and Tobias, 2009). The level of suppression of bone turnover varies across the different classes of bisphosphonates, but may last for long periods after cessation of therapy. The ideal length of bisphosphonate therapy is not known. Bisphosphonates have the most extensive track record in osteoporosis therapy and are likely to remain the most commonly prescribed drug for the prevention of fractures in the immediate future (Villiers and Tobias, 2009).

Bisphosphonates are characterized by two phosphonate groups attached to a single carbon atom and have a strong affinity for the Ca^{2+} ions in calcium phosphate materials (Palazzo et al., 2007). This high affinity for bone may affect many important biological properties of the bisphosphonate including uptake and retention in the skeleton, diffusion of the drug within the bone, the release of the adsorbed drug from the bone, potential recycling of the desorbed drug back onto the bone surfaces, and effects of mineral dynamics and cellular function within the bone (Nancollas et al., 2006). A significant feature of the bisphosphonate structure is its basic P-C-P structure that can be widely modified by changing the substituent at the central carbon atom.

This will influence the behaviour of bisphosphonate in the biochemical process (Palazzo et al., 2007). The two phosphate groups are essential for binding of bisphosphonate to hydroxyapatite (HAp) and for its biochemical mechanism of action.

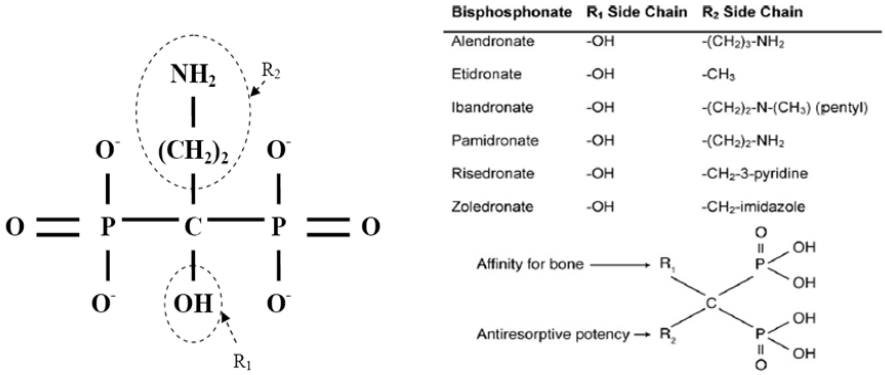

Figure 4.1 The basic chemical structure and difference classes of bisphosphonate based on different R1 and R2 side groups (Bell and Johnson, 1997).

Different classes of bisphosphonate are characterized by two covalently bonded side chains attached to the central carbon atom, termed R1 and R2 (Figure 4.1), which determines the anti-resorptive potency efficiency of the compound (van Beek et al., 1999). It is well known that the R1 substituents with additional capability to co-ordinate to calcium, such as hydroxyl (OH) or amino (NH_2), can display enhanced chemisorption to mineral. By varying the R2 substituents, it can in turn influence other surface properties, including the zeta potential and interfacial tension. The difference in binding affinities of the bisphosphonate and the effects on mineral surface properties will also affect the different clinical applications (Nancollas et al., 2006). Studies of the solid/liquid interfacial properties of hydroxyapatite/ bisphosphonate conjugates have shown that differences among the bisphosphonates may also influence their mechanisms for binding and inhibiting crystal growth and dissolution (Palazzo et al., 2007).

The presence of a nitrogen group within the R2 side group is associated with the ability of an individual bisphosphonates to inhibit farnesyl pyrophosphate (FPP) synthase, which is a major enzyme in the mevalonate pathway (Boanini et al., 2008). FPP synthase stimulates isoprenylation, a process that activates small GTPases (such as Rab, Rac, Ras and Rho) and is important in the control of sub-cellular protein trafficking.

There is also a morphological affect on osteoclasts, with cytoskeletal rearrangement and loss of "membrane ruffling" which are necessary for local generation of H^+ and bone resorption (Luckman et al., 1998, Alakangas et al., 2002, Kimmel, 2007, Pavlos, 2005). GTPases Rho and Rac are involved in the differentiation of osteoclasts and bisphosphonates that interfere with this will inevitably cause failure of proper osteoclast maturation and survival (Woo et al., 2005, Zhang et al., 1995). Additionally, Rho and Rac are involved in regulation of apoptosis. There is also evidence that nitrogen-containing bisphosphonates reduce recruitment of osteoclasts (Hughes et al., 1989) and induce osteoblasts to produce an osteoclast-inhibiting factor (Vitte et al., 1996).

Bisphosphonates are thus recognized as inhibiting osteoclastic activity by four main processes: 1) Induction of osteoclastic apoptosis, 2) inhibition of osteoclastic resorption of bone, 3) inhibition of osteoclastic maturation, and 4) inhibition of osteoclastic recruitment

Pamidronate is a class of bisphosphonate that has shown positive effects on implant fixation in osteoporotic bone, in addition to their well-documented potency to inhibit implant loosening in normal bone (Tengvall et al., 2004). A striking study has shown the application of immobilized bisphosphonate to prevent implant loosening to be more effective and efficient in osteoporotic bone than in normal bone (Tengvall et al., 2004). Studies conducted by Peter et al. (2005) reported an increase in the maximum push-out force in pamidronate by up to 2.9 fold. As briefly mentioned earlier, the elevated osteoclast activity in osteoporosis is considered to precipitate the dissolution of bone mineral and impair the tight coupling between bone formation and resorption, while incomplete filling of resorptive cavities in turn leads to the net bone loss and implant loosening. If compared with normal bone, osteoporotic bone provides a larger region capable of being exposed to any drugs being delivered; the local resorption and osteoclastic activities at the site of implantation are also much stronger.

In such conditions, immobilized bisphosphonate not only reduces the aseptic loosening associated with particulate debris but can also inhibit the osteoporotic related osteolysis around the implant which can in turn shift the dynamic equilibrium of bone metabolism in favour of stronger bone (Gao et al., 2009).

To summarize the effect of bisphosphonate at the cellular level, there is general agreement that a decrease in the osteoclast number can occur either through direction action on osteoclast precursors, or indirectly by stimulating the osteoblasts to produce an inhibitor of osteoclast formation.

4.1.2 Liposome Coatings

Radin et al. (1997) reported that antibiotic loading into calcium phosphate ceramics followed by lipid coating to slow antibiotic elution was a more effective method than drug loading without lipid coating. Over 30 years ago Bangham discovered that phospholipids spontaneously form closed spherical or oval structures in aqueous solutions which are often referred to as liposomes. Due to their similarity to biological membranes, liposomes have been used extensively in basic research to model cell membranes as well as drug delivery agents. Liposomes consist of a single or multiple concentric lipid bilayers that encapsulate an aqueous compartment. Biocompatibility, biodegradability, reduced toxicity and capacity for size and surface manipulations comprise the outstanding profile that liposomes offer compared to other delivery systems. Huang et al (1997) have used liposome-coated hydroxyapatite and tricalcium phosphate as bone implants. These studies were carried out in the mandibular bony defect of miniature swine, and they found that the liposome-coated materials were biocompatible.

Liposomes are of considerable interest as carriers for the controlled delivery of drugs which exploits the protective nature of the phospholipids to encapsulate and entrap a wide range of solutes including drugs, contrast agents, genetic material, enzymes, and other biomolecules and deliver them to a specific site *in-vivo*.

The primary functional characteristic of liposomes that render them useful for drug delivery technology can potentially be exploited to coat microspheres to control the release of encapsulated drugs. Pharmaceutical drugs can be incorporated without loss of their activity within the hydrophobic domain of vesicle membranes, acting as a size-selective filter, only allowing passive diffusion of small solutes such as ions, nutrients and antibiotics(Dwarakanadha and Swarnalatha, 2010). Thus, drugs that are coated are effectively protected from premature degradation. The drug molecule, however, is able to diffuse through the liposome membrane, driven by the concentration difference between the interior and the exterior of the microsphere.

4.2 Equipment and Procedure

The protocols utilized and developed for the bisphosphonate experiments are described in the following section. The incorporation of bishphosphonate to the β-TCP microsphere was observed under the scanning electron microscope. To identify the adsorption of the bisphosphonte to the β-TCP microspheres the sample was examined by EDS analysis by comparing the phosphate intensity since phosphate is present in both the microsphere and in the bisphosphonate structure and X-ray photoelectron spectroscopy (XPS) analysis. XPS analysis was utilized to identify the unique nitrogen element within the bisphosphonate's chemical structure. The presence of phosphorous is inherently present in β-TCP, and hence it was not an appropriate marker for the presence of pamidronate by XPS. Instead nitrogen, which is foreign to the β-TCP sample, provided a convenient marker element. Various analytical chemistry methods can be employed to study the bisphosphonate release profile, however they require strict sample preparation and are often time consuming. Due to instrumentation restrictions, the bisphosphonate release profile was measured using a newly developed and published technique by our research group (Chou et al., 2009) using quantitative nuclear magnetic resonance (NMR) spectroscopy.

Bisphosphonate loading - It is noted that due to the uniqueness of bisphosphonates high affinity for calcium it would bind strongly to the β-TCP microspheres. Each β-TCP microspheres were taken and weighed before and after BP adsorption for percentage loading calculations. The microspheres were immersed in 3mg/mL bisphosphonate solution (Pamidronate disodium salt hydrate, Sigma Aldrich) for two hours and removed and air-dried at room temperature. The loading efficiency of the bisphosphonate was calculated according to the following equation.

$$Encapsulation\ Efficiency\ (\%) = \frac{Actual\ drug\ incorporated}{Theoretical\ drug\ incorporated}$$

Bisphosphonate release profile study - The use of quantitative nuclear magnetic resonance spectroscopy (^{1}H -NMR) in determining the solvent residues of various pharmaceutical drugs has been proven to be successful for many years (Avdovich et al. 1991). Bisphosphonate powders (MW-279.03, Sigma Aldrich) were dissolved in deuterium oxide (D_2O,Sigma Aldrich) solution. D_2O solution was used as the solvent, the internal standard was 3-(trimethylsilyl) 3,3,2,2-tetradeuterapropionic acid Na salt. Benzylamine (Sigma Aldirch) was chosen as the reference. Benzylamine has similar a functional group CH_2-NH_2 to that of the bisphosphonate drug. The bisphosphonate was measured using liquid-state proton nuclear magnetic resonance spectroscopy (300 MHz Bruker (DRX) Nuclear Magnetic Resonance Spectrometer). β-TCP microsphere was immersed in 1mL of distilled water at 37°C. The concentration of bishphosphonate in the solution was measured every 2h for 24h. D_2O (Sigma Aldrich) was used as the internal standard and benzylamine (Sigma Aldrich) was used as the reference.

Identifying Bisphosphonate on Surface - Adsorption of bisphosphonate onto the microsphere was determined by the unique nitrogen N 1s signal from the spectrum around 400eV by x-ray photoelectron spectroscopy (XPS) using Mg Kα radiation source. The elements detected from the surface analysis spectrum were taken from 0-1100eV.

Electron Microscopy - The surface characterization of the β-TCP microspheres following adsorption of bisphosphonate, was performed on a Philips (FEI) XL 30 ESEM. The microscope was operated in low vacuum mode at 0.8 Torr, 20kV accelerating voltage and a working distance of 10mm, using the back scattered electron detector (BSE).

Liposome Coating - Liposomes were prepared by mixing DMPC and cholesterol in a 10:1 molar ratio. Cholesterol, 1,2-Dimyristoyl-sn-glycero-3 phosphocholine (DMPC), chloroform and rhodamine dye were purchased from Sigma-Aldrich Australia Ltd. Briefly 100mg of DMPC were dissolved in 1 mL of chloroform and 14mg of cholesterol were dissolved in 100 µL of chloroform. Both were then mixed together and aliquots of 200 µL were transferred to each test tube. To ensure the complete removal of the chloroform, the test tubes were put on a rotator while having nitrogen gas flow over the lipid film for 2 hours. The lipids were than further dried in a desiccator, leaving a thin film of lipid and cholesterol at the base of the test tube.

Lipid coating of Microspheres - The lipid-cholesterol film was reconstituted by rehydrating with 2mL of phosphate-buffered saline (PBS) and sonicated for 10 mins with the microspheres in the PBS solution. To test the successful coating of the lipids to the β-TCP microspheres, rhodamine dye was used to stain the lipid. They were then observed under the fluorescent microscope. Rhodamine dye (200µL) was introduced into the lipid coated microsphere solution for 40 minutes followed by washing with PBS to wash off any excess dyes. A positive and negative control was used for testing the staining of the lipid coating.

4.3 Results and Discussions

4.3.1 Bisphosphonate Loading

β-TCP microsphere samples loaded with bisphosphonate were weighed before and after loading to obtain the average loading per sample. The average loading per sample was found to be 0.8 mg for n=10. The encapsulation efficiency of bisphosphonate was 84% ± 9. Figure 4.2 is an SEM image showing pure bisphosphonate powder resembling platelet structures. This image serves as a control for visual verification of bisphosphonate loading onto the microsphere in the following section.

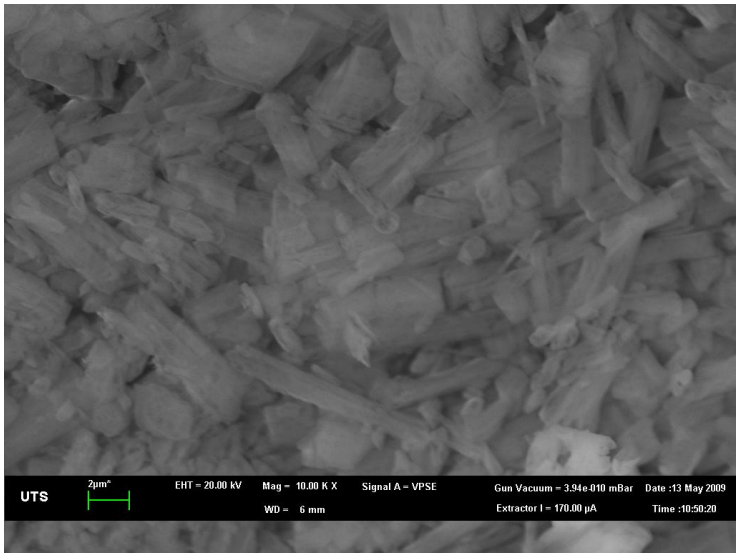

Figure 4.2 SEM micrograph showing pure bisphosphonate powder having a long platelet structure.

4.3.2 Surface Characterization After Bisphosphonate Loading

The presence of bisphosphonate was visually confirmed by means of environmental scanning electron microscopy (ESEM). Figure 4.3 showed that after loading the surface of the β -TCP microspheres had successfully adsorbed the bisphosphonate platelets throughout the entire surface, in large abundance. The amount adsorbed as noted visually, would suggest a high loading efficiency. These observations were made over six samples.

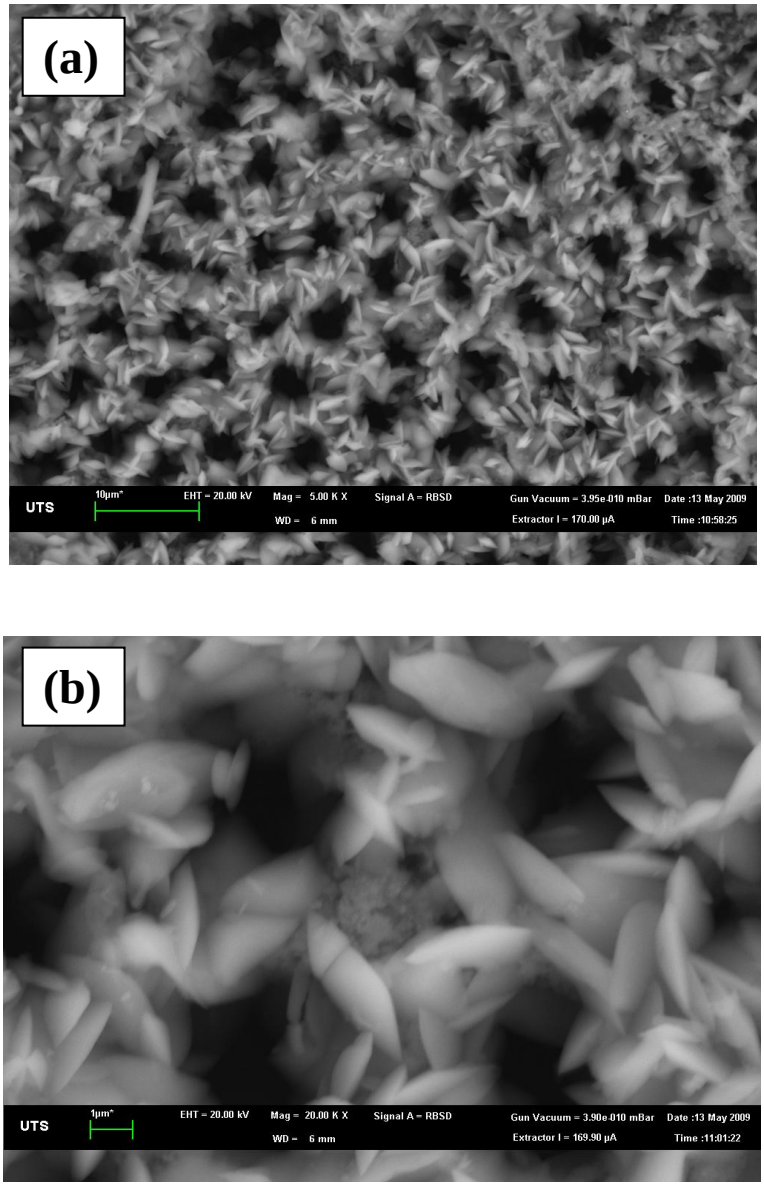

Figure 4.3 ESEM image showing bisphosphonate adsorb to surface of β-TCP microspheres aligned as platelets at (a) lower magnification and at (b) higher magnification.

The loaded microspheres were then broken in half to observe the adsorption penetration of the bisphosphonate into the interior of the microspheres. Figure 4.4 (a) is a cross section view of the central core chamber of the microsphere and it can be seen under 500x magnification that there are particulates present in the core. To verify this a higher magnification SEM image was taken as shown in Figure 4.4 (b) which clearly shows the presence of platelet structures of the bisphosphonate had been adsorbed.

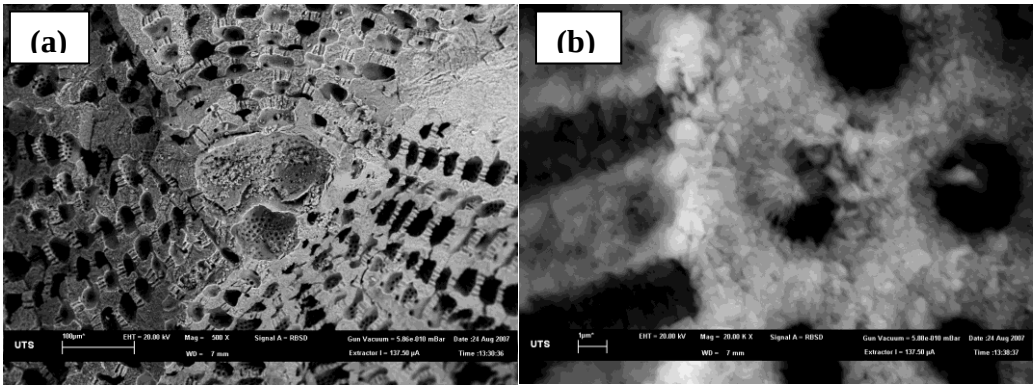

Figure 4.4 SEM image showing a) bisphosphonate adsorption all the way to the central core of the β-TCP microsphere and b) higher magnification of the pores from the core of the microsphere.

It can be concluded that due to the high affinity of bisphosphonate for calcium phosphate, the β-TCP microsphere is not only capable of adsorbing drugs, but these drugs can permeate within the interconnected porous network which is highly advantageous for slow drug delivery applications to delay the release of the drug rather than their release occurring as an initial burst.

4.3.3 Identifying the presence of bisphosphonate by EDS Analysis

Upon visually confirming the presence of bisphosphonate adsorption to the microsphere the next step was to confirm this by chemical analysis. The presence of phosphate can be found in the chemical composition of bisphosphonate which would suggest the area where the bisphosphonate was adsorbed should have a higher phosphate concentration compared to the microsphere. The EDS intensity count for the phosphate (P) contributed by the bisphosphonate and by the β–TCP microsphere was 261 (Figure 4.5 (a)) and 210 (Figure 4.5 (b)) respectively. This increase in the phosphate intensity further strengthens the case for confirming the presence of bisphosphonate on the microspheres. As phosphate is present in both the drug and the sample this can cause conflicting results, so an additional method was employed to resolve this discrepancy.

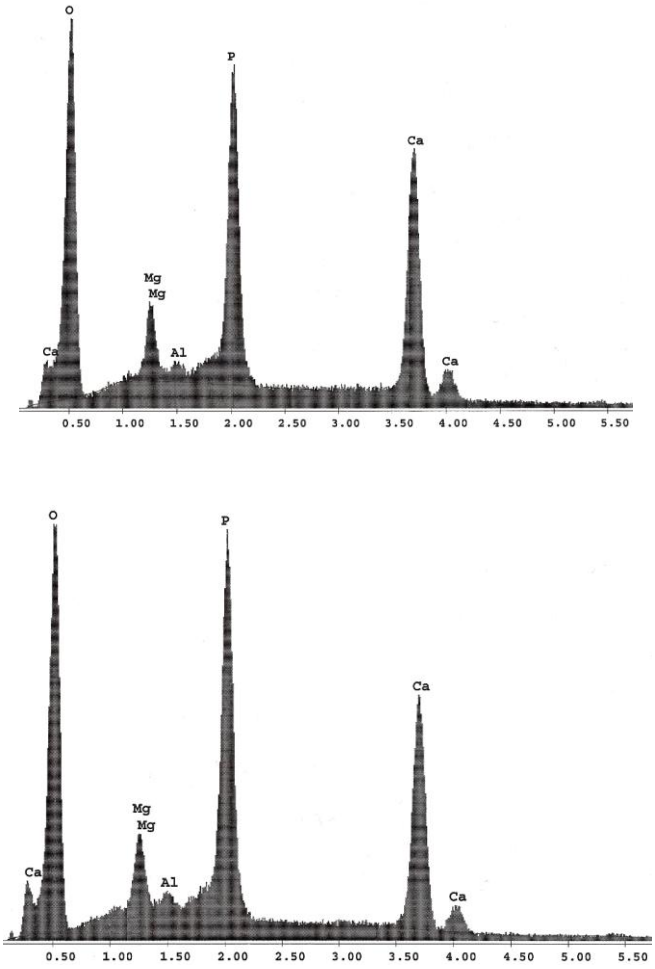

Figure 4.5 EDS image of (a) β–TCP microsphere and (b) bisphosphonate powder on surface of microsphere.

4.3.4 X-ray photoelectron spectroscopy (XPS) chemical state analysis

The nitrogen (N 1s) photoelectron signal was chosen as the identifying marker of the bisphosphonates as it is foreign to the β -TCP microsphere sample. The phosphate (P 2p) signal from the bisphosphonate could suffer from interference from the P 2p contributed by the underlying β -TCP sample hence it was not used. The XPS survey spectra in Figure 4.6 shows the detected photoelectron signals to be nitrogen (400eV), carbon (284.8) and oxygen (531eV). From the spectra the detected N 1s photoelectron signal is relatively weak, as was expected, since the presence of nitrogen in bisphosphonate only constitutes 6.7 at. % of the chemical composition and therefore its XPS sensitivity factor will be relatively low. This further confirmed that bisphosphonate had been successfully adsorbed onto the β –TCP microspheres.

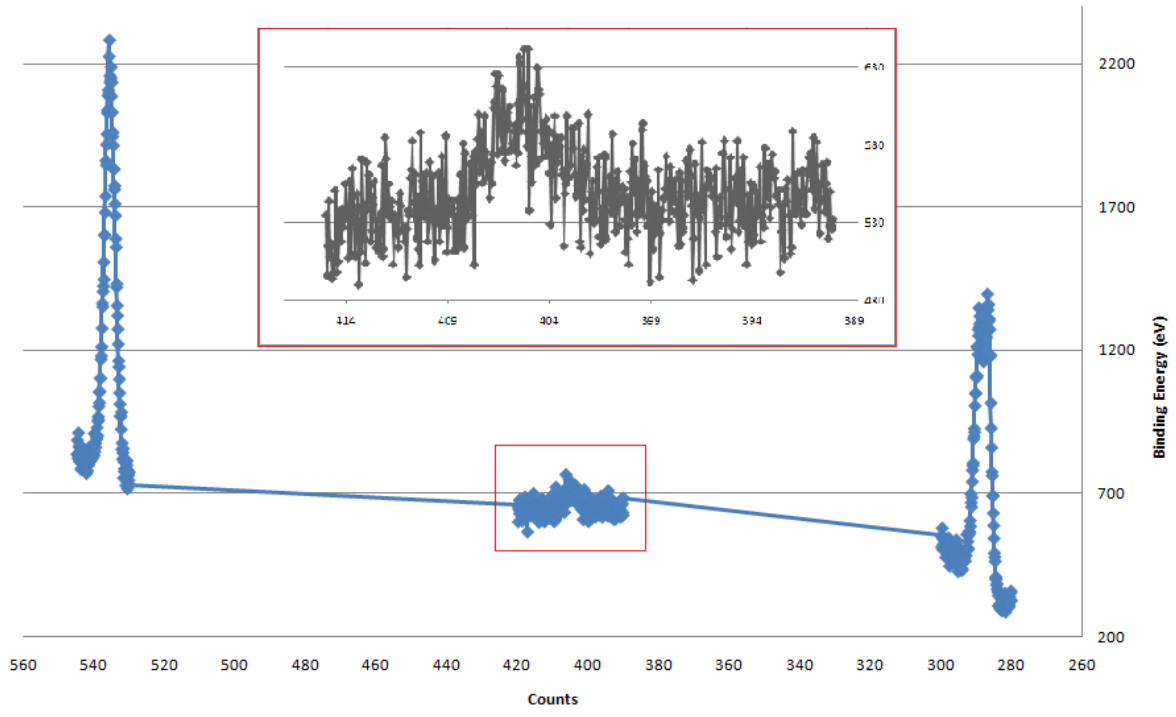

Figure 4.6 XPS chemical spectra showing identifying the nitrogen (N 1S) band contributing from the bisphosphonate at 400eV.

4.3.5 Bisphosphonate Release Profile

In-vitro release of bisphosphonate from β-TCP microsphere was profiled for 21 days, with a new and accurate method of measurement using quantitative NMR spectroscopy developed for this research project. Figure 4.7 shows the coupled dissolution of bisphosphonate and β-TCP microspheres.

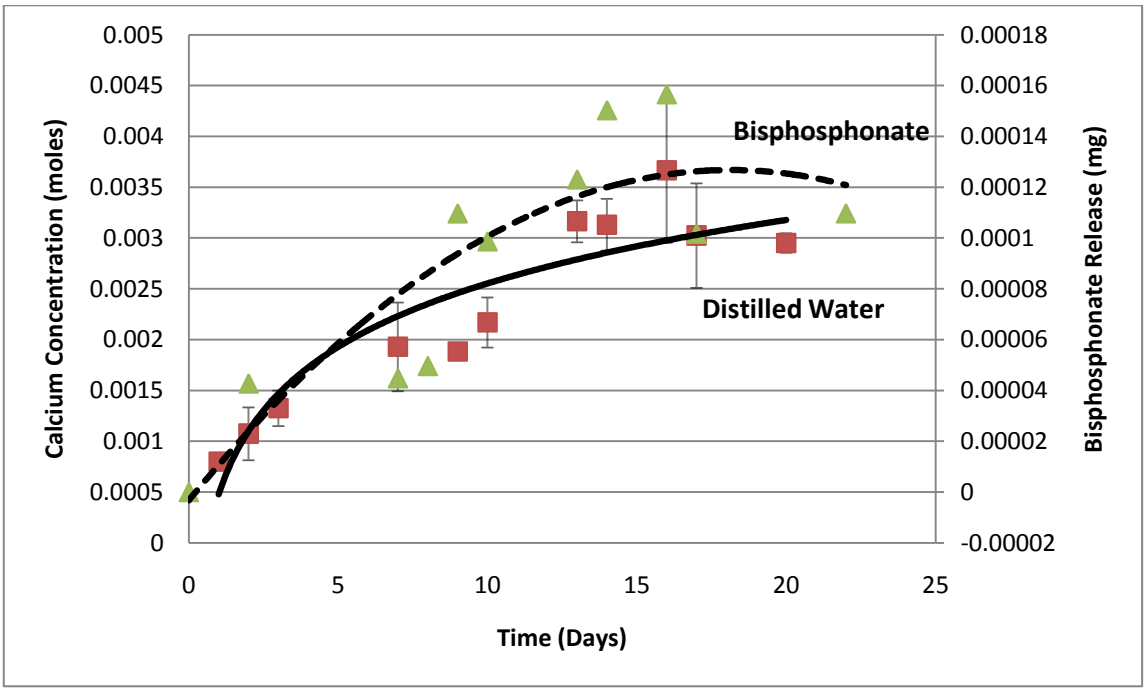

Figure 4.7 Coupled release profiles of bisphosphonate (mg released) and microspheres (n=3). The close correlation shows that shell degradation is an important mechanism for bisphosphonate release. It also shows the slow gradual cumulative release of bisphosphonate for 21 days.

The upper dashed-line profile shows a cumulative release of bisphosphonate sustained over 21 days reaching 12mg, while the lower unbroken line profile shows a similarly gradual decomposition of the β-TCP microsphere closely coupled to bisphosphonate release which total 12% decomposition of the bisphosphonate incorporated. However it is important to note that the presence of the bisphosphonate was still detectable during an observation period of more than 21 days, which is a key period for the early bone formation and implant-bone osseointegration. It is postulated that the bisphosphonate binds directly to the β-TCP microspheres and is released slowly over time.

As a bone graft it can be expected that it would exert apoptotic effects on osteoclast cells and improve implant fixation in osteoporotic bone. This can only eventuate when these compounds are internalized by the osteoclasts and the intracellular concentration has increased up to sufficient amount to induce apoptosis (van Beek et al., 1999).

4.3.6 Lipid Coating of β-TCP Microsphere

Fine tuning of drug elution is a necessity if we are to synchronize drug action with host biochemistry. A first important step to this end was made by coating the microspheres in a lipid film. A sacrificial lipid layer was coated onto individual shells to provide a permeable barrier that could slow down bisphosphonate elution. Attached lipid was labelled with rhodamine and visualized using fluorescence microscopy by positive fluorescence expression as shown in Figure 4.8. The fluorescence signal was not attributable to auto-fluorescence as the microsphere in itself did not show any fluorescence.

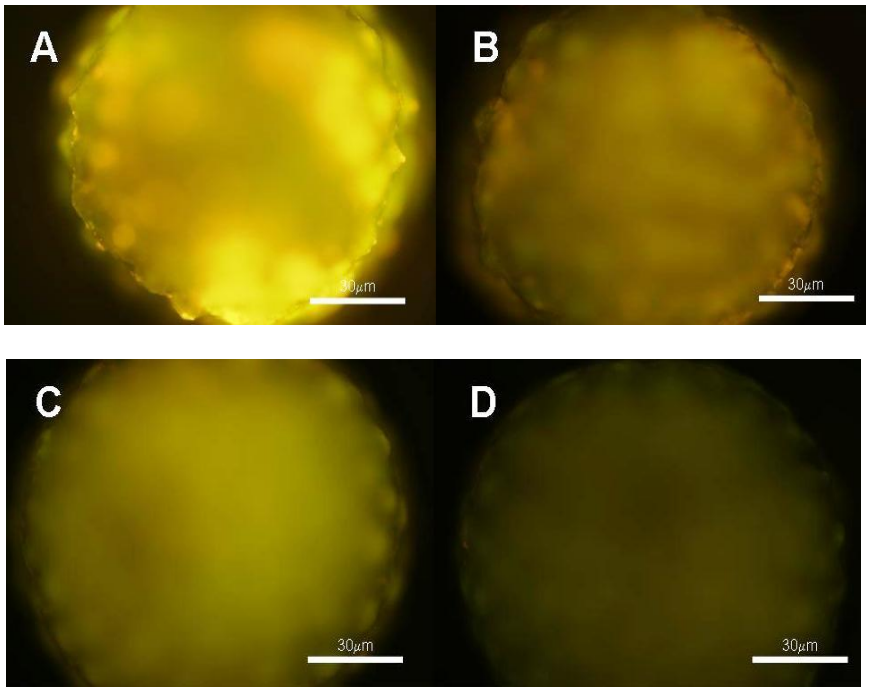

Figure 4.8 Demonstration of liposome coated β-TCP microsphere with fluorescent dye and its degradation over time. Lipid was stained with rhodamine and the strength of the dye was imaged at (A) 3, (B) 13, (C) 22 and (D) 72 days immersed in solution.

The spheres were then viewed at day 3, 13, 22 and 72 days. At day 3 a strong fluorescence signal was still visible. This however rapidly dissipates at day 13 (Figure 4.8 B) when the lipid coating de-couples from the shell and the level of observed fluorescence matches the non-lipid coated control at 72 days (Figure 4.8 D). Lipid was selected to provide a versatile platform for the effective attachment and presentation of any candidate biological molecule that can target specific tissue regions with much higher resolution such as a single cell type. We therefore, envisage decorating the lipid layer with homing peptides or antibody fragments so that each individual shell could remotely attach itself to a specific cell or tissue region expressing a complimentary receptor.

4.4 Conclusion

From the above experiments it can be concluded that bisphosphonate was successfully adsorbed onto the β-TCP microspheres. This is primarily determined by the detection of the key bisphosphonate element nitrogen in the XPS spectra and the comparison of the phosphate intensity increased from the EDS analysis. The adsorption onto the surface of the microsphere was confirmed by scanning electron microscopy which showed uniform distribution of bisphosphonate from the surface throughout the internal architecture of the microsphere. The bisphosphonate release profile showed that after 12 days, approximately 12% of the drug was released which is very promising as this would suggest that the rest remained within the sample. The successful coating of the liposome film is a proof of concept that the drug release can be further controlled for up to 72 days.

5 BIOLOGICAL EVALUATION OF CELL AND MICROSPHERE INTERACTIONS

5.1 Introduction

Biological evaluation is of great importance in assessing the potential benefit of implantable materials for biomedical applications. Biocompatibility testing allows us to evaluate the "biosafety" and the material's ability to perform with appropriate host responses in a specific application. *In-vitro* studies are an integral part of biological testing for potential implant materials. In today's competitive research environment time, effort, cost, increasing restriction and lack of precise basic data derived from animal experimentation, have lead to *in-vitro* testing becoming a major tool for evaluating the basal and specific cytocompatibility of new and modified materials for biomedical applications. *In-vitro* procedures are the basic starting point whereby biological response to materials are determined initially, as required by a number of standardization agencies (Kirkpatrick, 1992).

For the purpose of this research, it was necessary to evaluate the biological effects of bisphosphonate and observe its effect on the release of strontium using the human bone osteoblastic cell line (SaOS-2) and human moncytoid cell line (U937).

5.2 Equipment and Procedure

Osteoblast cell culture - Cultures of SaOS-2 cells were grown in 15% FBS in McCoy's 5A medium (Invitrogen 12330-031) and incubated at 37°C, 5% CO_2. Cells were passage with Trypsin-EDTA (Sigma T4299) for 15 minutes. SaOS-2 cells were cultured over the microsphere samples at a concentration of $3.3x10^4$ cell/mL and incubated for 3 and 7 days in a controlled atmosphere conditions. Tissue culture grade polystyrene was used as control and replicates were prepared. SaOS-2 cells were assayed for initial attachment, adhesion, viability and proliferation. After the prescribed incubation periods the live cells were incubated with 10% alamar blue in cell culture media for 2 hours and the fluorescence intensity of the supernatant was read by BioTek Synergy™ HT Multi-Mode Microplate Reader and the cell number was determined by standard curve.

Imaging of Osteoblast cells - The SaOS-2 cells incubated were imaged with the microspheres using the Philips (FEI) XL 30 environmental scanning electron microscope (ESEM). The microscope was operated in low vacuum mode at 0.8 Torr, 20kV accelerating voltage and a working distance of 10mm, using the back scattered electron detector (BSE).

U937 Monocytoid Cell Culture –

The U937 cell line is a human cell line established from a diffuse histiocytic lymphoma and displaying many monocytic characteristics It serves as an *in-vitro* model for monocyte/macrophage differentiation. Both cell cultures were maintained for appropriate time periods and culture conditions and cell behavior was assessed in terms of attachment and spreading, morphology and cell viability/proliferation. The cell response was evaluated by a direct assay, which involved culturing the cells on the material's surface. The major advantage of the direct assay is that is closely mimics physiological conditions by establishing a concentration gradient of chemicals, which diffuse away from the cells, as it would occur in intact tissues *in-situ*. In addition, studying such direct cell-surface interactions, the surface charge, surface topography and surface free energy play a

fundamental part in cell adhesion, spreading, growth, and, ultimately, function of the cell. In addition, cultures were observed by scanning electron microscopy (SEM). Human monocytoid cell line (U937) were maintained in RPMI1640 media supplemented with 20mM HEPES buffer solution (Gibco BRL), 2mM L-glutamine (Sigma Aldrich) and 10% fetal calf serum (Gibco BRL), in a humidified incubator at 37°C, 5% CO_2. U937 cells were cultured in the presence of microsphere samples in a concentration of $3.3x10^4$ cells/mL and incubated for 3 and 7 days in controlled atmosphere conditions. Tissue culture grade polystyrene was used as a control. All samples were prepared in duplicate.

Statistical analysis – The cell proliferation results are expressed as mean ± SD. The statistical differences among groups were evaluated using the Q- test with 99% confidence. All in-vitro cell culture experiment were conducted in triplicate.

5.3 Results and Discussion

5.3.1 SaOS-2 Human Osteoblast Cell Proliferation

To determine the effect of bisphosphonate on the viability of the osteoblast cells, proliferation experiments were undertaken to ensure that the adsorbed bisphosphonate is not toxic to the osteoblast cell survival. As mentioned previously, bisphosphonates are known to cause apoptosis in osteoclast cells and therefore should not have any detrimental effects to osteoblast cells. Figure 5.1 shows that the number of osteoblast cells exposed to the bisphosphonate loaded microspheres increased significantly over a seven day period when compared with just the osteoblast cell with the microsphere (control). The experiment was repeated 3 times for reproducibility. Interestingly the results would suggest bisphosphonate has the ability to enhance osteoblast cell proliferation.

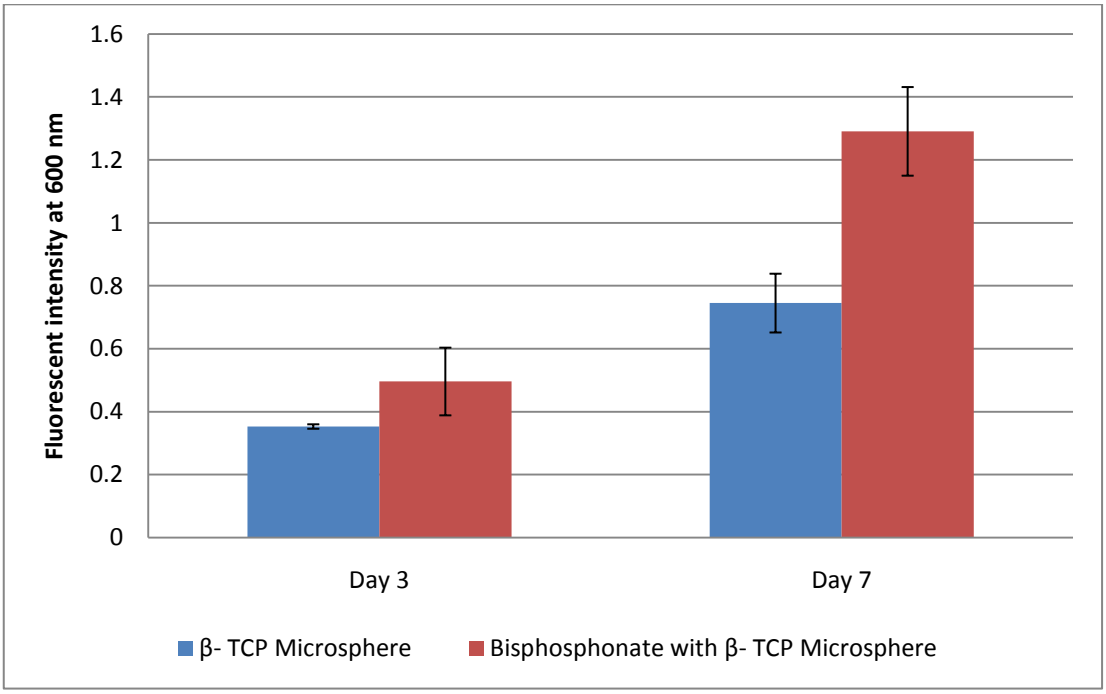

Figure 5.1 Osteoblast cell proliferation for 3 and 7 days showing an increase of cell numbers when exposed to bisphopshonate loaded β-TCP microsphere.

5.3.2 Examination of SaOS-2 Cell Attachment by ESEM

When examining the attachment of the SaOS-2 osteoblast cells on glass, they were first imaged in their natural state to help when identifying when exposed to the microspheres. Figure 5.2 is a light microscope image showing the cells possess an elongated structure after proliferation but when first seeded they have a circular structure.

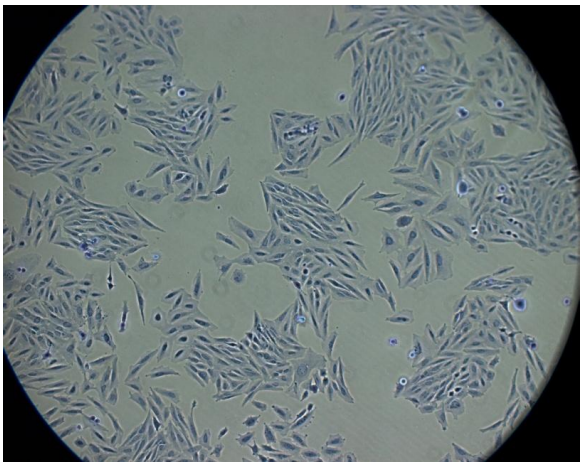

Figure 5.2 Light microscope image of SaOS-2 osteoblast cell showing the elongated structure of the cells after 3 days of seeding.

Figure 5.3 shows the SaOS-2 cell attached to the β-TCP microspheres which shows that the cells were still in the process of spreading.

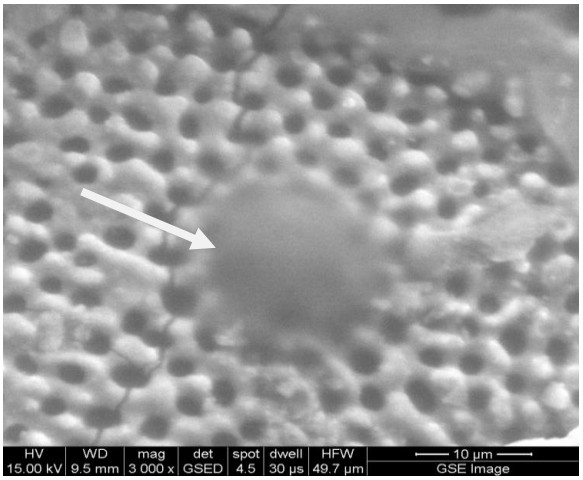

Figure 5.3 ESEM image of SaOS-2 cell after 3 days of seeding on β-TCP microsphere.

Figure 5.4 demonstrates the adhesion and spreading of an SaOS-2 osteoblast cell onto the bisphosphonate loaded microsphere after 3 days of seeding. These cells have the same physical structure (elongated) as the control cells observed in Figure 5.3

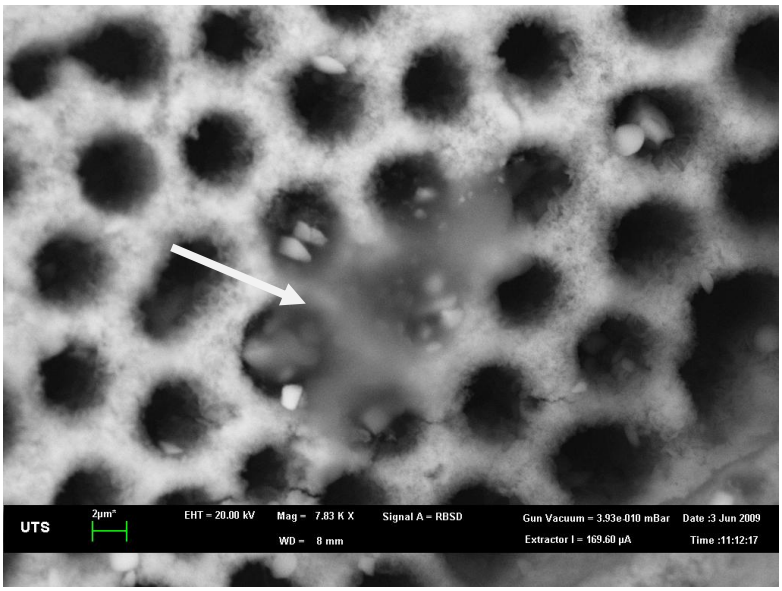

Figure 5.4 ESEM image showing attachment of SaOS-2 cell to the surface of the bisphosphonate incorporated β-TCP microsphere as indicated by the white arrow.

With the presence of the bisphosphonate incorporated on the surface, the cells presented a more flatten morphology, reflecting higher number of adhesion points to the surface as observed in figure 5.4. This behaviour indicates a superior affinity to this type of surface compared with the cells that adhered to the sample without the bisphosphonate. An important objective of bone tissue engineering is to develop improved scaffold materials or arrangement to control osteoblast behavior significantly affecting its response. Divalent cations including strontium are known to be active in cell adhesion mechanisms and proliferation (Reginster, 2002). The present investigation demonstrates that the SaOS-2 osteoblast cells are spreading well and it seems that the presence of strontium encourages the spreading and adhesion of osetoblasts cells onto the matrices. This makes bisphosphonate loaded β-TCP microsphere a promising candidate for bone tissue engineering.

5.3.3 Effect of Bisphosphonate on Human Monocytoid Cell Line (U937) Proliferation

The next important step was to confirm whether bisphosphonate remained active following its release from the β-TCP microspheres. As previously mentioned U937 cells were selected as they serve as an *in-vitro* model for macrophage differentiation. Bisphosphonate is known to act on U937 cells by inducing apoptosis through inhibition of cholesterol synthesis pathway and cyclosporin A-insensitive mitochondrial pathway (Hirofumi et al., 2004). In Figure 5.5 it can be seen that in a 3 day period, there was already a significant decrease in cell number. As expected U937 proliferation was inhibited showing that microsphere-derived bisphosphonate was active. Interestingly the microspheres by themselves also showed effects of inhibiting cell growth.

As mentioned in the previous chapter, the chemical composition of the microspheres had been determined by ICP-MS following hydrothermal conversion. The microspheres were found to only contain calcium, phosphates, magnesium and strontium. Research has shown that strontium is capable of promoting osteoblast cell growth, while inhibiting osteoclast cells. Contrary to other drugs used in osteoporosis treatment, which act by either increasing bone formation or decreasing bone resorption, strontium does both simultaneously. It increases bone cell replication and bone formation *in-vitro*, by increasing the pre-osteoblastic cell replication and by secondary or primary increases in the synthesis of bone matrix (Canalis et al., 1996). By monitoring the expression of carbonic anhydrase and fibronectin receptor it was concluded that osteoclast differentiation is decreased by strontium, leading to inhibition of bone resorption (Baron and Tsouderos, 2002). Strontium exerts its effects on bone cells through a novel mechanism of action, which is thought to result directly from the bone-seeking properties of strontium (Farlay et al., 2005). Sr^{2+} may increase in the bone micro-environment during the process of bone resorption, as shown for Ca^{2+} (Silver et al., 1988), and modulate the activity of osteoblasts and osteoclasts within the vicinity (Marie, 2005, Marie, 2006).

Thus, strontium increases osteoblastic replication and synthesis of the collagenous matrix (Edith et al., 2008, Canalis et al., 1996, Barbara et al., 2004) and reduces osteoclastic bone resorption (Baron and Tsouderos, 2002, Takahashi et al., 2003)

The results presented here suggest that the release of strontium from the microspheres is sufficient to have an effect on the proliferation of U937 and coupled with bisphosphonate this effect can be further enhanced. This research has shown that 159 μM is enough to observe the therapeutic effects of strontium in both the human osteoblast cells and the monocytoid cell lines in-vitro.
This is a clear demonstration of biomimicry at its best.

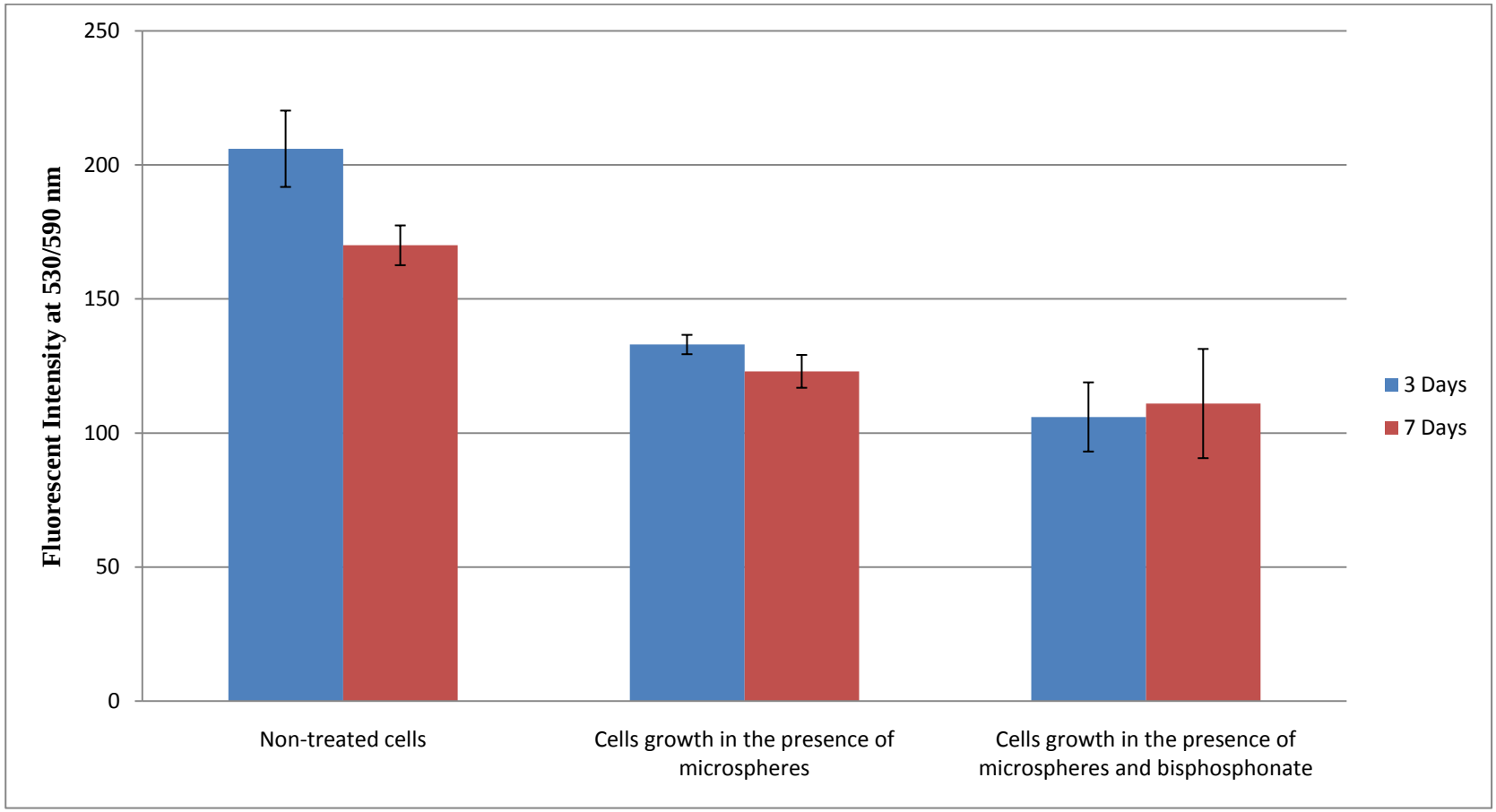

Figure 5.5 Demonstration of functional activity of bisphosphonate from β-TCP microsphere upon macrophages at 3 and 7 days. Inhibition of U937 proliferation by bisphosphonate loaded shells is significant compared to cells cultured in their absence. Interestingly inhibition is also affected by the shells themselves (n=6).

5.4 Conclusion

The effect of adsorbed bisphosphonate on osteoblasts at 3 and 7 days, was found to be non-detrimental to osteoblast survival. Bisphosphonates at a concentration of 159 μM cause apoptosis in macrophages (Hirofumi et al., 2004) but this should not be detrimental to osteoblast cells. We see that the number of osteoblast cells increased significantly over a seven day period compared with cells seeded on just the microsphere. From microscopic examination the osteoblasts presented a more flatten morphology an indication of more cell attachment points on the surface. This behaviour could indicate a stronger affinity to this type of surface compared with the cells that adhered to the sample without bisphosphonate. This biomaterial is composed of a hydroxyapatite matrix with bioresorbable β-tricalcium phosphate phase, which is more soluble than single hydroxyapatite and thereby would be liberating Ca and P ionic species to the local environment. Surface reactions occurring as a result of ongoing dissolution/deposition events appeared to also induce osteoblastic growth and differentiation. Supplementary to this is the inhibition of U937 by the shells themselves. The results showed significant decrease in cell number by both the microsphere and bisphosphonate loaded microspheres. The release of strontium ions from the microsphere may also have a positive contribution, as this ion is known to have potent influence on osteoblast cell proliferation and osteoclast cell inhibition (Bonnelye et al., 2008).

6 ANTIBIOTIC LOADED MICROSPHERES INHIBIT BACTERIAL GROWTH

6.1 Bacterial Infections Associated with Implants

One of the major challenges in using biomaterials is the occurrence of bacterial infections during and after implantation. Bacterial adhesion to biomaterials and the ability of many microorganisms to form biofilms on foreign bodies are well-established as major contributors to the pathogenesis of implant-associated infections (Katsikogianni and Missirlis, 2004). Bacteria adhere to the bone matrix and to orthopaedic implants and elude both the host's defences and antibiotics by developing a slimy film or acquiring a very slow metabolic rate (Moran Aviv, 2007). Bacterial contamination can occur at the time of operation by air pollution or by direct contagion. Control and prevention are effective by an aseptic ritual, by operating only on patients free from overt sepsis, and by using prophylactic antibiotics systemically or locally. The effects of late deep infection (pain and loosening at the implant interface) can subsequently lead to implant failure (Elson et al., 1984).

Orthopaedic implants are susceptible to microbial infections such as *Staphylococcus aureus (S. aureus) which* is a normal skin commensal of low virulence, but has the ability to adhere to, and colonise, implanted material. This infection may take weeks or months to become clinically apparent (Thomes B, 2002). These infections often lead to osteomyelitis which can eventually lead to the failure of the implant due to localised bone destruction. Osteomyelitis is refractory because of the characteristics of bone. The soft tissues of bone are surrounded by hard walls, and inflammation of the contained tissues cause circulatory disturbances which can readily lead to necrosis of various parts of the bone. These anatomical features provide an environment suited for the localization and colonization by bacteria. Osteolysis with loosening of the prosthesis is the most common cause of failure in total joint arthroplasty and it us usually initiated by a number of material, device, site and host specific biological and mechanical events. These include fragmentation and wear of the implant materials, release of particles into the tissue to provoke a foreign body reaction, stress shielding due to stiffness mismatch between the implant material and the

surrounding bone, and activation of cells to produce a variety of cytokines and proteolytic enzymes. It is therefore vital to develop successful strategies to minimise ostoelysis, as these would reduce the costs to both the patient and healthcare providers associated with revision surgery to replace failed prostheses (Ganguli et al., 2005).

6.1.1 Biofilm Formation

According to the National Institutes of Health, “more than 60% of all microbial infections are caused by “biofilms” (Lewis, 2001). The development of microbial biofilms and their importance in medical implant infections have being extensively researched over the years. Microbial biofilms cause over 2 million infections annually, generating over $11 billion in additional patient costs (Emerson and Camesano, 2004).

The development of a biofilm is initiated when bacterial cells attach to a surface and begin to excrete slimy, glue-like substances, which serve to anchor the cells (O'Toole and Kolter, 1999). The adhesion of microorganisms that occurs on the surface is facilitated by bacterial signalling. Biofilms are enclosed within an exopolymer matrix that can restrict the diffusion of substances and bind antimicrobials (Lewis, 2001). This effectively provides resistance for biofilm cells against large molecules such as antimicrobial proteins lysozyme and complement. The negatively charged exopolysaccharide is very effective in protecting cells from positively charged aminoglycoside antibiotics by restricting their permeation, possibly through binding (Emerson and Camesano, 2004). A mature biofilm is characterised when adherent bacteria produce extracellular polymeric substances (EPSs) that aid in trapping nutrients from the surrounding environment. The final stage is the release of microorganisms back into their surroundings.

The environment created by the biofilm enhances antimicrobial resistance. The EPSs of biofilms contain considerable amounts of polysaccharides, proteins, nucleic acids and lipids, which are responsible for maintaining the structural integrity of the biofilm and providing an ideal matrix for bacterial cell growth. Intermolecular interactions between the functional groups within these macromolecules serve to strengthen the overall mechanical stability of the EPSs and the survivability of the microorganisms. The biofilm exopolymer physically protects the cells from body's immune system. One can envisage the survival dynamic of a biofilm *in-vivo* in which an initial application of antibiotic eradicates most of the population, leaving behind a small fraction of survivors. If the concentration of the antibiotic temporarily drops or if symptoms disappear due to the eradication of the planktonic cells and therapy is thus discontinued, the remaining bacteria will reform the biofilm, which will begin to shed off new planktonic cells. This dynamic explains the relapsing nature of biofilm infections and the need for lengthy antibiotic delivery (Emerson and Camesano, 2004).

6.1.2 Bacterial Infections in Biomaterials

After implantation there is a "race for the surface" between bacteria and tissue cells for reactive domains at a conditioned surface. If bacterial colonization is established on a synthetic surface, it is difficult to eliminate because of the enhanced bacterial resistance to both antibiotics and host defence mechanisms for organisms encased in biofilm. To combat these infections antibiotics are administered to the affected area to eliminate the bacteria. However, one must remember that antibiotics do not kill cells but cause damage that triggers cell suicide which results in cell apoptosis induced by damage from toxic factors. As antibiotics cannot be intravenously delivered directly to an infected bone at a sufficiently high concentration without producing systemic toxic effects, local administration such as closed irrigation and suction, local injection and implantable pumps are widely used but are regarded as clinically inconvenient (O'Gara and Humphreys, 2001).

Currently the most extensively studied and commercially available material for local antibiotic delivery is polymethylmethacrylate (PMMA), which is typically combined with antibiotics like gentamicin (Blaha et al., 1993, Mohanty et al., 2003), tobramycin (Chisholm et al., 1993) and vancomycin (Scott et al., 1988).
The use of antibiotic incorporated PMMA beads as drug delivery systems have been shown to be reasonably successful but have been limited due to their low biocompatibility, low release ratio and possible thermal damage to the antibiotics. To achieve the desired therapeutic effect without any of the side effects, it is necessary to ensure that the initial release of an active drug should exceed the minimum effective concentration into the systemic circulation but should be less than the minimum toxic concentration. After its initial release, the rate of dissolution should be at a constant or near-constant rate with accordance to zero-order kinetics, which would result in a constant, non-fluctuating plasma drug concentration. Attention has therefore been focused on biodegradable antibiotic delivery systems which provide a high, effective concentration at the site of infection with no systemic side effects. Therefore the development of resorbable bone-filling biomaterials with drug incorporated would allow a coupled therapeutic approach, drug release, and bone substitution in a one-step process (Lucas-Girot A., 2005). For example, antibiotic-loaded bone cement has been commercially available in Europe for many years. However, these bone cements were, until recently, not cleared for sale in the United States. In 2003, the FDA approved several antibiotic loaded bone cements for the purpose of preventing further infections in two-stage joint revisions impelled by an infection of the original joint replacement prosthesis (Neut et al., 2005).

Bioceramic drug delivery systems are a suitable candidate in this respect as it is biocompatible in the physiological environment and biodegradable. For slow drug release, porous calcium phosphate is considered more suitable as there is no risk of thermal damage to the antibiotic, that is commonly associated with production of bone cements. Antibiotic incorporated calcium phosphate can serve as both a bone substitute and as a drug carrier to the infected site.

Porous β–tricalcium phosphate (β-TCP), on the other hand, is one of the most biocompatible, resorbable synthetic hard tissue implant materials that can be directly bonded to bone via natural mechanisms to stabilized traumatized bone fractures.

There is a need for a stable drug delivery system that can promote both bone growth and prevent bacterial infections without the need for post surgical operations. Though the threat from bacterial infections can be limited in most modern medical facilities, however one must be practical when it comes to real world surgical applications. Even though antibiotic release from currently available drug delivery systems has proven to be effective towards reducing infection, none of these systems has been investigated for simultaneous or subsequent bone regeneration. Searching for more effective treatments, this study was designed to evaluate the use biodegradable β-TCP microspheres for the controlled release of gentamicin sulfate in the treatment of invasive bacterial infections.

6.2 Equipment and Procedure

Gentamicin loading - Gentamicin sulphate (cell culture tested), *o*-phthaldialdehyde (3µg/mL), isopropyl alcohol (propanol) and pamidronate disodium salts were purchased from Sigma Aldrich. Two different types of microspheres were prepared for antibacterial testing. The first type of sample was gentamicin loaded microsphere (100mg of gentamicin sulphate, Sigma Aldrich) and the second type was gentamicin and bisphosphonate loaded microsphere (100mg/mL of gentamicin sulphate and 3mg/mL of pamidronate, Sigma Aldrich). Gentamicin loading was calculated by taking the difference between the weight of the microspheres before and after loading. All measurements were performed in n=6.

Antibacterial efficacy test - The bacterial strain used in this experiment was *Staphylococcus aureus* (*S. aureus*). The bacterial strain was tested for gentamicin susceptibility by a broth dilution method. The minimum inhibitory concentration (MIC) was defined as the lowest concentration of gentamicin that inhibited growth of the test bacteria. The MIC of *S. aureus* used this study were determined using the broth dilution technique as recommended by the National Committee for Clinical Laboratory Standards (NCCLS). Briefly, serial dilutions of gentamicin (100, 10, 1, 0.1, 0.001 mg/L) in Brain Heart Infusion broth were prepared. Bacterial suspensions were then added to each tube. Tubes containing growth media alone or bacterial culture without gentamicin were included as ngative and positive controls, respectively. The cultures were inspected for bacterial growth after incubation at 37°c for 24 h and the MICS of the gentamcins for each were recorded. *S. aureus* strain was grown overnight in shaking cultures at 37°C in brain heart infusion (BHI) broth and was then subcultured for 3 hours before introducing the gentamicin microspheres. All bacteria were stored on plates at 4°C. Every 30 minutes for up to 350 minutes, 1mL of the bacterial media was extracted to determine the optical density (OD) and subsequently a plot was made for the bacterial growth curve and compared.

Bacterial adhesion test - The bacterial adhesion test was conducted with an overnight culture (16 h) of S. aureus prepared in 10 mL of brain heart infusion (BH1) broth (Merck). By reference to a standard optical density calibration curve the cells were resuspended at a concentration of approximately 10^4 cells/mL. The samples included β-TCP microspheres as control, microspheres with gentamicin and microspheres with gentamicin and bisphosphonate incorporated. 1 mL of the bacterial suspension was added to each well and the plate incubated at 37°C for 24h. On completion of the incubation the β-TCP microspheres were placed into a fresh 24-well plate and repeatedly washed with 2 ml of sterile PBS to remove any loosely adherent bacteria. Each material was then placed into 1 ml of fresh BH1 broth and vortexed at maximum power for 3 minutes to remove bacteria which had adhered to the material. Previous work has shown that few bacteria remain attached to surfaces after this vortex process. 100 µl aliquots of the vortex solutions were serially diluted (200 µl in 2mL) and plated in triplicate onto brain heart infusion (BH1) plates and incubated at 37°C for 17h. The colonies formed from the incubation solutions and vortex solutions were subsequently counted.

Electron microscopy - Scanning electron microscopy (SEM) images of the gentamicin sulphate powder and the gentamicin loaded microspheres were taken with a Philips (FEI) XL 30 ESEM. The microscope was operated in low vacuum mode at 0.8 Torr, 25kV accelerating voltage and a working distance of 10mm, using the back scattered electron detector (BSE).

6.3 Results and Discussion

6.3.1 Gentamicin Loading

β-TCP microsphere samples loaded with gentamicin were weighed before and after loading to obtain the average loading per sample. The average loading per sample was found to be 4.2 mg for n=10.

6.3.2 Surface Analysis of Gentamicin Adhesion

Scanning electron microscopy (SEM) was used to investigate the homogeneity and coating of the gentamicin to the microspheres. Figure 6.1 is an image of pure gentamicin powders.

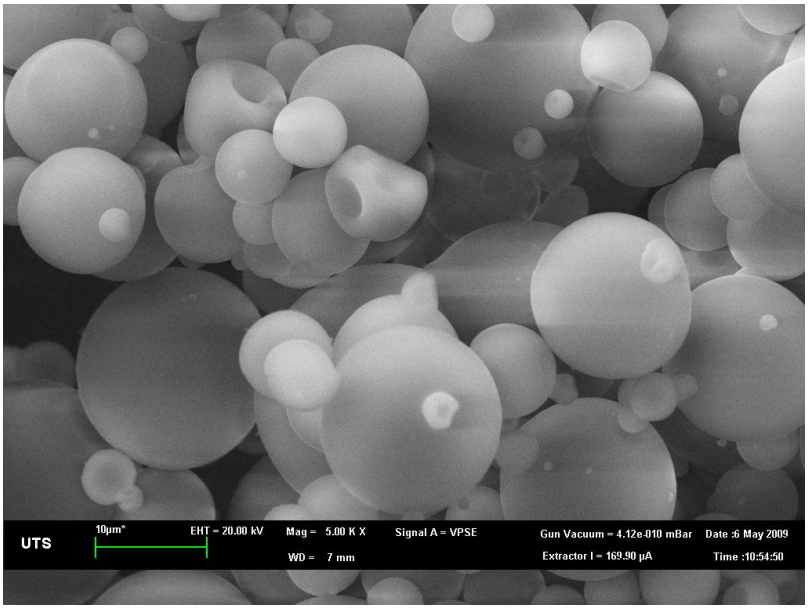

Figure 6.1 SEM image of pure gentamicin sulphate powder in its natural state.

As shown in Figure 6.2 after suspending the microsphere in a concentrated gentamicin solution it can be seen that the gentamicin was successfully incorporated to the microsphere and is evenly distributed throughout the surface as well as within the pores.

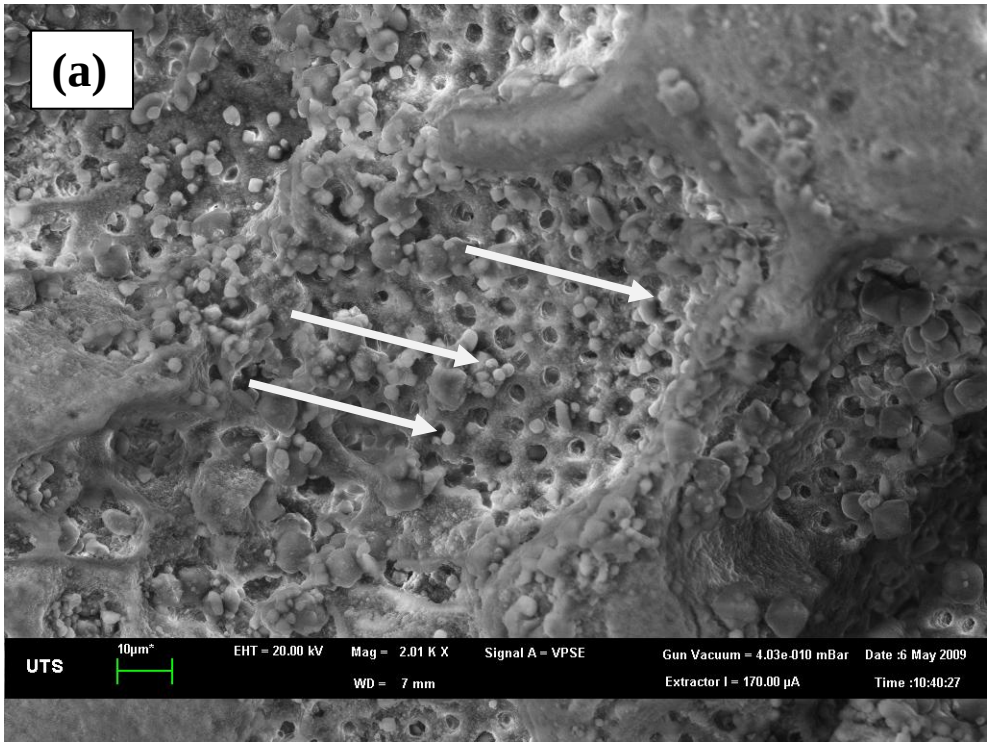

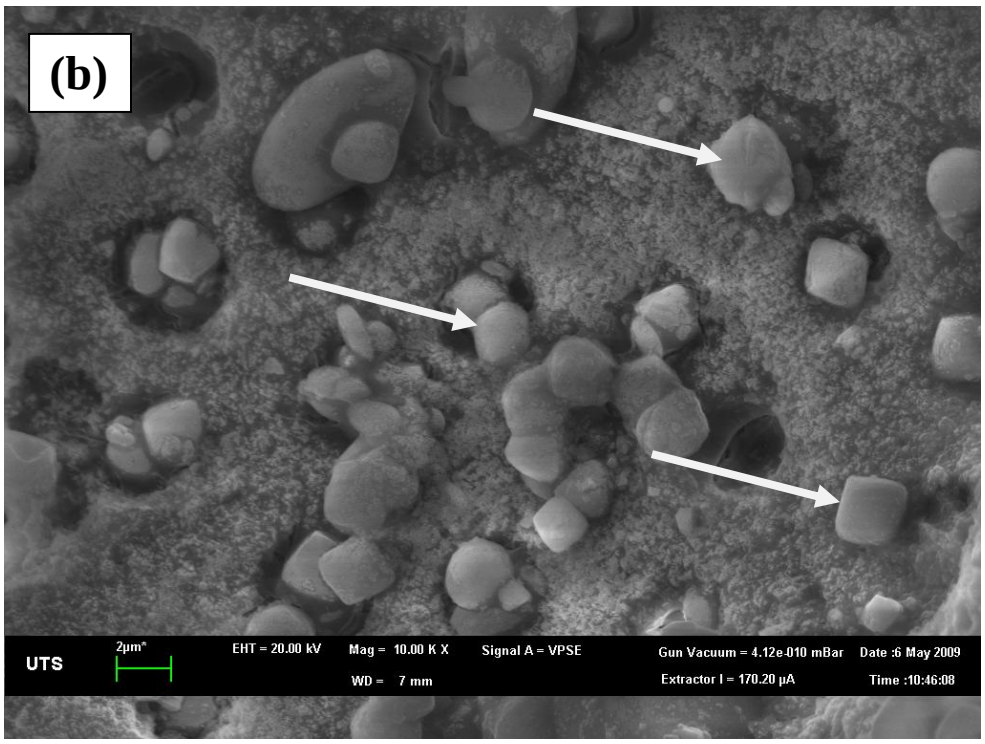

Figure 6.2 SEM image of gentamicin crystals incorporated onto the β –TCP microsphere as indicated by white arrows at (a) low magnification and (b) at higher magnification.

6.3.3 Effect of Dual Loaded Bisphosphonate and Gentamicin Microspheres on Human Osteoblast Cell SaOS-2

It was also important to determine the effect of both bisphosphonate and gentamicin loaded microspheres was not detrimental to human osteoblast survival. Figure 6.3 details the effects on the proliferation of human osteoblast SaOS-2 to the dual loaded bisphosphonate and gentamicin β-TCP microspheres. The relative number of osteoblasts, as determined by fluorescent labeling, shows an increase during the first day but maintained a slight increase compared with the untreated cells during day 3 and 5 (n=6 statistical analysis was based on a 95% confidence interval). This verifies that dual-loaded microspheres maintain their benefits on both osteoblast proliferation and antibacterial efficacy.

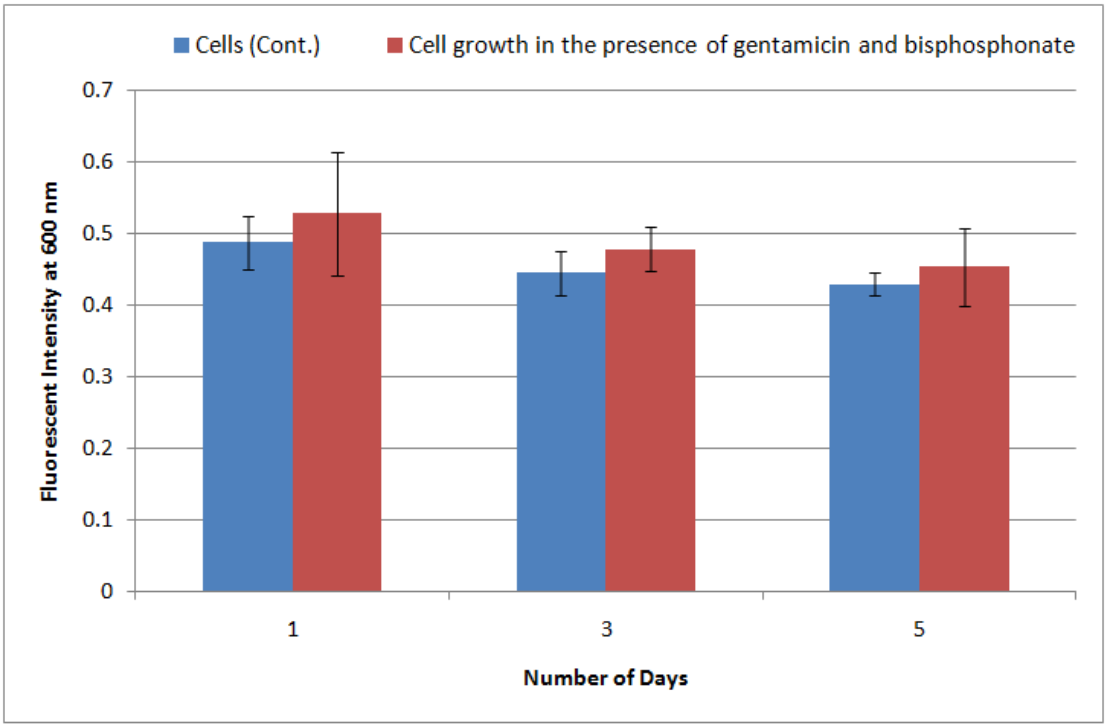

Figure 6.3 Human osteoblast (SaOS-2) growth responses to bisphosphonate and gentamicin incorporated β-TCP microspheres at 1, 3 and 5 days.

Figure 6.4 shows osteoblast attachment to the surface of the dual-loaded β-TCP microspheres. A closer examination of the osteoblast cell shows high numbers of adhesion points (Figure 6.5 (b)) to the surface which indicates strong affinity to the microspheres. The osteoblast cells were observed throughout the surface of the microspheres and this shows a good biocompatibility of the microsphere with the cells which is crucial to promote bone ingrowth and integration.

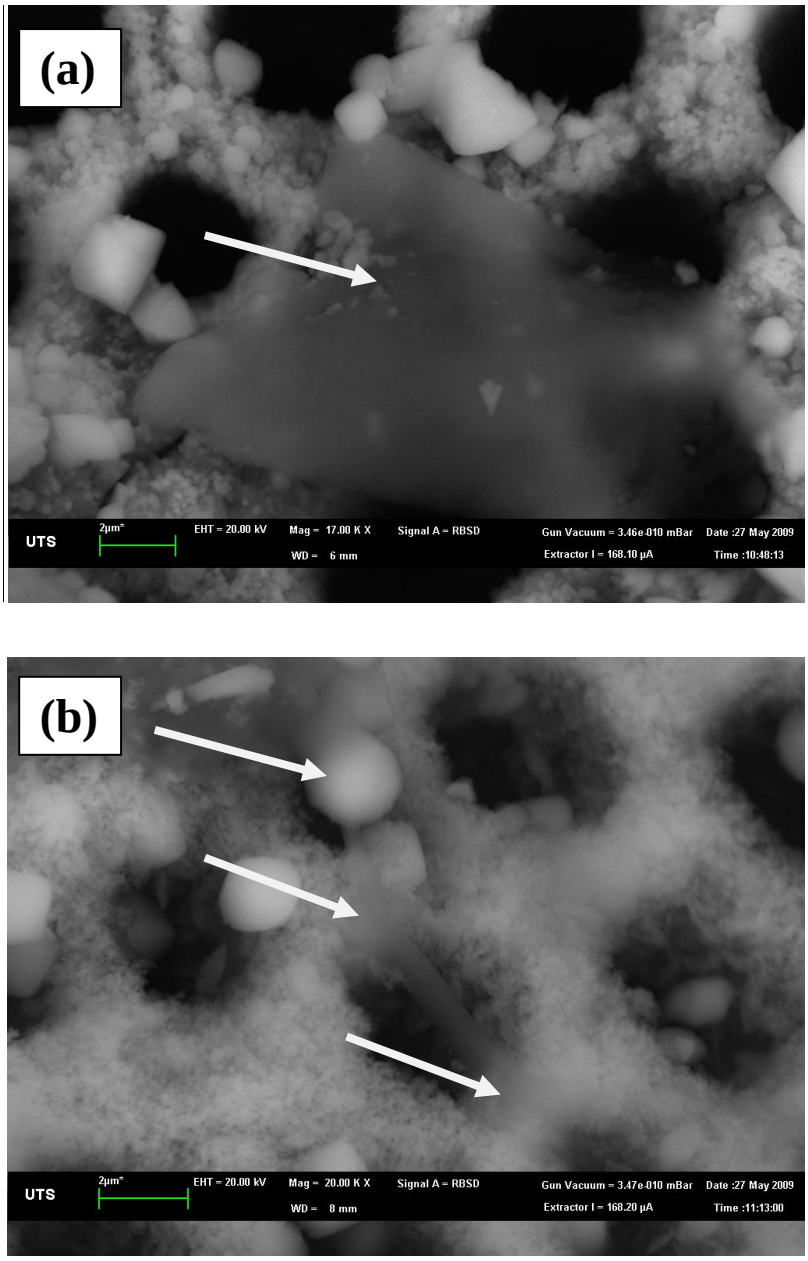

Figure 6.4 SEM image of β –TCP microsphere incorporated with bisphosphonate and gentamicin showing (a) the attachment of a human osteoblast cell and (b) at higher magnification the multiple attachment point over multiple pores.

6.3.4 Antibacterial Efficacy Testing

Before testing the antibacterial efficacy of the microspheres the minimum inhibitory concentration (MIC) of *S. aureus* was first identified and was found to be 10 µg/mL. Figure 6.5 is a growth curve graph of *S. aureus*. It can be observed from Figure 6.6 that there is bacterial growth for the normal β –TCP microspheres and zero growth from microsphere with the bisphosphonate and gentamicin incorporated. The result shows that if one introduces gentamicin and bisphosphonate into the β-TCP microspheres, it is capable of inhibiting the growth of *S. aureus* and should thus allow the bisphosphonate to promote bone growth without the interference from any bacterial infection that may occur in clinical application.

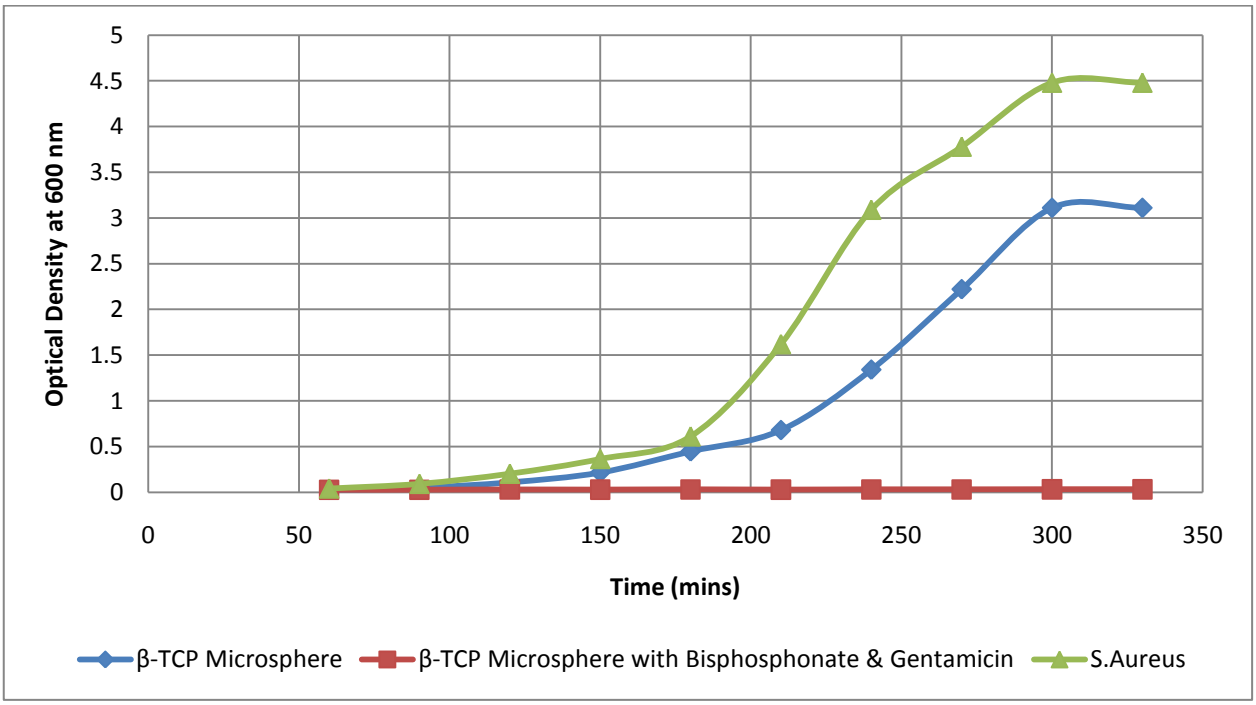

Figure 6.5 Bacterial growth curve showing the inhibition on the growth of S. aureus when exposed to β –TCP microsphere incorporated with bisphosphonate and gentamicin.

6.3.5 Time Delayed Antibacterial Efficacy Testing

For the microspheres to be utilized as a bacterial prevention delivery system, it was necessary to determine the actual release rate of the gentamicin and its affect on the growth of *S. aureus*. A time delayed antibacterial efficacy test was designed to introduce the *S. aureus* at predetermined time intervals. This allowed the examination on the relationship of gentamicin release and bacterial inhibition. Figure 6.6 shows the *S. aureus* growth curve after being exposed to the gentamicin incorporated microspheres at different time intervals.

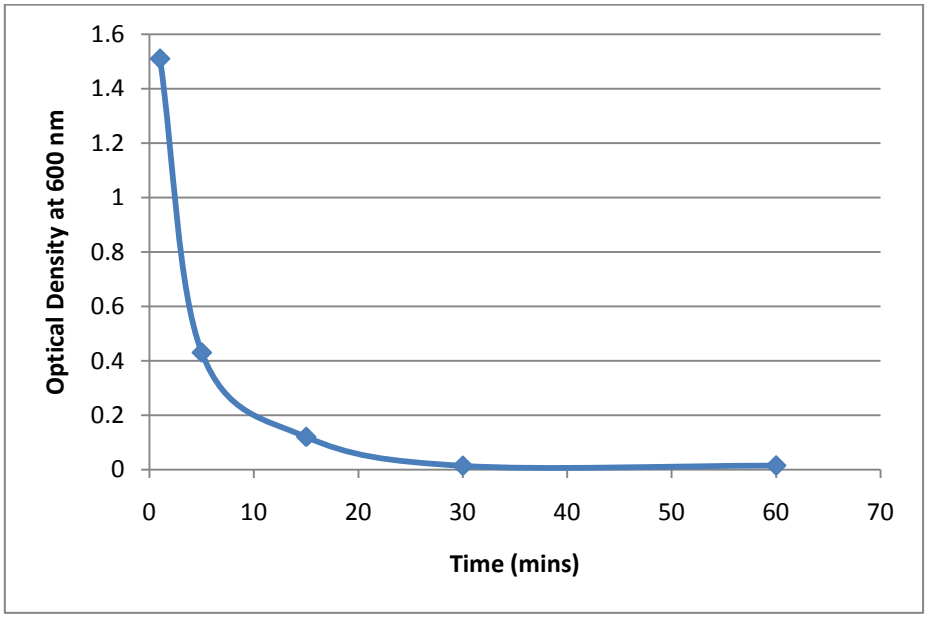

Figure 6.6 Time delayed S. aureus growth curve revealing after 30 mins the bacteria is inhibited from growing from the gentamicin released from the β-TCP microspheres.

As discussed previously there will naturally be an initial burst of the gentamicin which can be seen from the drop in the OD reading at 1 min followed by the dramatic decrease to zero at 30 mins. The test was carried out for 24 hours but no changes were noticed after the 30 min period. From the growth curve the complementing gentamicin release profile is shown in Figure 6.8. This shows that *S. aureus* infection can be inhibited after 30 mins of introducing the microspheres.

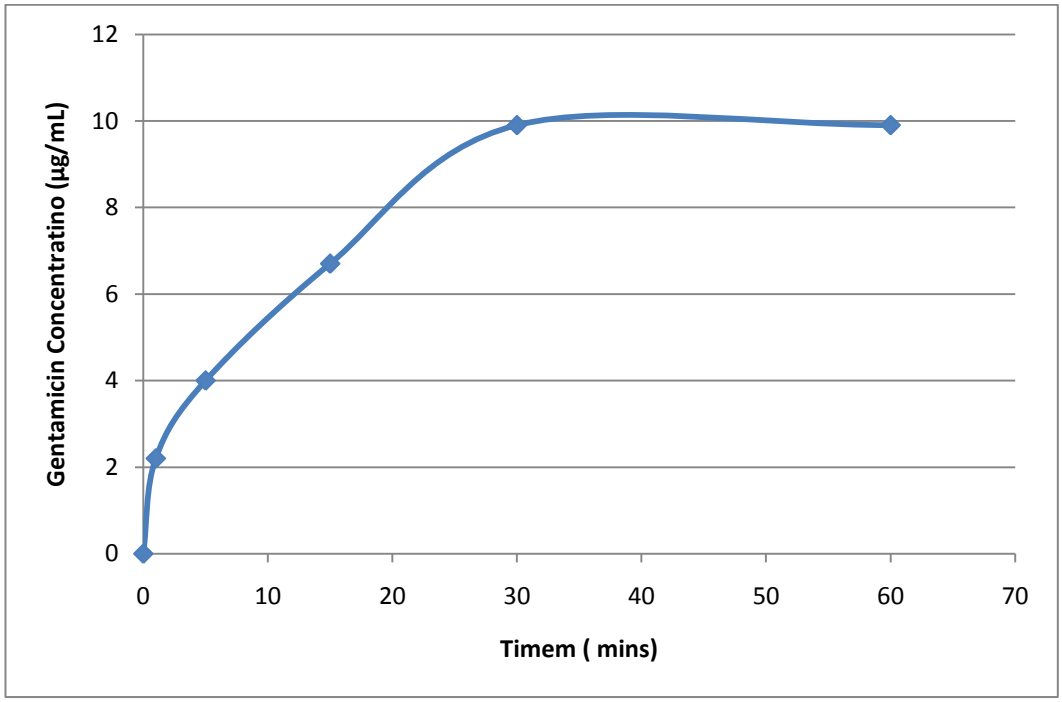

Figure 6.7 Gentamicin release profile calculated from time-delayed antibacterial experiment.

6.3.6 Bacterial Adherence Assay

An adapted modified vortex device (MVD) method which relies on a whirlpool-type force to remove bacteria from a solid matrix was used to determine bacterial adhesion, as this procedure has been used successfully to quantify adhesion (R.White, 1995). This method was used to quantify the number of adherent bacteria on the microspheres loaded with gentamicin and gentamicin with bisphosphonate. The adhesion of *S. Aureus* to some surfaces has been shown to be due to its ability to bind specific host matrix proteins (Montanaro L., 1999). The adhesions that mediate the binding to host proteins, termed MSCRAMMs, are 'microbial surface components which recognise adhesive matrix molecules'. These MSCRAMM components could mediate adhesion on prostheses by binding to host proteins that cover the implant surface *in-vivo* (Ganguli et al., 2005, Paulsson et al., 1993). The cationic amino group on the phosphate of the bisphosphonate chemical structure may attract bacteria by either direct electrostatic interaction or through a direct surface protein interaction.

It is possible that phosphates provide an amino acid mimic on the surface of hydroxyapatite which interacts with the MSCRAMM component. It thus recognizes the simulated host protein on the surface of the material, and mediates increased bacterial adhesion to the hydroxyapatite surface. A prosthesis coated with bisphosphonate would therefore be prone to infection. Therefore it was necessary to demonstrate that with the combination of gentamicin and bisphosphonate incorporated in the microsphere, bacterial adhesion can be prevented. Figure 6.8 shows the bacterial adhesion results which clearly demonstrate that with the gentamicin by itself, there was very limited bacterial cell attachment. The result from the gentamicin and bisphosphonate group shows very minimal bacterial cell attachments.

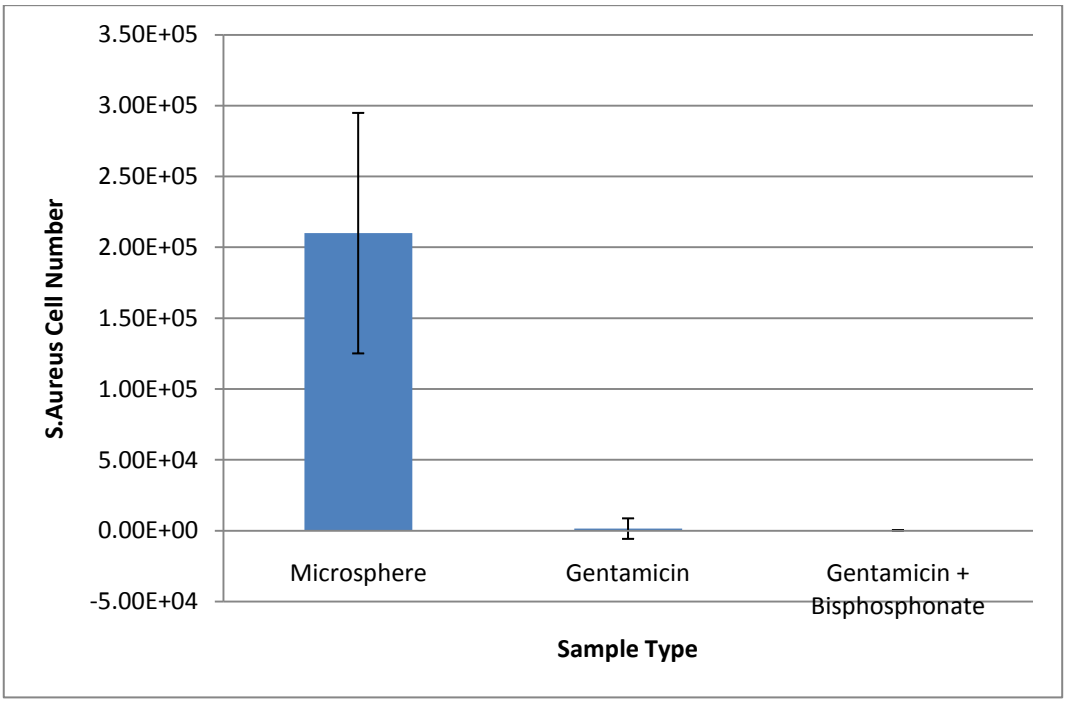

Figure 6.8 Adhesion of S. aureus to microspheres loaded with gentamicin, gentamicin and bisphosphonate and microspheres as control.

6.4 Conclusion

In all experiments, there was an initial rapid release of gentamicin. This initial "burst" results from the presence of the antibiotic crystals on the surface of the microspheres. The drug crystals are more soluble than the microsphere; therefore, their early dissolution will "free" up some of the pores allowing fluid to penetrate into the microsphere. This speeds up the dissolution of the drugs from within the microsphere and consequently leads to the burst effect. The initial burst effect ends because the channel formation ends when all the drugs on the surface, which are in direct contact with each other, are dissolved. After this point, the elution is no longer logarithmic and a constant release pattern is therefore observed as equilibrium has been reached. At this point, the breakdown of the microsphere controls the release of the antibiotic, allowing the exposure of the new drug crystals to the medium. The rapid burst release has shown to be beneficial from a therapeutic standpoint because the high initial release killed the bacteria introduced at the beginning and at various time periods.

The results from the bacterial adhesion tests shows that even though bisphosphonate has the potential to attract bacterial adhesion, it can be prevented or inhibited by the dual effect of having the addition of gentamicin in the microspheres. This demonstrate that the proposed β-TCP microspheres can act as a dual drug delivery system that can assist in implant success.

7 Conclusions and Future Directions

7.1 Key Achievements of this Research

Recycling natural structures and their functions for new applications may play a significant role in bone fracture treatment as an effective targeted delivery of therapeutic drug compounds. We may go further and view this as a generic archetype for bone rectification strategies where filler particles are used to restore bone volume/structure and correct bone metabolism in tandem. There are considerable practical benefits of using natural microspheres for processing and drug incorporation that are simple, cost-effective procedures that make drug delivery vehicle synthesis and assembly redundant. There seems to be no limit either, as to the type of drug that can be used. The fact that we can coat each individual shell in a bioactive lipid film and potentially attach any desired biomolecule to the outside surface will significantly enhance the therapeutic utility and purpose of this device. The biodegradability of coralline microspheres compared to other implant materials makes it a useful material for grafting certain bone defects. This research has shown that coralline materials may be used successfully to fill aseptic bone defects, e.g., after trauma, tumor resection, or removal of bone grafts from the iliac crest. They can also be used in grafting large bone defects, loose pseudarthrosis, bone lengthening, spine fusions, and maxillofacial reconstructions.

The main objective of this research was to develop an effective system to load bisphopshonate, known for its ability to reduce bone resorption, to hydrothermally converted microsphere for improved bone-implant fixation. Adsorption of bisphosphonate and/or with antibiotic onto coral derived calcium phosphate has not been previously investigated.

This study showed that both drugs could be successfully adsorbed onto the microsphere and therapeutic efficiency could be achieved.

The major findings of this study were:

- Microspherical coral sand (calcium carbonate) can be successfully converted to beta-tricalcium phosphate by hydrothermal method while preserving the original architectural characteristics.
- The dissolution rate of the β-TCP microspheres profiled at 21 days suggest the material is suitable for application as a bone filler or as a drug delivery system.
- Bisphosphonate was successfully adsorbed onto the microsphere and can be coated with a sacrificial lipid layer to further control the release rate. The bisphosphonate dissolution rate shows only a 12% release in 21 days thus maintaining the therapeutic efficiency of the drug.
- *In-vitro* evaluation shows the increase in osteoblast proliferation in the presence of bisphosphonate and the reduction of monocytes. Further observation was made of possibly the effect of trace amount of strontium on the reduction of monocytes.
- Antibiotics alone or combined with bisphosphonate was successfully adsorbed onto the microsphere and both were capable of inhibiting the growth of *Staphylococcus aureus* within 30 minutes of introducing the microsphere with the antibiotic. This effect can be observed with just one microsphere.

7.2 Future Investigations

These investigations have been based primarily on determining if pharmaceutical drugs can be adsorbed onto the converted microspheres and to examine if there therapeutic efficiency could be observed *in-vitro*. Further experiments and assays are required to examine in further detail the effect of strontium with osteoblast and osteoclast cells. Furthermore, growth factors, bone morphogenic proteins and mesenchymal stem cells can be incorporated to examine the effectiveness of these alternative strategies in promoting bone regeneration.

Further investigations required include *in-vivo* studies as to determine the effectiveness of the adsorbed bisphosphonate microsphere on a biomedical joint replacement bone implant. *In-vivo* studies have been reported in literature and show that commercially available partially hydrothermally converted corals (having HAp and unconverted calcium carbonate) resulted in imporved mechanical fixation of implants to bone, increase bone mineral density around implants and accelerated new bone formation. Therefore it can be postulated that our bisphosphonate incorporated microsphere would show similar or better results *in-vivo*. However, the effect of both antibiotic and bisphosphonate loaded microsphere is unknown and requires detailed *in-vivo* examination.

8 References

ALAKANGAS, A., SELANDER, K., MULARI, M., HALLEEN, J., LEHENKARI, P., MONKKONEN, J., SALO, J. & VAANANEN, K. 2002. Alendronate disturbs vesicular trafficking in osteoclasts. *Calcified Tissue International,* 70**,** 40-47.

BARBARA, A., DELANNOY, P., DENIS, B. & MARIE, P. 2004. Normal matrix mineralization induced by strontium ranelate in MC3T3-E1 osteogenic cells. *Metabolism* 53**,** 532-537.

BARO, M., SÁNCHEZ, E., DELGADO, A., PERERA, A. & EVORA, C. 2002. In vitro- in vivo characterization of gentamicin bone implants. *J Control Release.,* 83**,** 353-364.

BARON, R. & TSOUDEROS, Y. 2002. *In vitro* effects of S12911-2 on osteoclast function and bone marrow macrophage differentiation. *Eur J Pharmacol,* 450**,** 11-17.

BELL, N. & JOHNSON, R. 1997. Bisphosphonates in the treatment of osteoporosis. *Endocrine,* 6**,** 203-206.

BEN-NISSAN B. 2003. Natural bioceramics: from coral to bone and beyond. *Current Opinion in Solid State and Materials Science,* 7**,** 283-288.

BLAHA, J., CALHOUN, J., NELSON, C., HENRY, S., SELIGSON, D., ESTERHAI, J. J., HEPPENSTALL, R., MADER, J., EVANS, R. & AL., W. J. E. 1993. Comparison of the clinical efficacy and tolerance of gentamicin PMMA beads on surgical wire versus combined and systemic therapy for osteomyelitis. *Clin Orthop Relat Res.,* 295**,** 8-12.

BLOKHUIS, T., TERMAAT, M., DEN BOER, F., PATKA, P., BAKKER, F. & HAARMAN, H. 2000. Properties of calcium phosphate ceramics in relation to their in-vivo behavior. *J. Trauma,* 48**,** 179-186.

BOANINI, E., TORRICELLI, P., GAZZANO, M., GIARDINO, R. & BIGI, A. 2008. Alendronate–hydroxyapatite nanocomposites and their interaction with osteoclasts and osteoblast-like cells. *Biomaterials***,** 790-796.

BOHNER M. 2001. Physical and chemical aspects of calcium phsphates used in spinal surgery. *Eur Spine J.,* 10**,** 114-121.

BONNELYE, E., CHABADEL, A., SALTEL, F. & JURDIC, P. 2008. Dual effect of strontium ranelate: stimulation of osteoblast differentiation and inhibition of osteoclast formation and resorption in vitro. *Bone,* 42**,** 129-138.

BUCKELS, R. G. 1977. Principles of the Design of Controlled Drug Delivery System. *Biomedical Engineering Society, Chicago*.

BUCKLES, R. G. 1983. Biomaterials for Drug Delivery Systems *Journal of Biomedical materials Research,* 17**,** 109-128.

CANALIS, E., HOTT, M., DELOFFRE, P., TSOUDEROS, Y. & MARIE, P. 1996. The divalent strontium salt S12911 enhances bone cell replication and bone formation *in vitro*. *Bone,* 18**,** 517-523.

CHISHOLM, B., LEW, D. & SADASIVAN, K. 1993. The use of tobramycinimpregnated polymethylmethacrylate beads in the treatment of osteomyelitis of the mandible: report of three cases. *J. Oral Maxillofac Surg,* 51**,** 449-450.

CHOU, J., SHIMMON, R. & BEN-NISSAN, B. 2009. Bisphosphonate determination using 1H-NMR spectroscopy for biomedical applications. *Journal of Tissue Engineering and Regenerative Medicine,* 3**,** 92-96.

CROTEAU, S., RAUCH, F., SILVESTRI, A. & HAMDY, R. C. 1999. Bone morphogenetic proteins in orthopedics: from basic science to clinical practice. *Orthopedics,* 22**,** 686-695.

DE GROOT, J. H., NIJENHUIS, A. J., BRUIN, P., PENNINGS, A. J., VETH, R. P. H., KLOMPMAKER, J. & JANSEN, H. W. B. 1990. Use of porous biodegradable polymer implants in meniscus reconstruction. 1) Preparation of porous biodegradable polyurethanes for the reconstruction of meniscus lesions. *Colloid & Polymer Science,* 268**,** 1073-1081.

DEDHIYA, M. G., YOUNG, F. & HIGUCHI, W. I. 1972. Mechanism for the Retardation of the Acid Dissolution Rate of Hydroxyapatite by Strontium. *Journal of Dental Research,* 52**,** 1097-1109.

DEDHIYA, M. G., YOUNG, F. & HIGUCHI, W. I. 1974. Mechanism of hydroxyapatite dissolution. Synergistic effects of solution fluoride, strontium, and phosphate. *The Journal of Physical Chemistry,* 78**,** 1273-1279.

DOROZHKIN, S. V. 2002. A review on the dissolution models of calcium apatites. *Progress in Crystal Growth and Characterization of Materials,* 44**,** 45-61.

DOROZHKIN, S. V. 2009. Calcium Orthophosphate Cements and Concretes. *Materials,* 2**,** 221-291.

DRISKELL, T. D., HASSLER, C. R. & MCCOY, L. R. 1973. Significance of Resorbable Bioceramics in the Repair of Bone Defects. *Proceedings of the Annual Conference on Engineering in Medicine and Biology,* 15**,** 199.

DUCHEYNE, P., RADIN, S. & KING, L. 1993. THE EFFECT OF CALCIUM-PHOSPHATE CERAMIC COMPOSITION AND STRUCTURE ON INVITRO BEHAVIOR .1. DISSOLUTION. *Journal of Biomedical materials Research,* 27**,** 25-34.

DWARAKANADHA, R. P. & SWARNALATHA, D. 2010. Recent Advances in Novel Drug Delivery Systems. *International Journal of PharmTech Research,* 2 2025-2027.

EDITH, B., ANNE, C., FRÉDÉRIC, S. & PIERRE, J. 2008. Dual effect of strontium ranelate: Stimulation of osteoblast differentiation and inhibition of osteoclast formation and resorption in vitro. *Bone,* 42**,** 129-138.

ELEMA, H., DE GROOT, J. H., NIJENHUIS, A. J., PENNINGS, A. J., VETH, R. P. H., KLOMPMAKER, J. & JANSEN, H. W. B. 1990. Use of porous biodegradable polymer implants in meniscus reconstruction. 2) Biological evaluation of porous biodegradable polymer implants in menisci. *Colloid & Polymer Science,* 268**,** 1082-1088.

ELSON, R. A., JEPHCOTT, A. E., MCGECHIE, D. B. & VERETTAS, D. 1984. Antibiotic-loaded acrylic cement *Journal of Bone and Joint Surgery - British Volume,* 59-B**,** 200-205.

EMERSON, R. J., IV & CAMESANO, T. A. 2004. Nanoscale Investigation of Pathogenic Microbial Adhesion to a Biomaterial. *Appl. Environ. Microbiol.,* 70**,** 6012-6022.

FARLAY, D., BOIVIN, G., PANCZER, G., LALANDE, A. & MEUNIER, P. J. 2005. Long-term strontium ranelate administration in monkeys preserves characteristics of bone mineral crystals and degree of mineralization of bone. *J Bone Miner Res,* 20**,** 1569-1578.

FRAYSSINET, P., FAGES, J., BONEL, G. & ROUQUET, N. 1998. Biotechnology, material sciences and bone repair. *European Journal of Orthopaedic Surgery and Traumatology,* 8**,** 17-25.

GANGULI, A., STEWARD, C., BUTLER, S. L., PHILIPS, G. J., MEIKLE, S. T., LLOYD, A. W. & GRANT, M. H. 2005. Bacterial adhesion to bisphosphonate coated hydroxyapatite. *Journal of Materials Science: Materials in Medicine,* 16**,** 283-287.

GAO, Y., ZOU, S., LIU, X., BAO, C. & HU, J. 2009. The effect of surface immobilized bisphosphonates on the fixation of hydroxyapatite-coated titanium implants in ovariectomized rats. *Biomaterials,* 30**,** 1790-1796.

GAREY, D., WHITTAKER, J. M., JAMES, R. A. & LOZADA, A. L. 1991. The histologic evaluation of the implant interface with heterograft and allograft material - an eight months autopsy report. *J. Oral Implantol,* 17**,** 404-408.

GINEBRA, M., TRAYKOVA, T. & PLANELL, J. 2006. Calcium phosphate cements as bone drug delivery systems: A review. *J Control Release.* , 113**,** 102-110.

GUILLEMIN, G., LAUNAY, M. & MEUNIER, A. 1993. Natural coral as a substrate for fibroblastic growth in vitro *Journal of Materials Science: Materials in Medicine,* 4**,** 575-581.

GUILLEMIN, G., PATAT, J. L., FOURNIE, J. & CHETAIL, M. 1987. The use of coral as a bone graft substitute. *Journal of Biomedical Materials Research,* 21**,** 557-567.

HARAKAS, N. K. 1984. Demineralized bone-matrix-induced osteogenesis. *Clin Orthop Relat Res.,* Sep**,** 239-251.

HENCH, L. L., AND E.C. ETHRIDGE 1982. *Biomaterials. An Interfacial Approach,* New York, London, Academic Press.

HENCH, L. L. & WEST, J. K. 1990. The sol-gel process. *Chem. Rev.,* 90**,** 33-72.

HENRIKSEN K, L. D., BYRJALSEN I, NIELSEN RH, SORENSEN MG, DZIEGIEL MH 2007. Osteoclasts prefer aged bone. *Osteoporos Int,* 18.

HIGUCHI, T. 1963. Mechanism of sustained-action medication. Theoretical analysis of release of solid drugs dispersed in solid matrices. *J. Pharm. Sci.* , 52**,** 1143-1149.

HIROFUMI, F., TOMOKO, K., TOSHIHIKO, U., SHIKIBU, M., TAKUZO, F., CHOSEI, M., JITSUO, A., TATSUJI, Y. & KOZO, U. 2004. Mechanism of risedronate-induced apoptosis in U937 cells. *Japanese Journal of Medicine and Pharmaceutical Science,* 51**,** 697-710.

HOLLINGER, J. & WONG, M. E. K. 1996. The integrated proess of hard tissue regeneration with special emphasis on fracture healing. *Oral Surg Oral med Oral Pahtol Oral Radiol Endod.,* 82**,** 594.

HUANG, J., LIU, K., CHEN, C., HO, K., WU, Y., WANG, C., CHENG , Y., KO, W., LIU, C., HO, Y., WANG, Y. & HONG, K. 1997. Liposomes-coated hydroxyapatite and tricalcium phosphate implanted in the mandibular bony defect of miniature swine. *Kaohsiung J. Med. Sci.,* 13**,** 213-218.

HUGHES, D., MACDONALD, B., RUSSELL, R. & GOWEN, M. 1989. Inhibition of osteoclast-like cell formation by bisphosphonates in long-term cultures of human bone marrow. *Journal of Clinical Investigation,* 83**,** 1930-1935.

HUGHES, F. J., TURNER, W., BELIBASAKIS, G. & MARTUSCELLI, G. 2006. Effects of growth factors and cytokines on osteoblastic differentiation. *Periodontology 2000,* 41**,** 48.

JARCHO, M. 1981. Calcium phosphate ceramics as hard tissue prosthetics. . *Clin Orthop,* 157**,** 259-278.

JARCHO, M., J.F. LAY, K.I. GUMAER, R.R.H. DOREMUS AND H.P. DROBECK 1977. Tissue, cellular and subcellular events at a bone ceramic hydroxyapatite interface. *J. Bioeng.,* 1**,** 79-92.

KAJIWARA, H., YAMAZA, T., YOSHINARI, M., GOTO, T., IYAMA, S., ATSUTA, I., KIDO, M. A. & TANAKA, T. 2005. The bisphosphonate pamidronate on the surface of titanium stimulates bone formation around tibial implants in rats. *Biomaterials,* 26**,** 581-587.

KALFAS, I. H. 2001. Principles of bone healing. *Neurosurg Focus.,* 10**,** 1.

KASEMO, B., AND J. LAUSMAA 1991. The biomaterial-tissue interface and its analogoues in surface science and technology. *The Bone-Biomaterial Interface,* J.E.Davies (ed.)**,** 19-32.

KATSIKOGIANNI, M. & MISSIRLIS, Y. F. 2004. Concise review of mechanisms of bacterial adhesion to biomaterails and techniques used in estimating bacterial-material interactions. *European Cells and Materials,* 8**,** 37-57.

KIMMEL, D. 2007. Mechanism of action, pharmakinetic and pharmacodynamic profile, and clinical applications of nitrogen-containing bisphosphonates. *Journal of Dental Research,* 86**,** 1022-1033.

KIRKPATRICK, C. J. 1992. A critical view of current and proposed methodologies for biocompatibility testing: cytotoxic in vitro. *Regulatory Affairs,* 4.

KLEIN, C. P. A. T., DRIESSEN, A. A., DE GROOT, K. & VAN DEN HOOFF, A. 1983. Biodegradation behavior of various calcium phosphate materials in bone tissue. *Journal of Biomedical materials Research,* 17**,** 769-784.

KOKUBO, T., ITO, S., HUANG, Z. T., HAYASHI, T., SAKKA, S., T., K. & YAMAMURO, T. 1990. Ca,P-rich layer formed on high-strength bioactive glass-ceramic A-W. *J. Biomed. Mater. Res.,* 24**,** 331-343.

KOKUBO, T., OYANE, A., KIM, H. M., FURUYA, T., MIYAZAKI, T. & NAKAMURA, T. 2003. Preparation and assessment of revised simulated body fluid. *J. Biomed. Mater. Res.,* 65A**,** 188-195.

KOKUBO, T. & TAKADAMA, H. 2006. How useful is SBF in predicting in vivo bone bioactivity? . *Biomaterials,* 27**,** 2907-2915.

KUHNE JH., B. R., FRISCH B., HAMMER C., JANSSON V., ZIMMER. 1994. Bone formation in coralline hydroxyapatite. Effects of pore size studied in rabbits. *Acta Orthop Scand,* 65**,** 246-252.

LANZA RP., C. W. 1997. Transplantation of encapsulated cells and tissues. *Surgery,* 121**,** 1-9.

LAUFFENBURGER D.A., G. L. G. 2001. Who's Got Pull Around Here? Cell Organization in Development and Tissue Engineering. *Proc. Natl. Acad. Sci.,* 98**,** 4282-4284.

LAURENT F, B. A., GOLDNADEL J, CHEVALIER J, FANTOZZI G, VIGUIER E, ROGER T, BOIVIN G, HARTMANN D. 2008. A New Concept of gentamicin loaded HAP/TCP bone substitute for prophylactic action: in vitro release validation. *J Mater Sci Mater Med.,* 19**,** 947-957.

LEE, J. J. & ANDERSON, O. R. 1991. *Biology of foraminifera* San Diego Academic Press

LEGEROS R.Z. 2001. Formation and transformation of calcium phosphates: relevance to vascular
calcification. *Z Kardiol.,* 90**,** Suppl. 3, III116-III125.

LEGEROS, R. Z. 1988. Calcium phosphate materials in restorative dentistry: a review. *Adv Dent Res,* 2**,** 164-180.

LEGEROS, R. Z. 1993. Biodegradation and bioresorption of calcium phosphate ceramics. *Clinical Materials,* 14**,** 65-88.

LEGEROS, R. Z. & DACULSI, G. 1990. In Vivo transformation of biphasic calcium phosphate ceramcis: ultrastructureal and physicochemical characterizations. *In:* YAMAMURO, T., HENCH, L. L. & WILSON, J. (eds.) *Handbook of Bioactive Ceramcis Volume II.* Boca Raton: CRC Press.

LEWIS, K. 2001. Riddle of Biofilm Resistance. *Antimicrobial Agents and Chemotherapy,* 45**,** 999-1007.

LUCAS-GIROT A., V. M., TRIBUT O., SANGLEBOEUF JC., ALLAIN H., OUDADESSE H., 2005. Gentamicin-loaded calcium carbonate materials: Comparison of two drug-loading modes. *J Biomed Mater Res B Appl Biomater. ,* 73B**,** 164-170.

LUCKMAN, S., HUGHES, D., COXON, F., RUSSELL, R. & ROGERS, M. 1998. Nitrogen-containing bisphosphonates inhibit the mevalonate pathway and prevent post-tranlational prenylation of GTP-binding proteins, including Ras. *Journal of Bone and Mineral Research* 13**,** 581-589.

MALONE JD, T. S., GRIFFIN GL, SENIOR RM, KAHN AJ. 1982. Recruitment of osteoclast precursors by purified bone matrix constituents. *J Cell Biol,* 92**,** 227-230.

MARIE, P. 2005. Strontium ranelate: a novel mode of action optimizing bone formation and resorption. *Osteoporos Int,* 16**,** S7-10.

MARIE, P. 2006. Strontium ranelate: a physiological approach for optimizing bone formation and resorption. *Bone,* 38**,** S10-14.

MESEGUER-OLMO, L., ROS-NICOLÁS, M. J., CLAVEL-SAINZ , M., VICENTE-ORTEGA, V., ALCARAZ-BAÑOS, M., LAX-PÉREZ, A., ARCOS, D., RAGEL, C. V. & VALLET-REGÍ, M. 2002. Biocompatibility and in-vivo gentamicin release from bioactive sol-gel glass implants. . *Journal of Biomedical Materials Research Part A,* 61**,** 458-465.

METSGER, D. S., DRISKELL, T. D. & PAULSRUD, J. R. 1982. Tricalcium phosphate ceramic--a resorbable bone implant: review and current status. *J. Am. Dent. Assoc.,* 105**,** 1035.

MOHANTY, S., KUMAR, M. & MURTHY, N. 2003. Use of antibiotic-loaded polymethyl methacrylate beads in the management of musculoskeletal sepsis — a retrospective study. *J Orthop Surg (Hong Kong),* 11**,** 73-79.

MONTANARO L., A. C., BALDASSARRI L., BORSETTI E., 1999. Presence and expression of collagen adhesin gene (cna) and slime production in Staphylococcus aureus strains from orthopaedic prosthesis infections. *Biomaterials,* 20**,** 1945-1949.

MORAN AVIV, I. B. M. Z. 2007. Gentamicin-loaded bioresorbable films for prevention of bacterial infections associated with orthopedic implants. *Journal of Biomedical Materials Research Part A,* 83A**,** 10-19.

NANCOLLAS, G. H., TANG, R., PHIPPS, R. J., HENNEMAN, Z., GULDE, S., WU, W., MANGOOD, A., RUSSELL, R. G. G. & EBETINO, F. H. 2006. Novel insights into actions of bisphosphonates on bone: Differences in interactions with hydroxyapatite. *Bone,* 38**,** 617-627.

NASCA RJ., L. J., DEINLEIN DA, 1989. Synthetic biomaterials for spinal fusion. *Orthopedics,* 12**,** 543-548.

NEUT, D., GROOT, E. P. D., KOWALSKI, R. S. Z., HORN, J. R. V., MEI, H. C. V. D. & BUSSCHER, H. J. 2005. Gentamicin-loaded bone cement with clindamycin or fusidic acid added: Biofilm formation and antibiotic release. *Journal of Biomedical Materials Research Part A,* 73A**,** 165-170.

O'GARA, J. P. & HUMPHREYS, H. 2001. Staphylococcus epidermidis biofilms: importance and implications. *Journal of Medical Microbiology,* 50**,** 582-587.

O'NEILL W.C. 2007. The fallacy of the calcium phosphorus product. *Kidney International,* 72**,** 792-796.

O'TOOLE, G. A. & KOLTER, R. 1999. Flagellar and twitching motility are necessary for Pseudomonas aeruginosa biofilm development. *Molecular Microbiology,* 30**,** 295-304.

OHGUSHI, H., OKUMURA, M., YOSHIKAWA, T., INBOUE, K., SENPUKU, N., TAMAI, S. & SHORS, E. C. 1992. Bone formation processin porous calcium carbonate and hydroxyapatite. *Journal of Biomedical materials Research,* 26**,** 885-895.

OLIVEIRA, A. L., PEDRO, A. J., ARROYO, C. S., MANO, J. F., RODRIGUEZ, G., SAN ROMAN, J. & REIS, R. L. 2010. Biomimetic Ca-P coatings incorporating bisphosphonates produced on starch-based degradable biomaterials. *J Biomed Mater Res B Appl Biomater.,* 92**,** 55-67.

PALAZZO, B., IAFISCO, M., LAFORGIA, M., MARGIOTTA, N., NATILE, G., BIANCHI, C. L., WALSH, D., MANN, S. & ROVERI, N. 2007. Biomimetic Hydroxyapatite-Drug Nanocrystals as Potential Bone Substitutes with Antitumor Drug Delivery Properties. *Advanced Functional Materials,* 17**,** 2180-2188.

PARFITT, A. M. 2002. Targeted and nontargeted bone remodeling: relationship to basic multicellular unit origination and progression. *Bone,* 30**,** 5-7.

PARK, J. B. & LAKES, R. S. 1992. *Biomaterials: An Introduction,* New York, Plenum Publishing

PAUL, W. & SHARMA, C. P. 1999. Development of porous spherical hydroxyapatite granules: application towards protein delivery. *Journal of materials science. Materials in medicine* 10**,** 383-388.

PAULSSON, M., KOBER, M., FREIJ-LARSSON, C., STOLLENWERK, M., WESSLÉN, B. & LJUNGH, Å. 1993. Adhesion of staphylococci to chemically modified and native polymers, and the influence of preadsorbed fibronectin, vitronectin and fibrinogen. *Biomaterials,* 14**,** 845-853.

PAVLOS, N., XU, J, RIEDEL, D, YEOH, J, TEITELBAUM, S, PAPADIMITRIOU, J, REINHARD, J, ROSS, F AND ZHENG, M 2005. Rab3D regulates a novel vesicular trafficking pathway that is required for osteoclastic bone resorption. *Molecular and Cellular Biology*.

PETER, B., PIOLETTI, D. P., LAÏB, S., BUJOLI, B., PILET, P., JANVIER, P., GUICHEUX, J., ZAMBELLI, P. Y., BOULER, J. M. & GAUTHIER, O. 2005. Calcium phosphate drug delivery system: influence of local zoledronate release on bone implant osteointegration. *Bone,* 36**,** 52-60.

PILLIAR, R. 1987. Porous-surfaced metallic implants for orthopaedic applications. *J. Biomed. Mater. Res.,* 21**,** 1-33.

R.WHITE, S. C. L. P. M. R. S. D. 1995. Bacterial adhesion measurements on soft contact lenses using a modified vortex device and a modified Robbins device. *Journal of Industrial Microbiology and Biotechnology,* 15**,** 243-247.

RADIN, S., CAMPBELL, J. T., DUCHEYNE, P. & CUCKLER, J. M. 1997. Calcium phosphate ceramic coatings as carriers of vancomycin. *Biomaterials,* 18**,** 777-782.

RAO, M. S. A. K. P. 2002. Preparation, characterization and in vitro release of gentamicin from coralline hydroxyapatite-gelatin composite microspheres. *Biomaterials,* 23**,** 3175-3181.

RATNER, B. D., HOFFMAN, A. S., SCHOEN, F. J. & LEMON, J. (eds.) 2004. *Biomaterials science : an introduction to materials in medicine,* Amsterdam ; Boston Elsevier Academic Press.

REGINSTER, J. 2002. Strontium ranelate in osteoporosis. *Curr Pharm Design,* 8**,** 1907-16.

REIS, R. L. & MONTEIRO, F. J. 1996. Crystallinity and structural changes in HA plasma-sprayed coatings induced by cyclic loading in physiological media. *Journal of Materials Science: Materials in Medicine,* 7**,** 407-411.

REY C., C. C., DROUET C., SFIHI H. 2006. Chemical diversity of apatites. *Adv. Sci. Technol. ,* 49**,** 27-36.

RIBEIRO C.C., B. C. C., BARBOSA M.A., 2006. Preparation and characterisation of calcium-phosphate porous microspheres with a uniform size for biomedical applications. *J Mater Sci: Mater Med,* 17**,** 455-463.

ROSSI S, A. A., OMRI A. 2004. Antimicrobial efficacy of a new antibiotic-loaded poly(hydroxybutyric-co-hydroxyvaleric acid) controlled release system. *J Antimicrob Chemother.,* 54**,** 1013-1018.

ROY DM, L. S. 1974. Hydroxyapatite formed from coral skeletal carbonate by hydrothermal exchange. *Nature,* 247**,** 220-222.

SAMBROOK, P., SEEMAN, E., PHILLIPS, S. & EBELING, P. 2002. Preventing osteoporosis: outcomes of the Australian Fracture Prevention Summit. *Med J Aust***,** 176.

SCOTT, D., ROTSCHAFER, J. & BEHRENS, F. 1988. Use of vancomycin and tobramycin polymethylmethacrylate impregnated beads in the management of chronic osteomyelitis. *Drug Intell Clin Pharm,* 22**,** 480-483.

SHIMA T., K. J., ALVIRA MM., MAYFIELD FH., DUNSKER SB., 1979. Anterior cervical discectomy and interbody fusion. An experimental study using a synthetic tricalcium phosphate. *Journal of Neurosurgery,* 51**,** 533-538.

SILVER, I., MURRILLS, R. & ETHERINGTON, D. 1988. Microelectrode studies on the acid
microenvironment beneath adherent macrophages and osteoclasts. *Exp Cell Res,* 175**,** 266-276.

SIMS, N. A. & GOOI, J. H. 2008. Bone remodeling: Multiple cellular interactions required for coupling of bone formation and resorption. *Seminars in Cell & Developmental Biology,* 19**,** 444-451.

SOMIYA, S. 2006. Historical developments of hydrothermal works in Japan, especially in ceramic science. *Journal of Materials Science,* 41**,** 1307-1318.

SOMMERFELDT, D. W. & RUBIN, C. T. 2001. Biology of bone and how it orchestrates the form and function of the skeleton. *Eur Spine J.,* 10**,** S86-S95.

STEFFEN T., M. D., AEIBI M., 2000. Posterolateral and anterior interbody spinal fusion models in the sheep. *Clin Orthop* 371**,** 28-37.

TADIC, D., WELZEL, T., SEIDEL, P., WÜST, E., DINGELDEIN, E. & EPPLE, M. 2004. Controlled Release of gentamicin from biomimetic calcium phosphate in vitro. Comparison of four different incorporation methods. . *Materialwissenschaft und Werkstofftechnik,* 35**,** 1001-1005.

TAKAHASHI, N., SASAKI, T., TSOUDEROS, Y. & SUDA, T. 2003. S12911-2 inhibits osteoclastic bone resorption *in vitro*. *J Bone Miner Res,* 18**,** 1082-1087.

TEMENO, J. S. & ANTONIOS, G. M. 2000. Injectable biodegradable materials for orthopedic tissue engineering. *Biomaterials,* 21**,** 2405}2412.

TENGVALL, P., SKOGLUND, B., ASKENDAL, A. & ASPENBERG, P. 2004. Surface immobilized bisphosphonate improves stainless-steel screw fixation in rats. *Biomaterials,* 25**,** 2133-2138.

THOMES B, M. P., BOUCHIER-HAYES D. 2002. Development of resistant strains of Staphylococcus epidermidis on gentamicin-loaded bone cement in vivo. *J Bone Joint Surg Br,* 84-B**,** 758–760.

TRACY, B. M. & DOREMUS, R. H. 1984. Direct electron microscopy studies of the bone—hydroxylapatite interface. *Journal of Biomedical materials Research,* 18**,** 719-726.

TUNG, I. C. 1995. In-vitro drug release of antibiotic-loaded porous hydroxyapatite cement. *Artif. Cells Blood Substit. Immobil. Biotechnol. ,* 23**,** 81-88.

VAN BEEK, E., PIETERMAN, E., COHEN, L., LOWIK, C. & PAPOULOS, S. 1999. Nitrogen-containing bisphosphonates inhibit isopentenyl pyrophsophate isomerase/farnesyl pyrophosphate synthase activity with relative potencies corresponding to their antiresorptive potencies in vitro and in vivo. *Biochem. Biphys. Res. Commun.* , 255**,** 491-494.

VILLIERS, J. D. & TOBIAS 2009. Bone health and osteoporosis in postmenopausal women. *Best Practice & Research Clinical Obstetrics & Gynaecology,* 23**,** 73-85.

VITTE, C., FLEISCH, H. & GUENTHER, H. 1996. Bisphosphonates induce osteoblasts to secrete an inhibitor of osteoclast-mediated resorption. *Endocrinology* 137**,** 2324-2333.

WEBSTER, T. J., KHANG, D., LIU-SNYDER, P., PARETA, R. & LU, J. 2009. Reduced Responses of Macrophages on Nanometer Surface Features of Altereed Alumina Crystalline Phases. *Acta Biomaterialia,* 5**,** 1425-1432.

WILLIAMS, D. F. 1985. *Biocompatibility of tissue analogs,* Boca Raton, FL, CRC Press.

WILLIAMS, D. F. 1990. *Biocompatibility,* Oxford, Pergamon Press.

WOO, J., NAKAGAWA, H., KRECIC, A., NAGAI, K., HAMILTON, A., SEBTI, S. & STERN, P. 2005. Inhibitory effects of mevastatin and a geranylgeranyl transferase I inhibitor (GGTI-2166) on mononuclear osteoclast formation induced by receptor activator of NFκB ligand (RANKL) or tumor necrosis factor-α (TNF-α). *Biochemical Pharmacology,* 69**,** 87-95.

WOPENKA B., P. J. D. 2005. A mineralogical perspective on the apatite in bone. *Mater. Sci. Eng.C,* 25**,** 131-143.

YOSHINARI, M., FURUYA, N., HAYAKAWA, T., YAMANISHI, Y., FUKUSHIMA, T. & SATO, M. 2009. Effect of Bisphosphonate Immobilization of Apatite Coated Titanium Web on Trabecular Bone Response. *Journal of Oral Tissue Engineering,* 7**,** 73-80.

ZHANG, D., UDAGAWA, N., NAKAMURA, I., MURAKAMI, H., SAITO, S., YAMASAKI, K., SHIBASAKI, Y., MORII, N., NARUMIYA, S., TAKAHASHI, N. & SUDA, T. 1995. The small GTP-binding protein, rho p21, is involved in bone resorption by regulating cytoskeleteal organization in osteoclasts. *Journal of Cell Science,* 6**,** 2285-2292.

ZHANG Q, C. J., FENG J, CAO Y, DNEG C, ZHANG X. 2003. Dissolution and mineralization behaviours of HA coatings. *Biomaterials,* 24**,** 4741-4748.